Ph. D. Thesis

Study on Separation and Recovery of Metal Ion from Wastewater Based on Environmental Crystallization Method

環境晶析手法に基づく排水中金属イオン分離および回収に関する研究

Feb. 2013

Yoshiharu Shimizu

清水　啓玄

Ph. D. Thesis

Study on Separation and Recovery of Metal Ion from Wastewater Based on Environmental Crystallization Method

環境晶析手法に基づく排水中金属イオン分離および回収に関する研究

Feb. 2013

Waseda University

Graduate School of Advanced Science and Engineering
Major in Applied Chemistry, Research on Chemical Engineering

Yoshiharu Shimizu

清水　啓玄

JUDGING COMMITTEE

Referee in chief

Waseda University — Prof. Izumi Hirasawa

Referee

Waseda University — Prof. Suguru Noda

Martin-Luter University — Prof. Joakim Ulrich

Abstract

Nowadays, metal resources are exhaustible and the establishment of technologies for recycling metals from wastewater is desired. This thesis proposes an environmental crystallization method for separating and recovering metal ions and attempts to organize and systematize this method. Drainage treatment technologies based on environmental crystallization have the following advantages: 1. Feedstock and equipment are inexpensive, 2. Sludge production is minimized, and 3. Particular materials can be recycled. In this study, a metal sulfate solution is reacted with a sodium carbonate solution and poor water-soluble metal carbonates or hydrates are precipitated. In the reactive crystallization, stock solutions are provided in the tank continuously on the basis of a double-jet method. Effluents are drained so that the solution volume in the tank is constant during the reaction.

Metal ions we treated are cobalt, copper, manganese, nickel and zinc divalent ions. The method of incorporating metal ions in spherical seeds such as metal carbonate basics is effective as a means of recovery metals as materials. For this reason, this thesis attempts to determine the optimum seed inputs and to solve the mechanisms of incorporating metal ions onto seeds. The reactive crystallization designed for applying to actual industrial wastewater containing impurities and examined how the impurities affect the ions uptake and seeds growth. At this time, the crystal growth over time was observed, and the roughness of the recovered crystals and target metals purities have been examined because they can be major factors contributing to the crystals formation and the ions uptake rate.

This metal ions separation and recovery technique can be expanded in two directions. One is the application to real wastewater. For realization, it is necessary to confirm conditions that can enlarge crystals continuously during the single metal ions reaction. The effect of other metal ions and anions such as phosphate and borate ions on the metal ions separation and recovery should also be a point of consideration. In addition, conditions and methods for the selective treatment need to be explored. The other direction is the examination of products availability as metal materials. The following aspects seem to be desirable in metal materials: highly mono-dispersed, uniform in size, and high purity. This study approaches the realization of drainage systems from the view of the above two points.

In chapter 1, metal wastewater treatment technologies were summarized and the environmental crystallization advantages and disadvantages are clarified with the discussion of the feasibility. Metal wastewater is widely treated by the coagulation method. This method is through the use of solubility products and metal ions are precipitated as poor water-soluble chemicals. This

method is inexpensive and effective from the view of treating a large amount of drainage at once. In contrast, the solvent extraction and the filtration are more favorable for separating and recovering metal ions selectively. However, they are suffered from the high cost of solvents, membranes and treatment facilities. The environmental crystallization can be the method of accomplishing water treatment and materials generation. Nonetheless, industrial wastewaters often contain a variety of metal ions, dispersants and chelate agents, so it seems to be difficult to treat wastewater only via this method. Basically, several technologies are used in combination for the water treatment, and it is important to examine the position of this method in total treatment. In this chapter, current situations about metal ions containing wastewater treatment technologies are investigated from official reports.

In chapter 2, general statements of the reactive crystallization are summarized and the results of manganese and zinc ions reactive crystallization were represented. By performing this method, optimal pH ranges that form crystals have been verified. Manganese and silver carbonates can be crystallized even in the neutral solutions; whereas nickel, copper and zinc ions can form hydrates or oxides only in the basic solutions. About manganese carbonates and zinc oxides that shape spherical crystals, the reactive crystallization was performed, changing the providing speed, initial pH in the tank solution or the metal ions concentration of the stock solution. As a result, recovered manganese carbonate particles have grown larger with an increase in the feeding rate and in the metal ions concentration. Similarly, the metal recovery rate was decrease with a decrease of the feeding speed and with an increase of the metal ions concentration in the stock solution. Obtained zinc oxide particles size has continuously changed depending on the initial pH. From the above, for the answer to host needs, obtained particles size, surface roughness, metal ions recovery rate and mono-dispersion can be controlled to some extent by fixing the reactive conditions.

In chapter 3, findings of seeding effect in recovering copper and nickel ions were summarized. Nickel and copper ions are crystallized by controlling pH but the product shapes are not regular. For recycling these materials, dispersion of their forms and sizes should be restricted. There, spherical metal carbonate basics are dosed in a tank preliminarily and the crystallization was performed aiming at the crystal growth on seed surfaces. In changing seed inputs, seed growth mechanisms were discussed from the crystal sizes data after the 8 hours reactive crystallization. As a result, it was indicated that seed growth mechanisms are different from the kind of seeds. In the recovery of nickel ions, granular fine particles were appeared around seeds or in the bulk and they accumulated on the surface of seeds to grow. Meanwhile, in recovery of copper ions, needle-like crystals were grown from the center of seeds. In the recovery of nickel and copper

ions, optimal seed input that can enlarge seeds, remaining the shape sphere was discovered. At this time, crystal sizes depend on one third power of the reaction time. Many fine particles were produced in providing less or more seed inputs.

In chapter 4, the reactive crystallization with the use of the solution containing multiple metal ions or anions was summarized. The difference in metal ions uptake rate and the purity improvement by the centrifugation have been found out, and the adaptability of this method against the complex systems was examined. Based on the nickel and copper ions recovery as dealt in chapter 3, the reactive crystallization was performed against the solution containing impurity ions. Metal existence mole ratio in produced crystals was analyzed and metal ions initial uptake rate per unit seed surface area R was calculated. In case that nickel carbonate basics were used as seeds, R value was small and impurities uptake rate: R_I was about one fourth of target ions uptake rate: R_T. Whereas, in case of copper carbonate basic, R_I was half the value of R_T and metal ions were indicated to be easily taken in. Perhaps the reason is that copper carbonate basics are easy to uptake other metal ions and that they form needle-like crystals so uptake site per unit surface area can be enlarged. The centrifugation was performed against recovered crystals and the purity improvement was examined. The purity was improved by from 10 to 20 % for copper carbonate basics; however, no improvement was seen for nickel carbonate basics. Components that were not separated were thought to be taken into crystals. In addition, the effect of anions such as phosphate or borate ions to crystal growth was examined. Phosphate ions only roughed particles surface but the average particles size has not changed. Whereas, borate ions produced many fine particles and the average size becomes reduce in size with the increase of anion concentration.

In chapter 5, phenomena in the reaction tank were embodied by the numerical simulation. And from the results, the generality of this technology has been discussed and problems were clarified. In one of analyses, the numerical model of time variation of metal ions concentration in the reaction tank was designed. After that, from these data, parameters about the nucleation and the growth rate of spherical crystals were determined. And also, the method of separating metal ions selectively from the view of the difference of the uptake rate has been considered.

As can be seen above, a method of separating and recovering metal ions by reactive crystallization was devised. Against isolated metal ions, crystal sizes, forms and dispersing qualities were highly controlled by adapting this method. Against solutions containing impurities, particular metal ions uptake can be controlled to some extent. This environmental crystallization can be used after highly condensing metal ions via solvent extraction or electrolytic refining.

Contents

Chapter 1

Crystal engineering for the wastewater treatment

This thesis proposes the reactive crystallization for separating and recovering metal ions from the wastewater. In this prologue chapter, general statement about metal resources and metal wastewater treatment strategies is summarized as the preliminarily part. Also, the availability of recovered metals as materials is indicated by citing some examples.

1.1 Metal resources and metal wastewater treatment/strategies

Metal resources underground exist in finite amount as well as oils, and offshore government would take political measures such as increasing prices or regulating export quantum. Metals are mainly used in the industrial arena and discharged in the wastewater. Therefore, recycling metals that scattered on the ground can be one of effective procedures for utilizing metals in a sustainable way. Essential data related to the amount of production and deposition, the fatigue life and the cost of representative metals in 2010 period are summarized in **Table 1-1** [1]. From these data, some rare metals such as cadmium and strontium, and even base metals such as tin, zinc, also, novel metals such as gold and silver cannot be endured around 30 years in a trial calculation. Furthermore, some rare metals such as cobalt, nickel and selenium are so valuable that they cost several dozens of U.S. dollars per kilogram.

Especially in Japan, rare metal materials are dependent on offshore. And so, Resources and Energy Agency in METI: Ministry of Economics and Trade and Industry announced four strategies for rare metals in 2009 [2]. These consist of I protection of resource interests, II recycling/ recovery from used products or wastewaters, III development of alternative materials and IV stockpiling. And in this thesis, the main focus is on the second term, especially the efficiency of recycling. The process of metals recycling is wide-ranging. Metals are, for the most part, processed via the following practical treatment methods (**Table 1-2**) which have already been developed for water purification and metal recovery operations. Each wastewater treatment has some critical factors on the efficiency such as treatable kind of metals, metal concentration in the stock solution, facility cost, and tolerability to the pressure.

In this chapter, reviews on the various treatment technologies for metals removals have been presented. And in **Tables 1-2~3**, basic information, advantages and disadvantages of each wastewater treatment methods are summarized [3-7].

Table 1-1 Metals reserve protection ratios in 2010 (from Mineral Commodity Summaries 2011, USGS in the U. S.).

Metal	Unit	P [Unit/y.]	R [Unit]	R/P [y.]	[U.S.$/kg]
		Produce amount	Deposit amount	Fatigue Life	Cost
Cd	t	22,000	660,000	30.0	3.9
Co	t	88,000	7,300,000	83.0	46.3
Cu	kt	16,200	630,000	38.9	7.5
Au	t	2,500	51,000	20.4	42328.8
Pb	kt	4,100	80,000	19.5	2.3
Li	kt	25,300	13,000,000	513.8	-
Mn	t	13,000	630,000	48.5	0.008
Hg	kt	1,960	67,000	34.2	-
Ni	t	1,550,000	76,000,000	49.0	21.7
Rare earth	t	130,000	110,000,000	846.2	6.9
Se	t	2,260	88,000	38.9	77.2
Ag	t	22,200	510,000	23.0	626.1
Sr	t	420,000	6,800,000	16.2	0.04
Sn	t	261,000	5,200,000	19.9	1.8
Zn	kt	12,000	250,000	20.8	0.2

Chemical precipitation is the most generally applied treatment method for metals, particular for the wastewater that complex chemical compounds are not involved. This treatment removes metals such as copper, zinc, iron, manganese, nickel and cobalt in the form of almost complete hydroxide precipitates [3]. This method also includes coagulation precipitation, Fenton reaction, sulfide deposition, reduction precipitation and so on. Any above treatments enable to remove particular metals selectively by controlling solution's pH. However, in most cases, produced sediments are co-precipitates that contain many types of ions, and won't do for recycling materials. These precipitation methods are called the primary treatment and contribute to the rough treatment for the mass wastewater at the first stage of treatment flow.

Other treatments such as solvent extraction, ultra-filtrate, electro-deposition, ion exchange and

activated carbon adsorption are more suitable for the metal recycling. These methods are limited to somewhat small concentration drainage, however, the metal recovery rates are almost near 100 %, and this is the reason that they are called second or high-class treatments. Above all, the solvent extraction is primarily utilized for recovering metals because high concentration solutions can also be treated and particular metals can be recovered selectively and quickly by the difference of solvent solubility. This treatment has drawback on high cost solvents.

And the "environmental crystallization" is a word-formation that describes the crystallization treatment method for removing some materials from wastewater, air, groundwater, or other environment. Crystal engineering for the wastewater treatment doesn't seem to be utilized revolutionarily. However, this treatment method has some merits on the point of wastewater treatment and resources recovery, such as, I not producing sludge, II getting high purity materials, III saving energy, IV operating easily, and so on. This technology can treat a mass of drainage at one time, and desired metals might be recovered selectively.

Table 1-2 Basic information of metal treatment technologies.

Solvent extraction
Solvent extraction involves extracting a particular metal from liquid-liquid system. This reagant reacts with the heavy metal ion of interest and converts it to a form soluble in appropriate organic reagant.
Ion exchange
Ion exchange is a reversible chemical reaction and the metals removal is accomplished by the exchange of ions on the resin. When the resin is saturated, it must be regenerated with an acid or a base to remove the metal ions from resin bed.
Membrane operation
The basis of this process is letting the solution flow under pressure through an appropriate membrane and withdrawing permeated water at atmospheric pressure.
Activated carbon adsorption
Metal ions accumulate and adsorve to the layer of a negative charged activated carbon particle.
Electrochemical operation
In elecrolytic recovery, a direct current is passed through aqueous solution containing metal ions between cathode plates and insoluble anodes.

Table 1-3 Advantages and disadvantages of metal contaminant removal processes.

Precipitation and coprecipitation	**Solvent extraction**
Advantages	***Advantages***
>Low cost for high volume	>High degree of recovery efficiency
>Simple reaction and equipment	>High degree of ions selectivity
>Rather high degree of removing efficiency	>Simple operation and equipment
>Treatable a large amount at once	>Treatable a large amount at once
Disadvantages	***Disadvantages***
>Chemical additions required	>High cost of solvents
>High-water-content sludge is disposed of	>Limited ability to concentrate metals
>Not efficient for small flow	>Some solvents are harmful
>Not for recycling but for removing	
Ion exchange	**Membrane operation**
Advantages	***Advantages***
>Enable to operate on demand	>Almost all contaminant are removed
>High degree of recovery efficiency	>Low effluent concentration possible
>High degree of ions selectivity	>Enable to coordinate the degree of purifying
>Large variety of specific resins available	>Free from secondary pollution
Disadvantages	***Disadvantages***
>Loading capacity	>Loading capacity
>High cost of operation	>High capital and operation costs
>Spent regenerant must be disposed of	>High level of pretreatment required
>Not feasible for high concentration	>Membranes are prone to fouling
Activated carbon adsorption	**Electrochemical operation**
Advantages	***Advantages***
>Enable to oerate on demand	>High degree of recovery efficiency
>Relatively insensitive to flow variations	>High degree of ions selectivity
>Low effluent contaminant level possible	>Low effluent concentration possible
>High degree of ions selectivity	
Disadvantages	***Disadvantages***
>Loading capacity	>Loading capacity
>Slow operation: adsorption	>High capital and operation costs
>Spent regenerant must be disposed of	>Not feasible for high concentration
>Not feasible for high concentration	>Time-consuming operation

1.2 Industrial metal wastewater and the efficient treatment

Most industrial wastewater contains primary product materials, by-products and residues produced by manufacturing chelate agents, dispersants, and medicinal agents and so on. Because many types of chemicals are immixed in the wastewater, it is hard to treat the wastewater only by one technology, and ordinarily, several types of water treatment technologies are used in combination. And it is important to examine the position of technologies in the total treatment flow. In **Table 1-4**, representative metals contained in the drainage in each industrial section are summarized [3]. According to this table, many types of metals seem to contain in the same drainage. Then, examples of metals composition ratio in wastewater from the automobile industry are described in **Table 1-5**. From these tables, the composition of wastewater is indicated to be different even in the same industry. And contents in the drainage and process flow-sheets for treating metal wastewater vary based on wastewater. There is no wastewater that is the same. The common point is that concentrated substances are removed together by the primary treatment at first. As for technologies, the coagulating sedimentation method is often used to remove metals and remaining fine particles are filtrated after that, as shown in **Fig. 1-1**. Metals wastewater treatment methods in some industries are described below [8-9].

In steel industries, many types of metallic substances: such as iron, manganese, nickel, and zinc are discharged. COD sources like coal powder, phenols, cyanogens, oil are also contained in the wastewater. When removing ammonia, an ammonia stripping facility is placed in the previous step. Substances other then metals discharged from coke plants are often treated by activated sludge treatment. After removing bulk of metals by sedimentation, filtration is often post-processed.

In metal industries, metallic substances related to the business: copper, zinc, manganese, nickel, lead are mainly discharged. Especially, the wastewater from metal-processing plants and plate processing plants are often treated by the alkaline precipitation. Metal ions concentration in the drainage is so high that the reaction system is effective for the treatment. After removing the bulk of metals by sedimentation, filtration is often post-processed in common with steel industries.

In machinery industries, as well as metals such as nickel, zinc, or copper, surface acting agents used for the washing operations (for example, 2-amino ethanol, poly-oxyethylene) are much contained in the wastewater. The flotation method is applied to the oil treatment, and suspended solids and CODs are mainly treated by the filtration or the activated carbon adsorption in the final process flow. In the semi-conductor manufacturing process, ammonia water is used in the

washing operation and the ammonia stripping or the system combined nitrification tank and denitrification tank is often applied in the early stage.

In most industries, activated sludge method and coagulation sedimentation method are installed for removing main substances. For treating particular contaminant speciation (ammonia, oils, CODs, BODs and so on), technology like aeration, screening, ammonia stripping or floating separation is prefixed. And filtration or activated carbonate adsorption is often used in final stage.

Table 1-4 Metals contained in the drainage in major industries.

Industry / Metal	Al	Ag	As	Cd	Cr	Cu	F	Fe	Hg	Mn	Pb	Ni	Sb	Sn	Zn
Pulp, paper mills, paperbord, building paper, board mills					•	•			•		•	•			•
Organic chemicals, petrochemicals	•		•	•	•		•	•	•		•			•	•
Alkalis, chlorine, inorganic chemicals	•		•	•	•		•	•	•		•			•	•
Fertilizers	•		•	•	•	•	•	•	•	•	•	•			•
Petroleum refining	•		•	•	•	•	•	•			•	•			•
Basic steel works, foundries			•	•	•	•	•	•	•		•	•	•	•	•
Basic non-ferrous metals-works, foundries	•	•	•	•	•	•	•		•		•		•		•
Motor vehicles, aircraft-plating, finishing	•	•		•	•	•			•			•			
Flat glass, cement, asbestos products, etc.					•										
Textile mill products					•										
Leather tanning, finishing					•										
Steam generation power plants					•										
Note: plastic materials, synthetics; meat products; dairy products; fruits and vegetables; grain milling; beat sugar ; beverages; and livestock feedlot industries have no heavy metal discharges.															

Table 1-5 Examples of metals composition in the automobile industry wastewater.

Ex. 1	Fe	Cr	Mo	Mn	Nb	Ti
mass [kg]	346.98	1.78	0.71	5.33	0.11	0.11
ratio [%]	97.7	0.5	0.2	1.5	0.0	0.0

Ex. 2	Fe	Nb	Co	Cu	Sn	Zn	Pb	Ni
mass [kg]	0.05	-	0.001	0.59	0.009	0.11	0.11	0.001
ratio [%]	6.1	<0.01	0.1	67.4	1.0	12.4	12.8	0.1

In **Figs. 1-2~4**, examples of metal recycling technologies from wastes are introduced. Actual flow-sheets are a bit complicated. The reason is that many types of substances are contaminated in the wastewater, and each contaminant should be separated and treated fairly. In terms of the early stages of these charts, various measurements like acid treatment, reduction, magnetism separation are used for extracting and separating metals from wastes. Then, high-class treatment methods like ion exchange, solvent extraction or electrolysis are installed in the final stage.
Given the introduction of crystallization method in metal recovery, one strategy is replacing by the coagulation sedimentation equipment, and another is applying to highly-isolated single metal solution by the extraction or the electrolysis. A small amount of impurities are contained in the treated solution, and determining the impurities effect on the crystals growth is essential. By adding the crystallization in the process, qualities of the metal recycling will be improved.

Actually, various innovations about the wastewater management are created for treating metal ions effectively. First, planning to simplify the process flow-sheets leads to reduce running cost and secure the extra space in the long run. For example, installation of composite-type system that treats multiple substances at one time is effective. And also, introducing treatment technologies that are appropriate broad-ranging substances in advance enables to lead to a favorable treatment even if any chemicals will be limited in the future. Secondly, heavy metals are preferable to be treated individually and densely because concentrated solutions are easy to extract or precipitate and the management cost can be controlled. For example, in the plating companies, cyanogens and chromium systems are desired to separate in the treatment. Moreover, the improvement of each wastewater technology and placing the right technology in the right site

will also contribute to the efficient management.

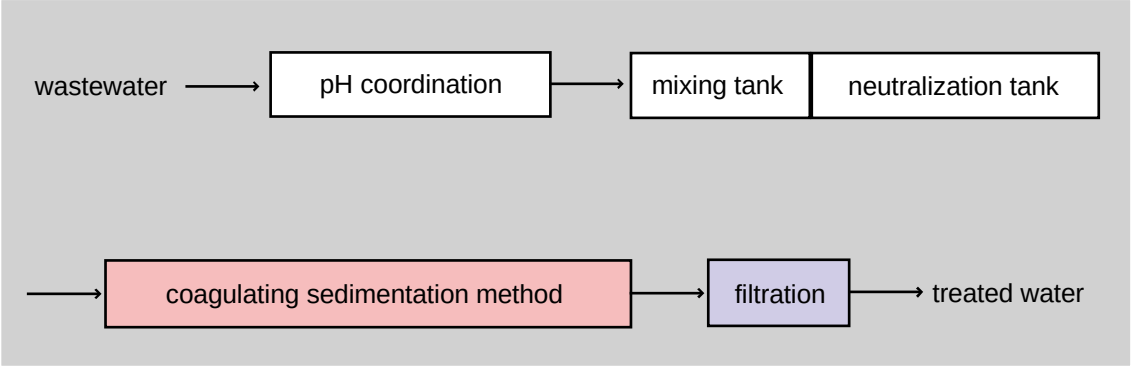

Fig. 1-1 A brief flow-sheet of metal wastewater treatment in industries.

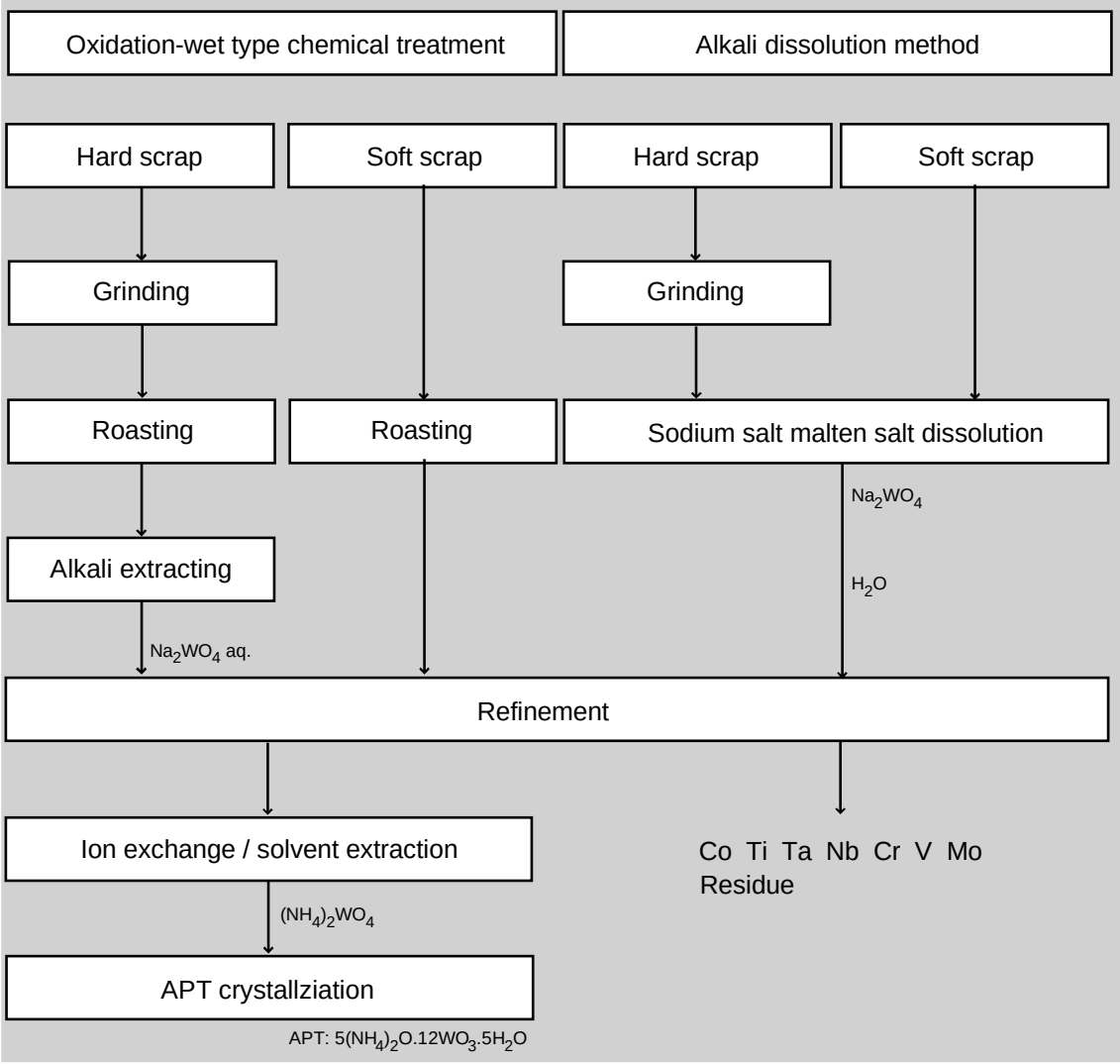

Fig. 1-2 Modernistic tungsten recycling process.

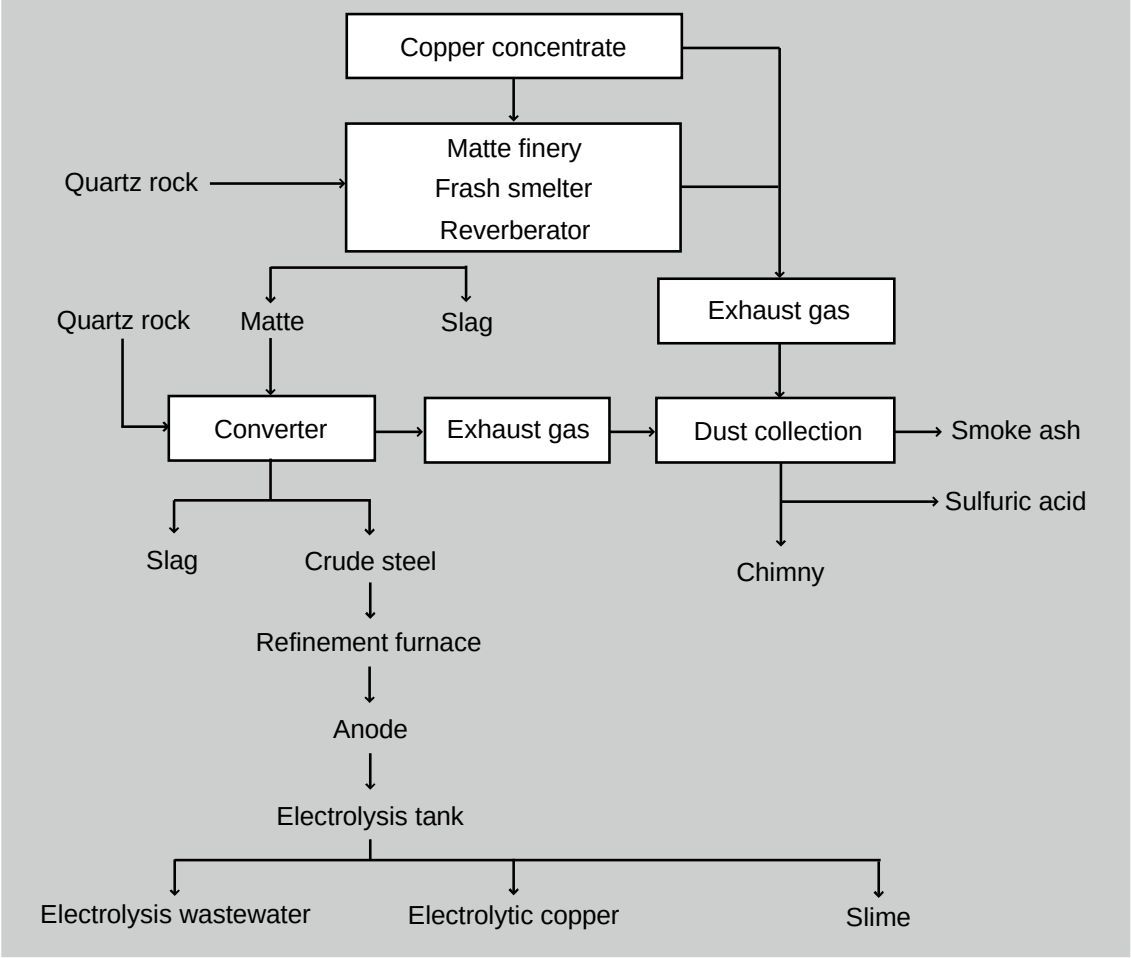

Fig. 1-3 An example of copper refining process.

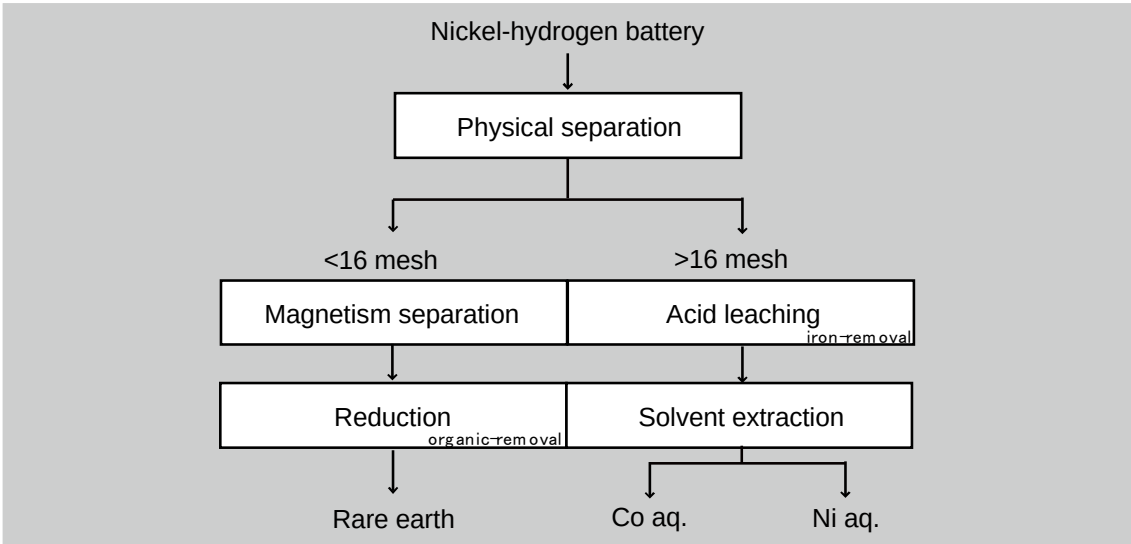

Fig. 1-4 An example of nickel-hydrogen battery recycling process.

When considering the process selection, the following would be the main factors: contaminant speciation, influent and effluent concentration, levels of dissolved solids, available treatment system size, and flow variability [6]. Treatment costs are, of course, always considered; they should be minimized while technical objectives are satisfied. And it is necessary to determine the treatment object; whether it is desirable to remove only one or two contaminants using precipitation or selective sorption or to remove essentially all contaminants by the membranes.

1.3 Beneficial materials recycling by the reactive crystallization

This thesis focused on divalent metals such as cobalt, copper, manganese, nickel and zinc in the situation of separating and recovering from the metal wastewater. Metals were chosen from the view of the low water-solubility of products, weak toxicity, tight fatigue life, valuable price and large demand. Metal carbonates, oxides or hydrates are utilized in a wide range of businesses as materials, such as plating solvents, or catalysts [10]. And they are often desired to be recovered spherical because of their handiness from the standpoint of coating on the surface of materials or valuating their sizes and the dispersibility.

Nickel carbonate basics are used in the electro-plating, in the preparation of nickel catalysts and as ingredients in ceramic colors and in glazes. Copper carbonate basics are used as a source of copper, pigments, and in jewelries. Zinc oxides are used in pigments, in ceramic glazes, and in opaque glass. And they are also used in the manufacture of magnetic ferrites and other specialized ceramics. Recently, they are developed for cosmetics as skin sunscreen ingredients. Manganese carbonates are commonly contained some iron and calcium. They are used as special steels, electrodes, and lithium batteries and so on. Silver carbonates are used to produce iridescent stains or sheens on glazes. And they are also used as a component of glass stains.

In crystallization technology, operation conditions such as supersaturation, temperature, pH, impurities and kind of solvents affect largely on crystals sizes, shapes, or habits [11-16]. As the example of effecting on crystal growth, some have presented phosphate and fluoride experiments as follows [12-16]. For recovery of phosphate, hydroxyapatite (HAP: $Ca_{10}(PO_4)_6(OH)_2$) and magnesium ammonium phosphate (MAP: $MgNH_4PO_4$) have been utilized as recovered materials from wastewater. Phosphate resources often exist as calcium phosphates, and MAP can be used as a slow-acting fertilizer. Experiments were operated on a basis of seed growth. Selection of suitable substances as seeds was required such that crystals are easily grown and fixed on the surface of the seeds. As seeds of HAP, Jordan phosphate mineral ores were selected because of having a relatively similar component. As seeds of MAP, crushed MAP crystals or MAP fine crystals produced in the equipment are used as seeds. Supersaturation was indicated to be a factor for influencing the nucleation and the crystal growth kinetics. The ideal condition of supersaturation for them has been found by changing the concentration of raw materials (supersaturtin ratio was set to 2.0-8.7) and pH (7.7-9.2). The optimum crystal growth condition was evaluated from the relationship between the phosphate recovery rate and the operation

condition. Then, the effect of phosphate loading on the phosphate recovery rate was determined. Especially, for MAP recovery, the optimum supersaturation ratio was set to 3.3 and pH to 8.6, considering the recovery efficient. When the supersaturation ratio of MAP solution was below 3.7, the recovery ratio of phosphate was low because a lot of fine crystals have been generated. For controlling the nucleation and growth speed, the relationship between the phosphate loading [g m^{-1} day^{-1}] per unit surface area of MAP crystals and the phosphate recovery rate [g m^{-2} day^{-1}] per unit surface area of crystals has been investigated. The phosphate recovery rate improved with the increase of the phosphate inflow loading, however, the maximum rate of recovery was almost constant at 13 g m^{-2} day^{-1}. In other words, the recovery rate has a maximum limitation, and excess load would contribute to producing fine crystals. The growth rate [m day^{-1}] was obtained by dividing the phosphate recovery rate by the crystal density, i.e., the growing rate also has a maximum limitation. Besides, when calcium ions were existed in the stock solution as impurities, their concentration has affected MAPs' seed growth. At lower concentration: Ca/Mg~0.2, impurities promoted the seed growth; whereas, at higher concentration: Ca/Mg~0.3, impurities inhibited the growth because they tend to fill seed airspace and the growth rate was diminished.

Concerning the fluoride ions recovery, fluorites (CaF_2) were utilized as seed crystals, and the most appropriate operation condition to produce the desired crystals was determined, operating the reactive crystallizer. The influence of pH (2.6-12.8) on the fluoride ion recovery rate was determined. The maximum recovery rate was observed in pH=7~8, and in pH≤5, incomplete precipitates were produced. In pH≥12, calcium hydrates generation inhibited the fluoride removal. The existence of metal ions was indicated to inhibit the crystallization rate. Also, phosphorous ions were indicated to act comparable to calcium ions against MAP: At lower concentration, the seed growth was promoted, while at higher concentration; the growth rate was prone to be small.

In recent, controlling of gold nano-particle has been performed by the reduction crystallization [17]. To control the size of gold particles, double-jet experiment was performed. Effect of the stock solution feeding rate (at this time, the feed amount was the same in each condition) and the feeding amount of reducing agent, AsA: ascorbic acid and basic ingredient, $HAuCl_4$ aqueous solution on the PSD: the particle size distribution and the C.V.: the coefficient of variability was investigated. TEM: transmission-type electron microscope images of gold particles obtained in the double-jet experiment are shown in **Fig. 1-5**. The influence of the stock solution feeding rate and

the feeding amount of AsA and $HAuCl_4$ on obtained particles' mean size and the C.V. are shown respectively in **Fig. 1-6 [A] and [B]**. In the result, grown particles' mean size increased with the decrease of the feed rate (**Fig. 1-6 [A]**). The value of C.V. was approximately 0.1 and particles were mono-dispersed. From **Fig. 1-6 [B]**, average size of gold particles was found to be increased with the increase of the feed amount of $HAuCl_4$, and 150-400 nm particles were obtained. Obtained particles were mono-dispersed (C.V. was around 0.1 in any condition). Gold nano-particles were precipitated as slurry just after the preparation; however, particles larger than 100 nm were obtained about one day after. The appearance of precipitates was different by particle size. Particles smaller than 200 nm were easily agglomerated, whereas, particles larger than 200 nm were precipitated and coated bottom of the vial container. SEM images of 100 and 300 nm precipitations are shown in **Fig. 1-7**. As seen in **Fig. 1-7**, although 100 nm particles massed together to change their size and shape from those of immediately after the preparation, 300 nm particles maintained their size and shape. The mechanism of the precipitation of 100 and 300 nm particles are illustrated respectively in **Fig. 1-8**. Based on the results above, following methods are effective for improving precipitations. For particles smaller than 200 nm, it can be effective to dilute the slurry for restraining the agglomeration, and for particles larger than 200 nm particles, applying energy by the ultrasonic for weakening the connection between particles is beneficial.

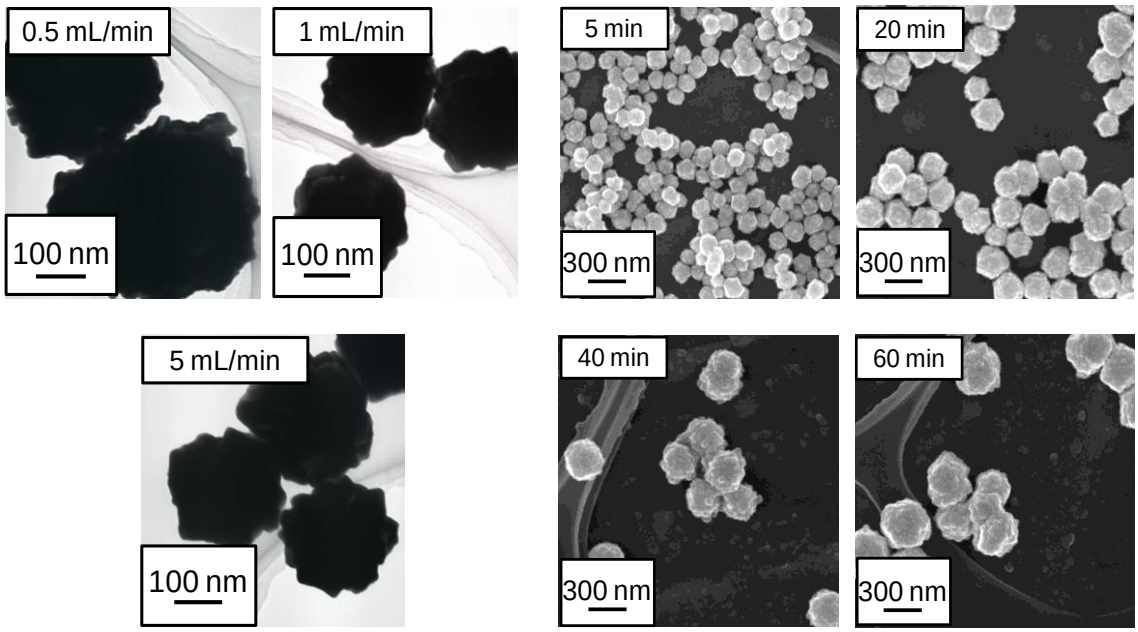

[A] Influence of the feeding rate [B] Influence of the feeding amount

Fig. 1-5 TEM images of gold particles obtained by the double-jet feeding method.

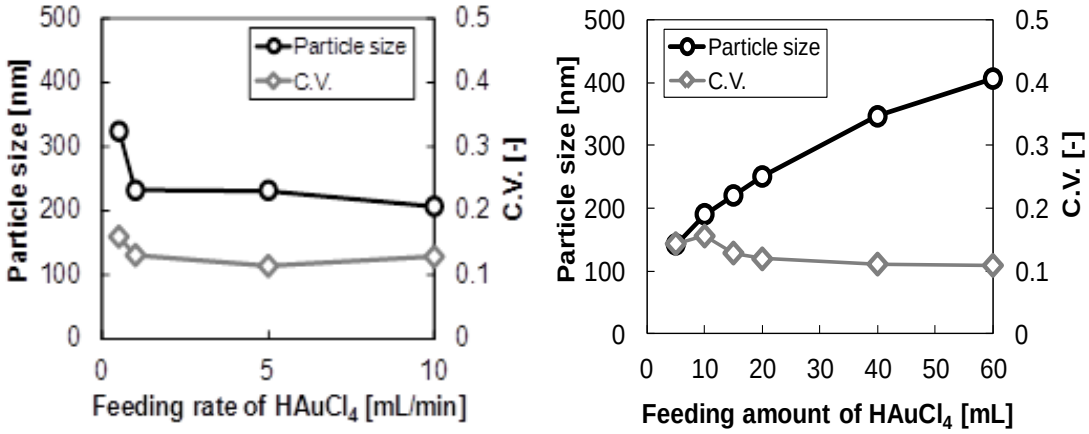

[A] Influence of feeding rate [B] Influence of feeding amount

(Feed amount of $HAuCl_4$: 20 mL, AsA: 10mL) (Feed rate of $HAuCl_4$: 1 mL min^{-1}, AsA: 0.5 mL min^{-1})

Fig. 1-6 Mean size and C.V. of gold particles obtained by double-jet feeding method.

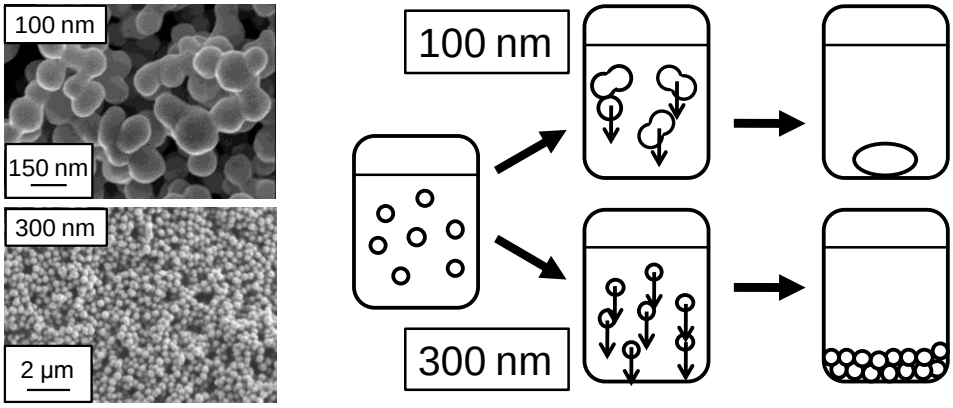

Fig. 1-7 SEM images of gold precipitations. Fig. 1-8 Mechanisms of gold precipitation.

Strontium carbonate ($SrCO_3$) particles with micro and nanomtreter size can also be controlled by changing feeding conditions. In the experiments on mixing strontium sulfate and sodium carbonate solutions, the influence of the feed pH on PSD and the aspect ratio of strontium carbonate have been examined [18]. Stock solutions were fed at 0.010 L min^{-1} for 10 min., and after that, agitated for 10 min. Obtained suspension was sampled and filtered by 0.1 μm membrane filter. Single-jet reaction crystallization process was proposed to clarify the possibility of controlling aspect ratio of strontium carbonate fine particles. Strontium solution was fed to the carbonate ground solution, to investigate the influence of initial pH on the quality of $SrCO_3$. **Fig. 1-9** shows SEM photographs obtained in various pH conditions. Also, the variation of aspect ratio

of crystals with the initial pH was examined (**Fig. 1-10**). From these results, it was clarified that superasaturation and initial pH could control aspect ratio of $SrCO_3$ fine particles to some extent.

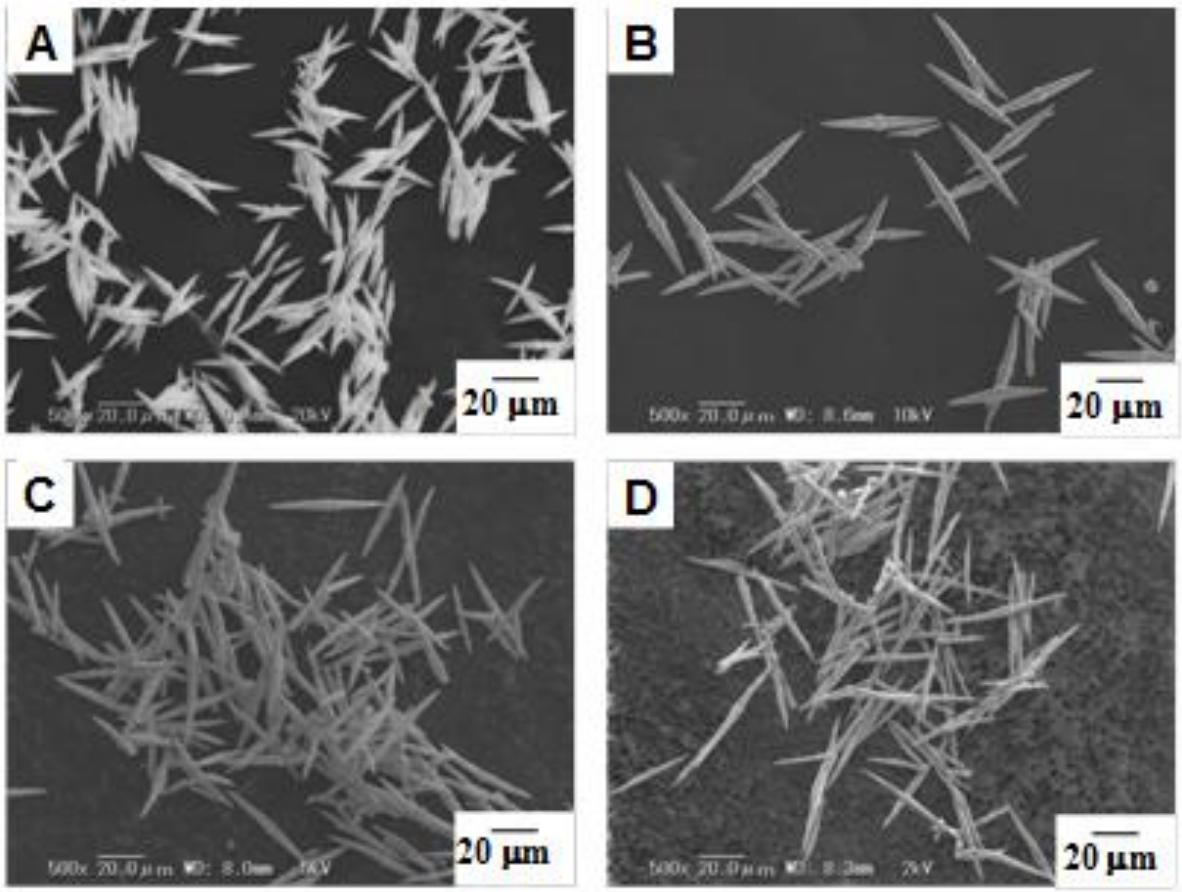

Fig. 1-9 SEM images of needle-like $SrCO_3$ particles obtained in pH-controlled reactive field [A] pH 6.3, [B] pH 9.0, [C] pH 10, [D] pH 11.

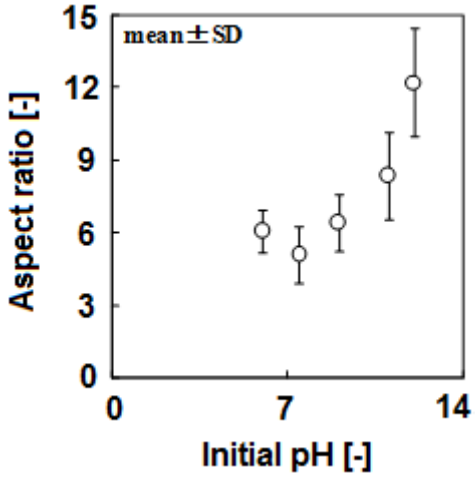

Fig. 1-10 The variation of obtained particles' aspect ratio with the initial pH.

Some researchers have evaluated the manganese carbonates and zinc oxides aspects from many viewpoints. Didier et al. [19] have performed the hydrolysis reaction for obtaining zinc oxides, and at higher precursor concentration, they have found that no aggregation occurs and tiny single particles are obtained. Su et al. [20] have examined the effects of reaction temperature, pH, or the raw solution concentration on the morphology and size of manganese carbonates. With reducing the reaction temperature, the dispersibility of obtained particles became better and their shapes also gradually trended towards unification and their size became larger. Also, the morphology and size of particles had not been affected obviously by the ingredient concentration.

Sugimoto et al. [21-24] have proposed that the establishment of technology that obtains mono-dispersed colloidal particles is of obvious importance in industries including catalysts, ceramics, pigments, pharmacy, photographic emulsion and so on. There are two noteworthy advantageous conditions for constructing mono-dispersed particles. One is that separating the nucleation and growth terms definitely. For accomplishing this, the nucleation after the growth term must be avoided, and the uniform growth time must be provided against wide range of particles as possible. The other point is that restraining agglomeration. Controlling the operation condition such as the supersaturation ratio, the feeding rate, or the initial pH can be one strategy. And adding fluctuation by such as ultrasound, bead-mill to the reactive solution can also be a strategy for keeping particles mono-disperse.

1.4 Metal wastewater treatment in foreign countries

In the United States and EU regions, technologies for the wastewater treatment tend to be influenced by some laws or regulations.

In the United States, CWA: Clean Water Act has been enacted in 1972, designed to regulate the discharge of wastewater and to set the water quality criteria. NPDES is the institution for the enforcement of CWA and has seven programs [25]. Guiding principles and standards are classified roughly in terms of four [26, 27].

A. BPT: Best Practicable Control Technology Currently Available, Technical standard instituted for the water quality preservation. Ordinarily, "best technology" is calculated from the others capability average of belonging to the same industry.
B. BCT: Best Conventional Pollutant Control Technology. This technology standard has to be practical on construction/operation cost and high cost- benefit performance.
C. BAT: Best Available Technology Economically Available. The best economically available technology should be selected from the most effective treatment technologies.
D. NSPS: New Source Performance Standards. New equipments have to be controlled the discharge of contaminated substances more effectively than before.

Meanwhile, in the EU, The Sixth Environmental Action Programme was proposed in 2001 by the Commissions of the European Committees. Integrated Pollution Prevention and Control/ IPPC protocol (96/61/EC) was placed aiming for minimizing the discharged contaminant from the industrial facilities in the EU region [28]. Discharge standard and operation condition based on BAT are approved in IPPC protocol. Furthermore, in 2000, the EU Water Framework Directive (WFD, 2000/60/EF) came into force with the aim to protect and improve the quality of EU waters [29]. BATs provided in each industry sector are indicated in the BAT reference document (BREF note). BREF is the index value related to the adequate certification requirement based on BAT and these indexes are determined by the regulating authority in affiliated countries.

The way of selection of appropriate technology for the wastewater treatment is often based on the screening operation (**Fig. 1-11**) [29-31]. The destination for the effluent is a critical factor in the choice of technology for wastewater treatment. A number of parameters should be considered

when choosing the appropriate technology. These can be grouped as economic, institutional and political, climatic, environmental, land availability, sociocultural, and other local ones. Once these factors have been taken into account the most cost-effective system should be selected, unless the population being served is willing to pay more. To screen processes, three major levels of analyses should be considered [29]. First, required effluent quality should be undertaken. Second, a number of aspects that could restrict the applicability of some processes, as mentioned above should be examined. Third, a cost effectiveness analysis should be undertaken so that the optimum economically viable solution can be identified. In developing countries, the criterion of required effluent quality is considered after the other two criteria.

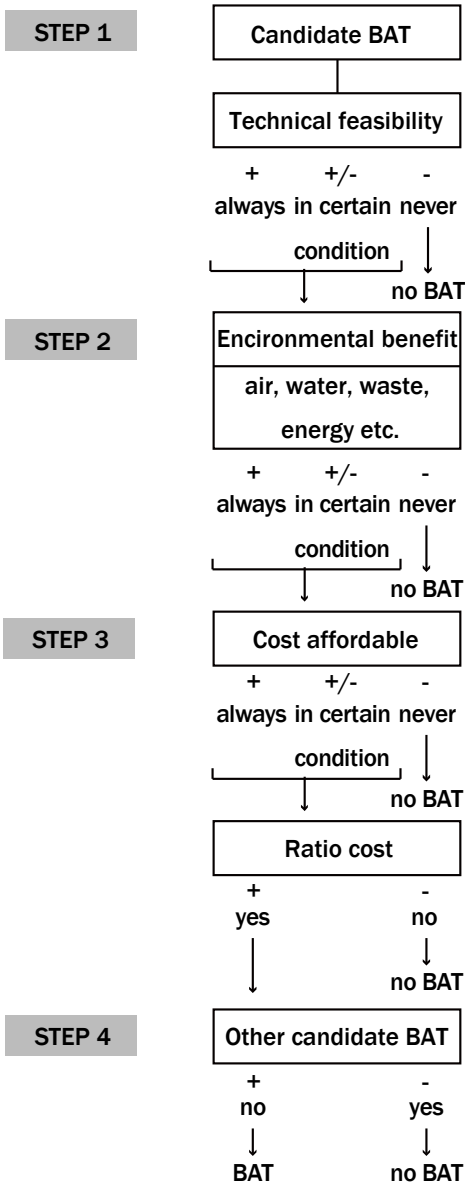

Fig. 1-11 Procedure for selection of BAT

And **Fig. 1-12** indicates the panoramic process of BAT extraction.

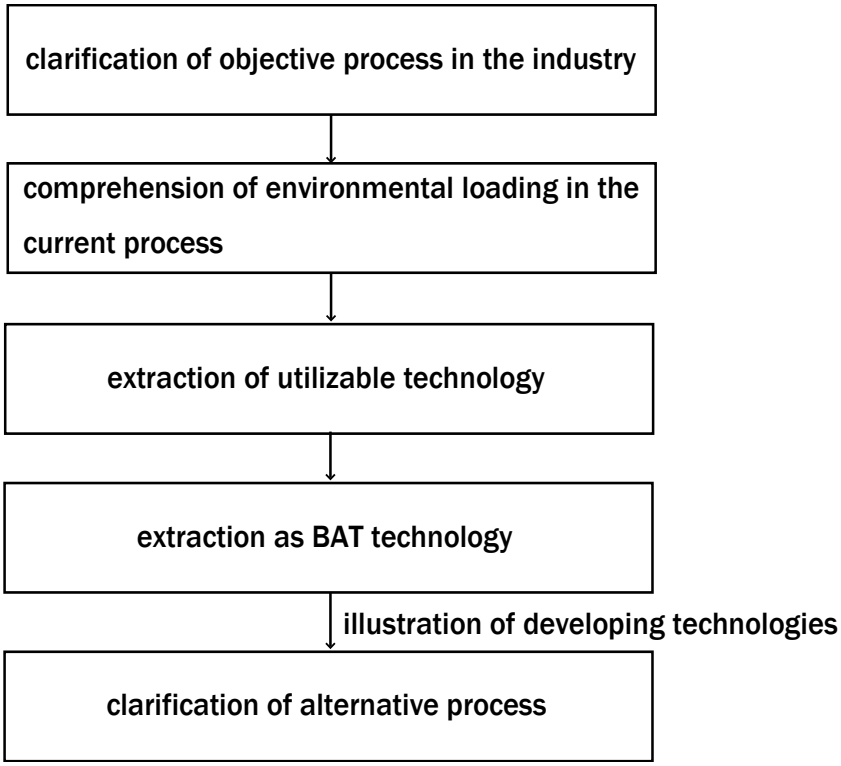

Fig. 1-12 Process of BAT extraction

BREFs do not prescribe techniques or emission limit values, however, the BREFs will inform the interested parts about what may be technically and economically available to industry in order to improve their environmental performance and consequently improve the whole environment [31].

References

[1] Mineral commodity summaries 2011, 2011, *U. S. Geological Survey (USGS).*

[2] Strategies for rare metal securement, 2009, *Japan Ministry of Economics and Trade and Industry (METI).*

[3] J. G. Dean, F. L. Bosqui and K. L. Lanouette, 1972, Removal of heavy metals from industrial wastewater, *Environ. Sci. Technol.*, **6 (6)**, 518-522.

[4] K. H. Lanouette, 1977, Heavy metals removal, *Chem. Eng.*, **84 (21)**, 73-80.

[5] T. Maruyama, S. A. Hannah and J. M. Cohen, 1977, Metal removal by physical and chemical treatment processes, *J. Water Pollut. Control Fed.*, **47 (5)**, 962-975.

[6] D. Clifford, S. Subramonian and T. J. Sorg, 1986, Removing dissolved inorganic contaminants from water, *Environ. Sci. Technol.*, **20 (11)**, 1072-1080.

[7] Carl E. Janson, Robert E. Kenson and Lawrence H. Tucker, 1982, Treatment of heavy metals in wastewaters, *Environ. Prog.*, **1 (3)**, 212-216.

[8] Heisasei kaiiki ni okeru mizukannkyomokuhyo minaoshito nikannsuru doukochousa houkokusho, 2008, *Japan association of industries and environment.*

[9] Electronic Journal Archives, 2011, *Electronic Journal*, **78**.

[10] A dictionary of mining, mineral, and related terms, 1997, *American geological institute*.

[11] R. W. Peters and L. Shem, 1983, Separation of heavy metals: removal from industrial wastewaters and contaminated soil, *Illinois.*

[12] Y. Shimizu and I. Hirasawa, 2012, Recovery of ionic substances from wastewater by seeded reaction crystallization, *Chem. Eng. Tech.,* **35 (6)**, 1051-1054.

[13] K. Shimamura, A. Mizuoka, H. Ishikawa and I. Hirasawa, 2008, Development of a process for the recovery of phosphorus resource from digested sludge by crystallization technology, *Water Sci. Technol.*, **57**, 451.

[14] I. Hirasawa, S. Kaneko, Y. Kanai, S. Hosoya, K. Okumura and T. Kamahara, 2002, Crystallization phenomena of magnesium ammonium phosphate (MAP) in a fluidized-bed-type crystallizer *J. Cryst. Growth*, **237**, 2183.

[15] S. Ishizuka, S. Sato and M. Shibata, 1998, *14th Int. Symp. On Industrial Crystallization.*

[16] K. Shimamura, I. Hirasawa, H. Ishikawa and T. Tanaka, 2006, Phosphorous recovery in a fluidized bed crystallization reactor, *J. Chem. Eng. Jpn.*, **39**, 1119.

[17] S. Kida, M. Ichiji, J. Watanabe and I. Hirasawa, Shape and PSD control of nanometer Au used as particle gun, 2012, *BIWIC 2012, Int. Workshop Ind. Cryst., 19th.*

[18] I. Hirasawa, C. Cha, Y. Ohtomo and R. Noda, Shape and size control of strontium carbonate fine particles by reactive crystallization, 2012, *BIWIC 2012, Int. Workshop Ind. Cryst., 19th.*

[19] Didier J., Jean G., Noureddine J. and Fernand F., 1995, Submicrometer zinc oxide particles: elaboration in polyol medium and morphological characteristics, *J. Mater. Res.*, **10(1)**, 77-83.

[20] Su H. F., Qu X.,Wen Y. X., Tong Z. F., Li X. H., 2008, Morphology control in preparation process of spherical manganese carbonate particles, *Chin. J. Process Eng.*

[21] T. Sugimoto, Preparation of monodispersed colloidal particles, 1987, *Adv. Colloid Interface Sci.*, **28**, 65-108.

[22] T. Mikami and I. Hirasawa, 2010, Quality-controlled reactive crystallization of $SrSO_4$ to produce high- valued chemicals, *Chem. Eng. Tech*., **33 (5)**, 775-779.

[23] T. Mikami and I. Hirasawa, 2010, Polyelectrolyte-assisted reactive crystallization of $SrSO_4$ to obtain monodispersed nano/micro particles, *Chem. Eng. Tech*., **33 (5)**, 797-803.

[24] T. Mikami, Y. Takayasu, J. Watanabe, I. Hirasawa, 2011, Influence of polyethyleneimine addition on crystal size distribution of Au nanocrystals, *Chem. Eng. Tech*., **34 (4)**, 583-586.

[25] EPA. Summary of the Clean Water Act in EPA website.
http://www.epa.gov/lawsregs/laws/cwa.html

[26] EPA. Effluent Limitation Guidelines and Standards in EPA website.
http:// cfpub.epa.gov/npdes/techbasedpermitting/effguide.cfm

[27] EPA. NPDES Glossary in EPA website.
http://cfpub.epa.gov/npdes/glossary.cfm?program_id=0#B

[28] Council Directive 96/61/EC concerning integrated pollution prevention and control, 1996.

[29] L. Hoibye, J. Clauson-Kaas, H. Wenzai, H. F. Laesen, B. N. Jacobson and O. Dalgaard, 2008, Sustainability assessment of advanced wastewater treatment technologies, *Water Sci. Technol*., **58 (5)**, 963-968.

[30] K. P. Tsagarakis, D. D. Mara and A. N. Angelakis, 2001, Wastewater management in Greece: experience and lessons for developing countries, *Water Sci. Technol*., **44 (6)**, 163-172.

[30] European IPPC Bureau,
http://eippcb.jrc.es/about/more_information.html

[31] R. Nowosielski, A. Kania and M. Spilka, 2008, Integrated recycling technology as a candidate for best available technologies, *Arch. Mater. Sci. Eng.*, **32(1)**, 49-52.

Chapter 2

Controlling metal substances recovery by the reactive crystallization

In this chapter, mono-disperse experiments were performed in manganese carbonate and zinc oxide by changing some crystallization condition: the initial pH, the feed rate, the feed concentration, and so on. As the preparatory for experiments, the introduction for the reactive crystallization and the measurement detecting metal ions concentration were summarized.

2.1 Introduction to carbonates and hydrates crystallization

The primary reaction in this study is described as the following reaction equation (Eq. 2-1): metal carbonates have been produced by mixing a metal sulfate solution with a sodium carbonate solution. Metal hydroxides or metal oxides were produced in the basic circumstance.

$$MSO_4 + Na_2CO_3 \rightarrow MCO_3 + Na_2SO_4 \quad (2\text{-}1)$$

The reactive crystallization is much related to hydroxide solubility products (K_{sp}). Here, K_{sp} is the equilibrium constant and the fundamental equilibrium in water is followed by the law of mass action (Eq. 2-2, 3). When the K_{sp} value is small, materials are present as solids, and this reaction is effective in being the sulfate K_{sp} large and in being the carbonate K_{sp} small [1-2].

$$M^{n+} + nOH^- \leftrightarrow M(OH)_n \quad (2\text{-}2)$$

$$[M^{n+}][OH^-]^n = K_{sp} \quad (2\text{-}3)$$

Representative metal ions solubility products are shown in the following **Table 2-1**. When the solution initial pH is high, poor water soluble metal hydrates are arisen as precipitates. Next, the relationship between metal ions water solubility and pH is shown as following **Fig. 2-1** [3-7]. Many types of metals are found to be precipitated in the basic circumstance. The pH that leads to the

crystallization cannot be necessarily coincident with this graph because crystals are not always formed when products have poor water-solubility. For example, zinc ions are easily precipitated at pH=10, however, they do not form crystals but amorphous. Therefore, it is necessary to determine the pH range they crystallize individually. In this study, solutions of sodium hydrate and hydrochloric acid are selected as pH adjusters.

Table 2-1 Solubility products of metal hydroxides (from 291 to 298 K).

Hydroxides	K_{sp}	Hydroxides	K_{sp}
$Al(OH)_3$	1.1×10^{-33}	$Fe(OH)_3$	7.1×10^{-40}
$Ca(OH)_2$	5.5×10^{-6}	$Mg(OH)_2$	1.8×10^{-11}
$Cd(OH)_2$	3.9×10^{-14}	$Mn(OH)_2$	1.9×10^{-13}
$Cr(OH)_3$	6.3×10^{-31}	$Ni(OH)_2$	6.5×10^{-18}
$Cu(OH)_2$	6.0×10^{-20}	$Pb(OH)_2$	1.1×10^{-20}
$Fe(OH)_2$	8.0×10^{-16}	$Zn(OH)_2$	1.2×10^{-17}

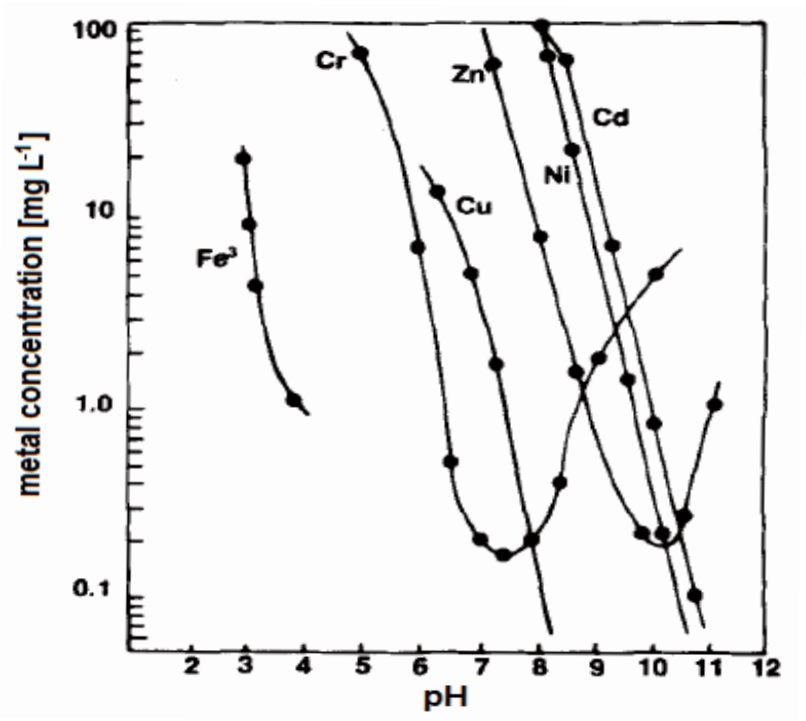

Fig. 2-1 The solubility curve of pure metal hydroxides as a function of pH.

Learning the behavior of pH is essential for discussing this reaction because pH continuously

changes during the reaction. One of factors that pH affects to the reaction is carbonate ions condition in the solution. Carbonate ions come in three types of ion figurations in the solution by changing pH, as shown in **Fig. 2-2** [8]. To precede the carbonate crystallizations stoichiometrically, providing sufficient amount of carbonate ions (CO_3^{2-}) is necessary. In addition, to let metal ions react 1:1 at all times, sodium carbonate concentration needs to be set considering at the lowest pH level of reactive solution during the reaction.

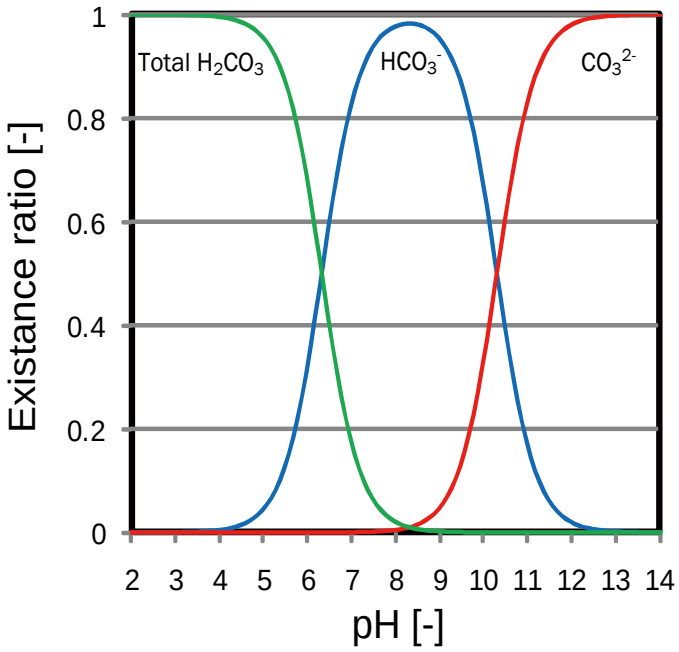

Fig. 2-2 Existence ratios about three forms of carbonate ions.

Initial pH is one of the most highly correlated factors with the crystallization. The pH ranges which can be obtained crystals by the reaction crystallization are different from kinds of metals. And so, experiments for determining pH ranges of crystallization were performed by the continuous stirred-tank reaction: CSTR method. **Fig. 2-3** represents pH ranges of metal substances crystallization. The boundary between crystals and amorphous seems rather vague. Then, **Fig. 2-4** represents crystals obtained by the CSTR treatment. Carbonates are transformed to hydrates or oxides as a result of basic treatment or drying process. And from these pictures, manganese carbonates, zinc oxides, silver carbonates are produced as typical crystals; while, nickel hydrates and copper oxides are produced atypical. Carbonates need to improve the dispersing quality for utilize as materials. And they also need to improve their shapes; in fact, they are desired to be spherical for the manufacturing process.

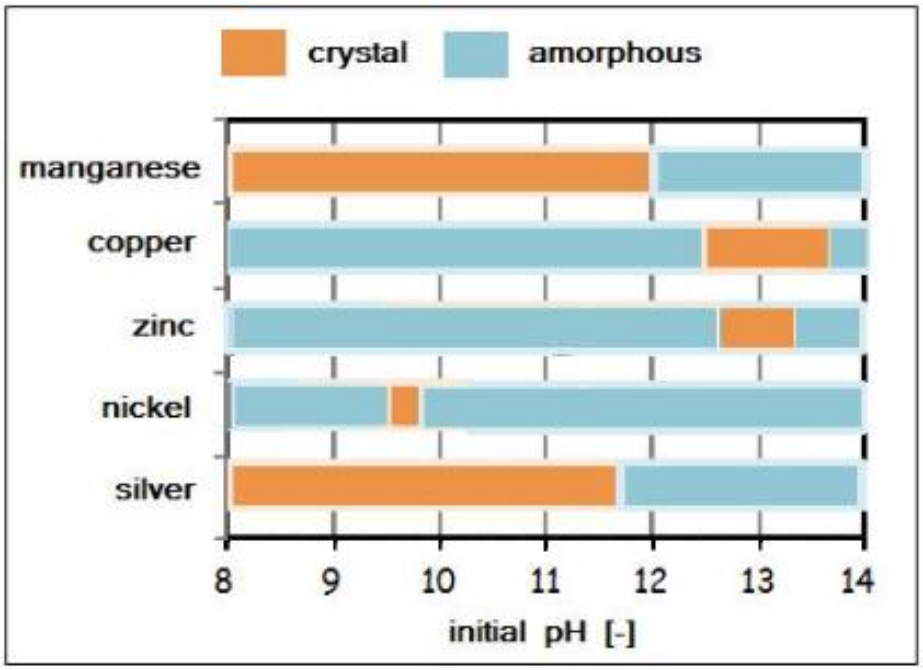

Fig. 2-3 Initial pH ranges of metal substances crystallization.

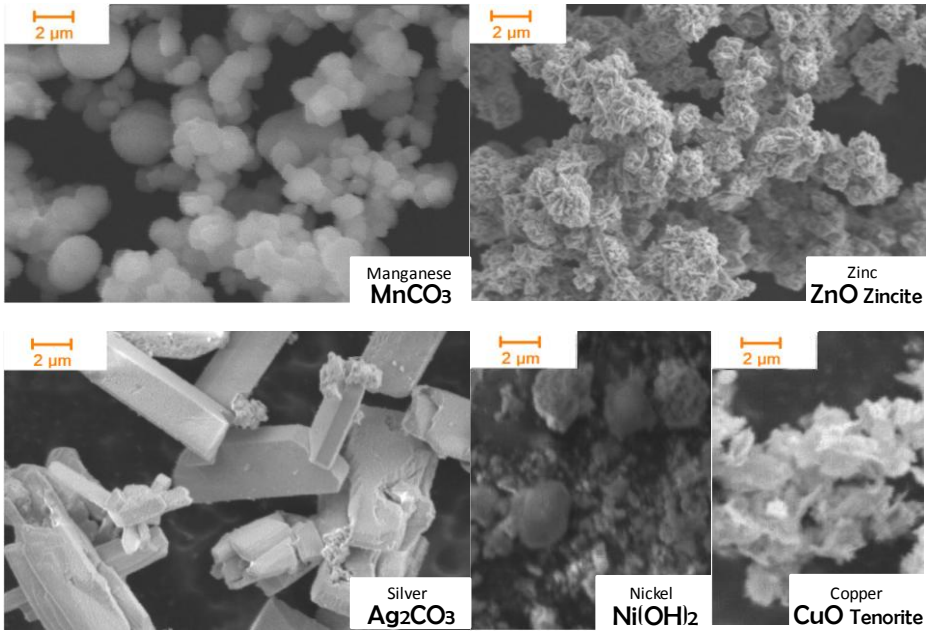

Fig. 2-4 Metal salt crystals obtained by the carbonate reactive crystallization.

The pH values in the reactive solution are changeable during the reaction, and so, pH changes were measured by operating 3 hours CSTR blank tests: metal ions in the feed solution was coordinated 1 000 mg L^{-1} and carbonate ions were large excess. Initial pH was set the value of

which metal ions crystallization was confirmed (about 13 in copper, and zinc, 9.7 in nickel and 7.7 in manganese experiment). From the pH changes results that have shown in **Fig. 2-5**, in most cases, solutions pH become constant near 10. In the copper ions crystallization, pH value falls below 10 but the total effluents pH is above 10 in any experiments. Therefore, CSTR experiments in this thesis were performed, assuming the total effluents pH is above 10.

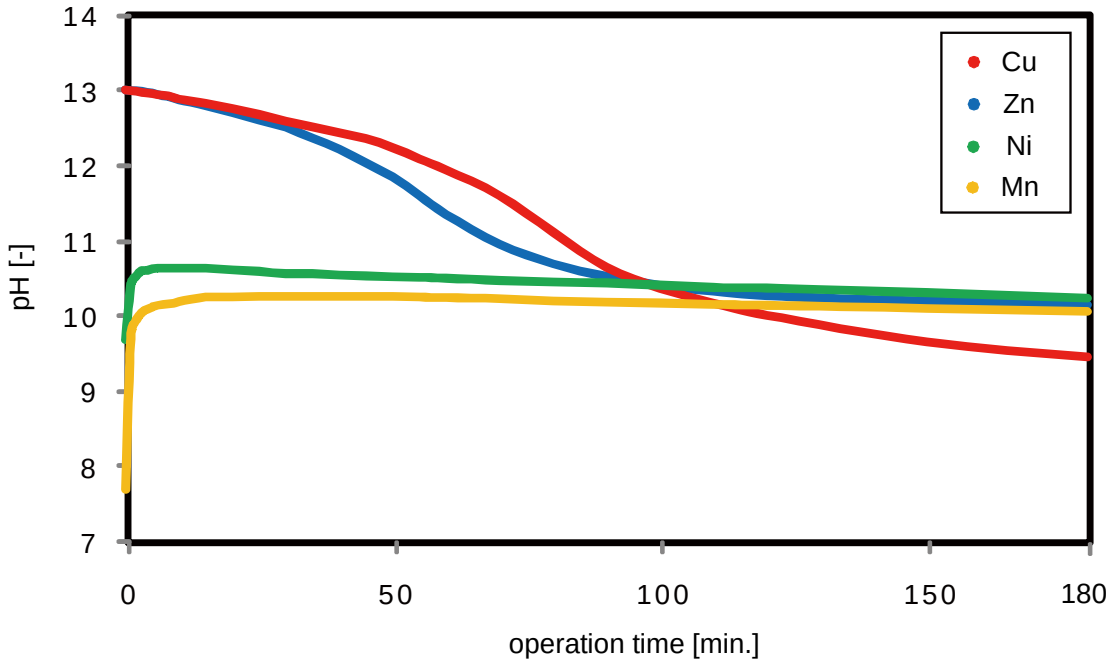

Fig. 2-5 pH changes during the CSTR blank reactive crystallization.

This reaction occurs depending on the initial pH for some reason. For example, nickel ions were crystallized and kept accumulating in setting the initial pH~9.7, despite that the value was soaring and becoming constant at about 10. Therefore, in experiments, the initial pH was especially paid attention and the pH change was regarded to be occurred with reproducibly.

2.2 Measurements for detecting metal ions concentration

Appreciating the metal ions concentration in the effluent filtrate is notable in this study. One method that can detect metal ions in solvents is that analyzing by Inducted-coupled plasma optical emission spectrometry: ICP. This is a popular method for measuring metal ions correctly and definitely. But when sample solutions are stayed for long time, metal solids are precipitated and metal ion concentration in solvent would be decreased owing to the degree of supersaturation. In this case, ICP method is applicable after diluting solids by acids such as hydrochloride. Another method for this case is that measuring electro-conductivity during the effluent filtrate flows out. This method has a merit on not likely to arise systematic errors by manual. Also, this method can detect metal ions concentrations on a real time basis and with no break. To obtain metal ion concentration, electro-conductivity needs to be converted by using below equations. After applying thermal correction, as shown in **Eq. 2-4**, metal ion concentration can be calculated by the compensation formula using a standard curve method such as **Eq. 2-5**. This equation can only be adapted in manganese ions detection. In addition, in below equations, *T* is temperature, λ is the electro-conductivity value and *C* is metal ions concentration and the index *0* means initial, and *t* means at time t, furthermore,. *Mn* represents manganese.

$$\lambda_t = \frac{\{1-0.02(T_0-T_t)\}}{\lambda_0} \tag{2-4}$$

$$\lambda_t = 1.66 \times C_{Mn} + 2.25 \tag{2-5}$$

2.3 Pre-exam for the carbonates separation by batch tests

A batch test is a simple measurement for confirming how the reaction occurs. Two neutral stock solutions whose concentration was each set 0.1 M were just mixed in a 100 mL conical flask. This is a simple mixing, and mixing point cannot be detected strictly because the way of providing are vary each time. In this experiment, three kinds of metal ions: manganese, nickel and zinc ions were reacted. The look of precipitates after the reaction is as following **Fig. 2-6**. Manganese ions crystallized in this operation but the others did not. **Fig. 2-7** shows $MnCO_3$ crystals observed by the optical microscope. The average size of $MnCO_3$ was 2.14 μm. After the ICP (IRIS-Intrepid, Thermo Fisher Scientific K.K., Yokohama) analyses of each supernatant, metal recovery rate was calculated. Each value was Mn^{2+}: 91.80 %, Ni^{2+}: 94.14 %, Zn^{2+}: 58.13 %. Zinc ions recovery rate was found to be small from this test.

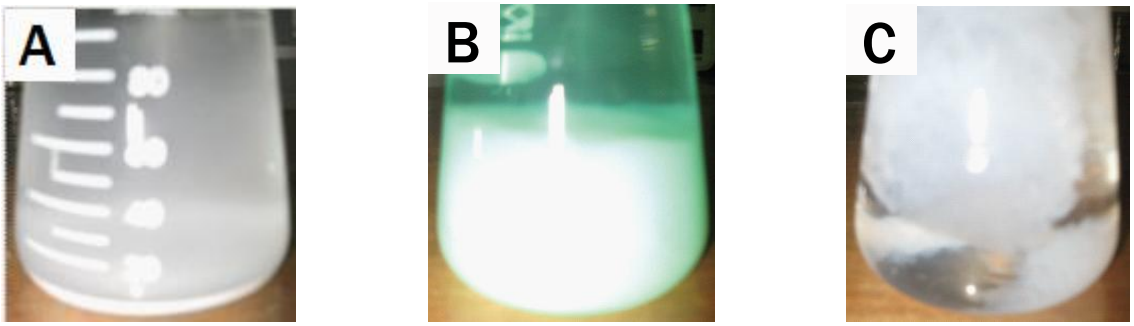

Fig. 2-6 Precipitates after the batch reaction in conical flasks (A: Mn^{2+}, B: Ni^{2+}, C: Zn^{2+}).

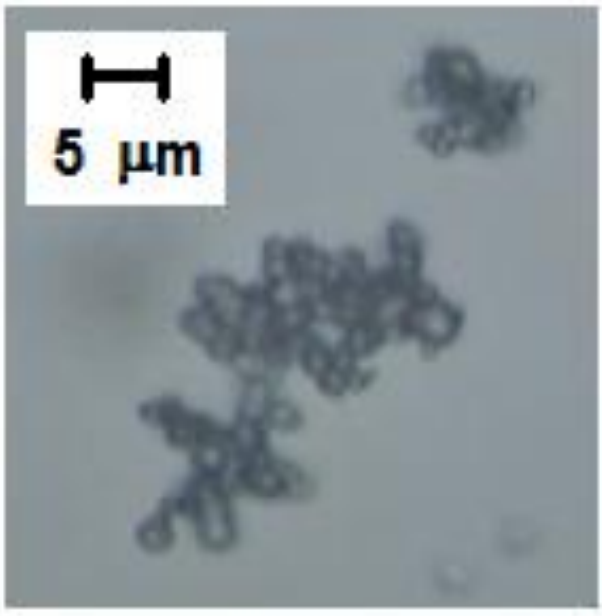

Fig. 2-7 $MnCO_3$ crystals obtained by batch reaction.

2.4 Separating and recovering manganese ions from the wastewater

This section focuses on the reactive crystallization about manganese carbonates by the continuous stirred-tank reactor. Recently, studies with creating mono-dispersed metal particles that have desired sizes and shapes in regular are much operated. Especially, calcium carbonates [9-11] have been investigated intensively in recent years because of their abundance in nature and their importance in the industrial applications in paints, plastics, rubber, and paper industries. Inorganic carbonate materials are also advantageous for the formation of polymeric micro/nanocapsules, as they can be synthesized from simple reactions. Manganese carbonate micro-particles can be used as templates not only for metal plating but also for functional materials like the system of biosensors, bioreactors, and drug-delivery systems [12]. Su et al. [13] have examined the effects of reaction temperature, pH, raw concentration on the morphology and size of manganese carbonate particles. With reducing the reaction temperature, the dispersibility of obtained particles became better and their shapes also gradually trended towards unification and their size became larger. In addition, the morphology and the size of particles had not been affected obviously by the ingredient concentration. Thereby, this research focuses on the carbonate reactive crystallization of manganese ions and summarizes the experimental studies in various aspects about obtained particles: such as the particles size data and the metal recovery rate from solution. Recovered manganese compounds are spherical, so it is adapted to evaluate their aspects. The purpose of this research is to examine the nature of the recovered crystals and the metal ions concentration of the filtrate after the reaction and then to determine the existence of optimal conditions.

In the reaction, manganese sulfate and sodium carbonate solutions are reacted in the water-laden 2 L beaker. A continuous stirred tank reactor which is illustrated in **Fig. 2-8** was employed for this reactive crystallization. A baffle plate was attached to improve and average the fluidized condition. An agitation stick has four-bladed paddles with the gradient are 45 degrees. This inclining contributes to improvement of the axial current and the emission flow. Distilled water (1 L) was poured in the tank in advance. Then, manganese sulfate ($MnSO_4.6H_2O$) and sodium carbonate (all from Wako Pure Chemical Industries, Osaka, Japan) solutions were provided at the same rate in the reactor. The effluent was drained to keep the solution volume in the tank constant. The agitation rate was set at 300 ± 1 rpm and the temperature in the reaction tank was kept at 303 ± 0.1 K. One-hour reactive crystallization was each conducted, changing the

flowing rate of stock solution (the standard value: 0.010 [L min^{-1}]) and the metal ions concentration in the stock solution (the standard value: 6.52 [g L^{-1}]). After the operation, recovered crystals' sizes were measured by the microscopic method and the manganese ions concentration in the effluent supernatant was calculated by converting from the electro-conductivity, which was measured continuously by the conductance meter. Manganese ions concentration was detected also by ICP in a few conditions and the accuracy of values have been confirmed. In addition, the transition of crystals shapes and habits were observed by the scanning electronic microscope (SEM: VE-8800, KEYENCE, Osaka). Thereafter, the best conditions for obtaining the high recovery rate and the dispersibility and for producing the desired crystals were examined. On this occasion, the C. V.: coefficients of variation [%] for obtained particles were determined by Eq.2-6. The absolute value of C. V. is sometimes known as relative standard deviation. It is a normalized measure of size dispersion. As follows, C. V. can be obtained by calculating the ratio of the standard deviation σ to the particles mean size μ.

$$\mathrm{C.V.} = \frac{100\,\sigma}{\mu} \tag{2-6}$$

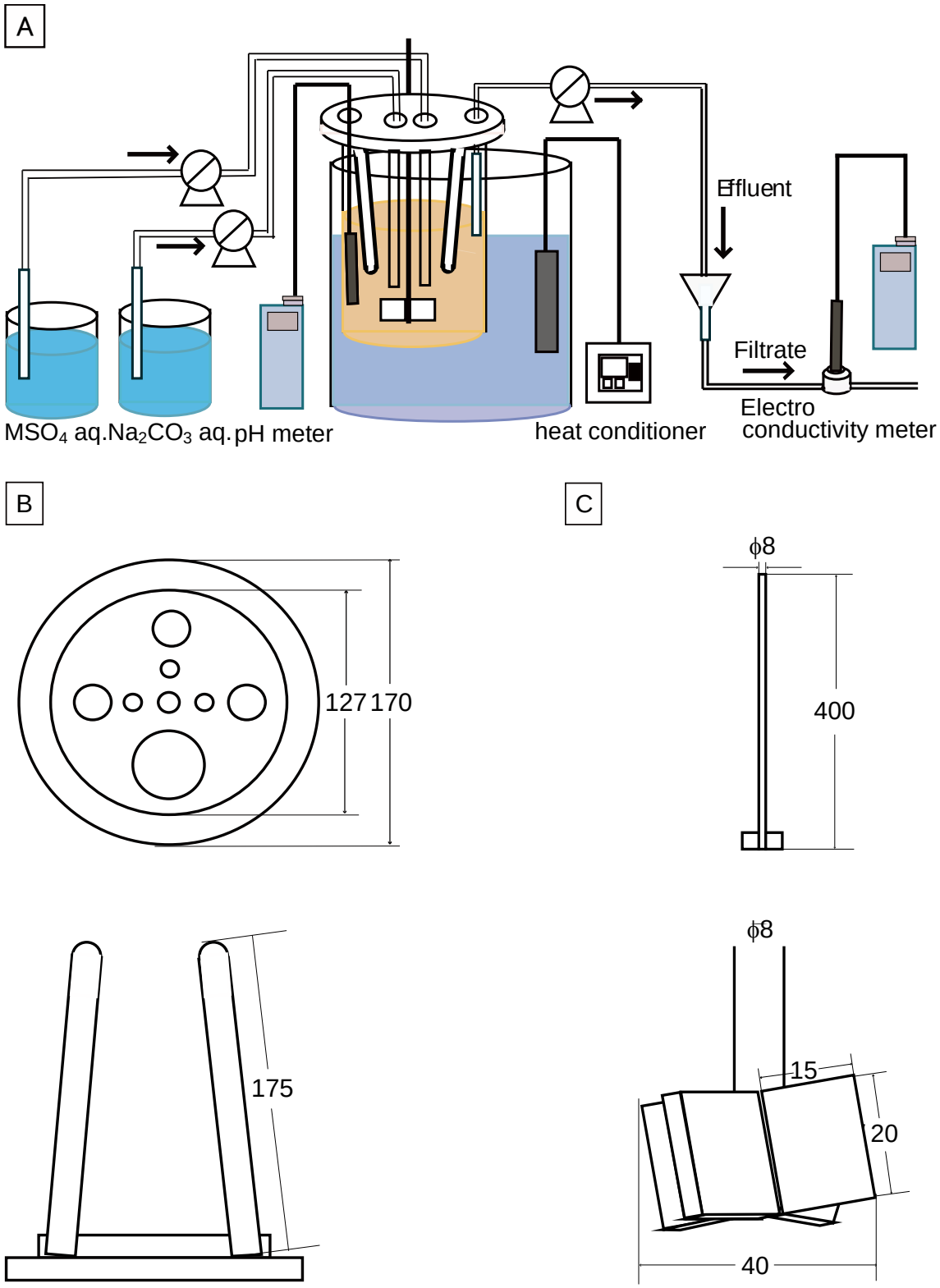

Fig. 2-8 Experiment apparatus for producing $MnCO_3$ particles [A] and the geometry of baffle plate [B] and agitation stick [C], [mm].

SEM images of obtained particles in changing crystallization conditions are shown in **Fig. 2-9.** The variation of recovered particles average size and manganese recovery rate with the feeding rate of the stock solution are indicated in **Fig. 2-10**. Meanwhile, **Fig. 2-11** shows the variation of recovered particle average size and manganese recovery rate with the metal ions concentration in the stock solution. From these illustrations, with the increase of the stock feeding rate or the metal ions concentration, crystals average size increased. The reason was estimated that the part of metal ions supersaturation in the tank has enlarged along with growing these two parameters. Particles dispersibility roughly improved with the increase of the feed rate and the metal ions concentration in the stock solution. Manganese recovery rates were determined from converting the manganese ions concentration in the effluent filtrate. They reduced with the increase of the stock solution feed rate and reached a value of near 91.8 %, which is a value from the batch-style mixed test. The recovery rate improved with the increase of metal ions concentration. As for the feed rate, rapid feed causes the recovery of coarse particles: whereas, slow feed recovers metal ions densely. If the feed rate is constant, high supersaturation degree produce large and dense particles and it estimates that manganese ions are well incorporated.

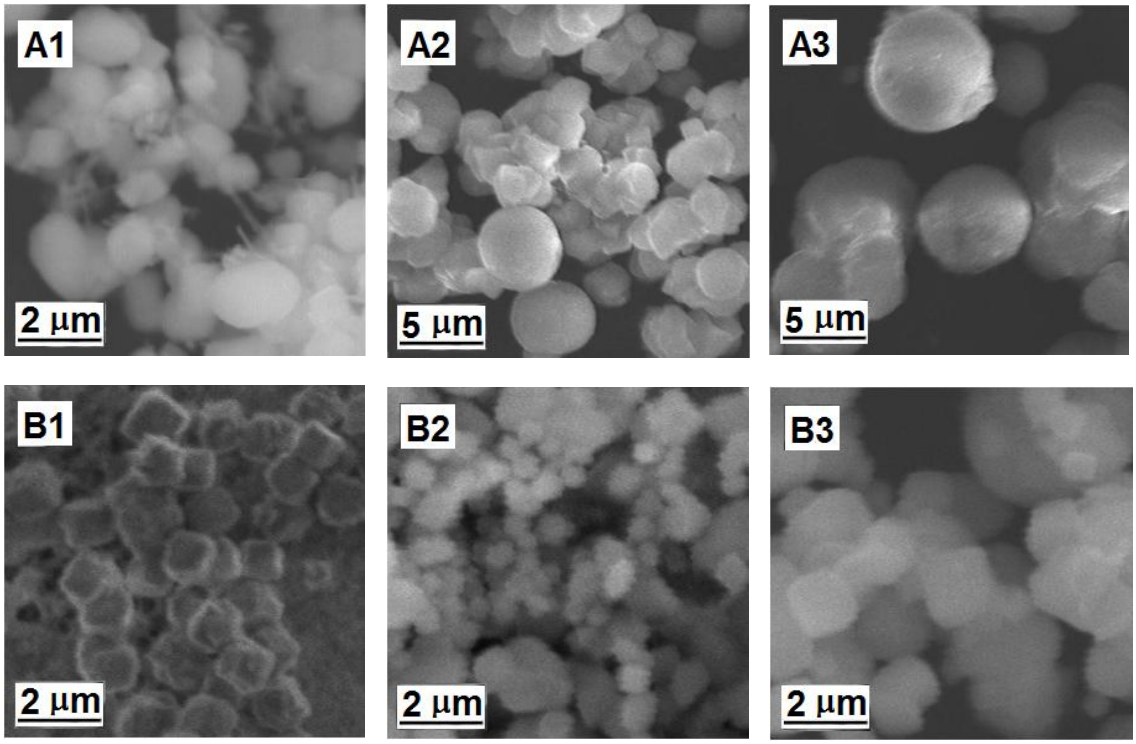

Fig. 2-9 SEM images of manganese carbonate particles (after 1 hour operation), [A1-3] feeding rate: 5, 10, 15 [mL min^{-1}], [B1-3] manganese ions concentration: 0.50, 1.0, 3.0 [g L^{-1}].

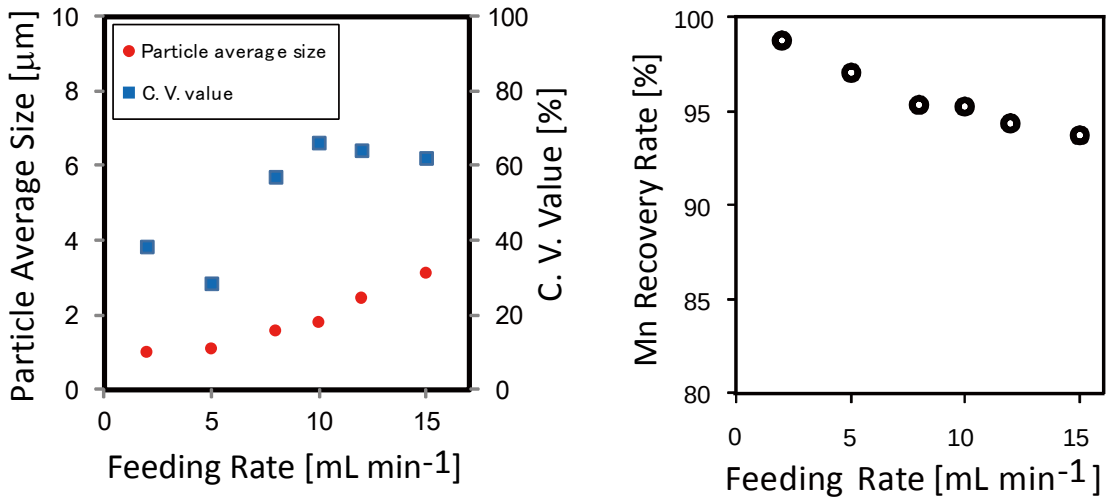

Fig. 2-10 The variation of recovered particle average size, C. V. value and manganese recovery rate with the feeding rate of the stock solution (after 1 hour crystallization, In these graphs, only conditions that can be obtained over 200 particles were plotted.).

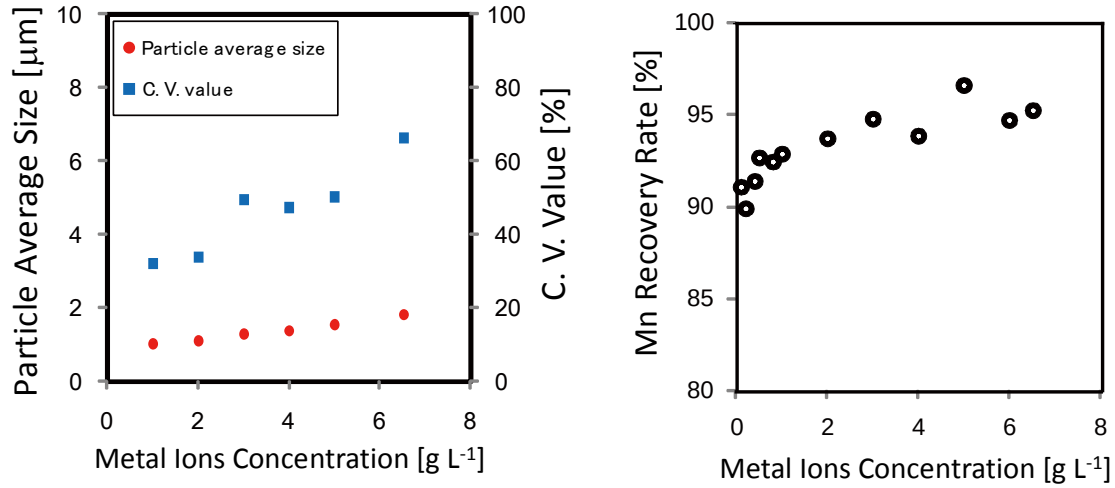

Fig. 2-11 The variation of recovered particle average size, C. V. value and manganese recovery rate with the metal ions concentration in the stock solution (after 1 hour crystallization, In these graphs, only conditions that can be obtained over 200 particles were plotted.).

These results indicate that crystals that have been desired sizes can be obtained by controlling crystallization operation conditions. With decreasing the feed rate, metal ions removal efficiency leads to improve. To produce large crystals with a high recovery rate in this case, the supersaturation ratio should be set to a high value. Performing reactive crystallization after the condensation of discharged water can be the effective strategy for the manganese ions removal.

2.5 Separating and recovering zinc ions from the wastewater

In this section, zinc ions reactive crystallization in the continuous stirred-tank reactor was focused on. Along with manganese carbonates shown in section 2.4, zinc oxides are also materials that are desirable to obtain regular in size and shape. Zinc oxides have been found their ceramic applications such as semiconductor and varistors and recently cosmetics such as sunscreens [14, 15]. Didier et al. [16] have performed the hydrolysis reaction for obtaining zinc oxides, and have found that the aggregation was not occurred and tiny single particles were obtained at higher precursor concentration. In the experiment, about zinc ions recovery, the nature of recovered crystals via changing the operation conditions: the initial pH, the solution feed speed, and the zinc ions concentration in the stock solution was examined. Then, the existence of optimal conditions has been determined as well as the manganese ions recovery.

In the reaction, zinc sulfate and sodium carbonate solutions are reacted in the water-laden 2 L beaker as well as the manganese recovery experiment, mentioned in the previous section. A continuous stirred tank reactor which is illustrated in **Fig. 2-12** was employed for this crystallization. Distilled water (1 L) was poured in the tank in advance. Then, zinc sulfate ($ZnSO_4.7H_2O$) and sodium carbonate solutions (both from Wako) were provided at the same rate in the reactor. The effluent was drained to keep the solution volume in the tank constant. The agitation rate was set at 300±1 rpm and the temperature in the reaction tank was kept at 303±0.1 K. In each occasion, one-hour reactive crystallization was conducted, changing the initial pH (the standard value: 13.02), the flowing rate of stock solution (the standard value: 0.010 [L min^{-1}]) and the metal ions concentration (the standard value: 1.0 [g L^{-1}]). After the operation, recovered crystals' sizes were measured by the microscopic method and the zinc ions concentration in the supernatant of the effluent was analyzed by the ICP (IRIS-Intrepid, Thermo Fisher Scientific K.K., Yokohama). In addition, the transition of crystals shapes and habits were observed. The appropriate conditions for obtaining particles that have high size uniformity and high dispersibility were examined. The agglomeration ratios of products α were also calculated from Eq. 2-7. This value represents the ratio of the number of aggregates n_a to the whole number of particles n (>1 000).

$$\alpha = \frac{n_a}{n} \tag{2-7}$$

SEM images of obtained particles in changing crystallization conditions are shown in **Fig. 2-12.** And then, the variation of recovered particles' properties, such as particles average size, C. V. value and agglomeration ratio with the initial pH, the feeding rate and the initial supersaturation ratio are indicated in **Fig. 2-13**. In these graphs, only conditions that can be obtained over 300 particles were plotted. The initial pH can highly affect the particles size, agglomeration ratio and surface condition (**Fig. 2-12, 13 [A]**). The most appropriate range seems to be 12.9-13.3, and the spherical forms become misshapen in other condition. Also, if the initial pH changes, the agglomeration ratio also changes drastically. Obtained particles were the largest around pH=13.33. The existence ratio of carbonate ions is not so different in this pH range, however, pH of the solution falls to 11~12 during the reaction, and a mass of carbonate ions makes a difference. Anyway, what we estimate is that the higher the initial solution's pH, the higher the metal ions supersaturation ratio. Then, zinc oxide particles enlarge to a threshold value with the increase of initial pH. When an initial pH set too high, strong alkali may affect to the surface of particles, and the condition was roughed and shrunken. Other parameters: the feeding rate and the metal ions concentration do not affect products so much, but the amount of fine particles or giant particles changes to a certain degree. With the increase of the feeding rate, obtained particles were little grown. Meanwhile, particles become reduce in size a little with enlarging the metal ions concentration in the stock solution. On this way, many fine particles appear but many giant particles produce at the same time, thus the materials production is likely to receive the influence from the high supersaturation in the tank as well as the manganese ions recovery. The values of coefficient of variance: C.V. have been in contrast to the obtained particles size, that is to say, the value of C.V. was small if the particles size was large. Zinc ions concentration in the effluent filtrate was around 2 mg L^{-1} in any experimental conditions.

From above experiments, some new findings were able to be obtained. One is that metal ions supersaturation can affect the growth of crystals at some level. Another is that materials that have one desired property will be obtained by coordinating some conditions. However, if the desired points are more than one, conditions that meet all will not exist. At this time, searching the meeting point, for example, the condition that small particles can be obtained but the recovery rate is poor will be the considerable way to evaluate results.

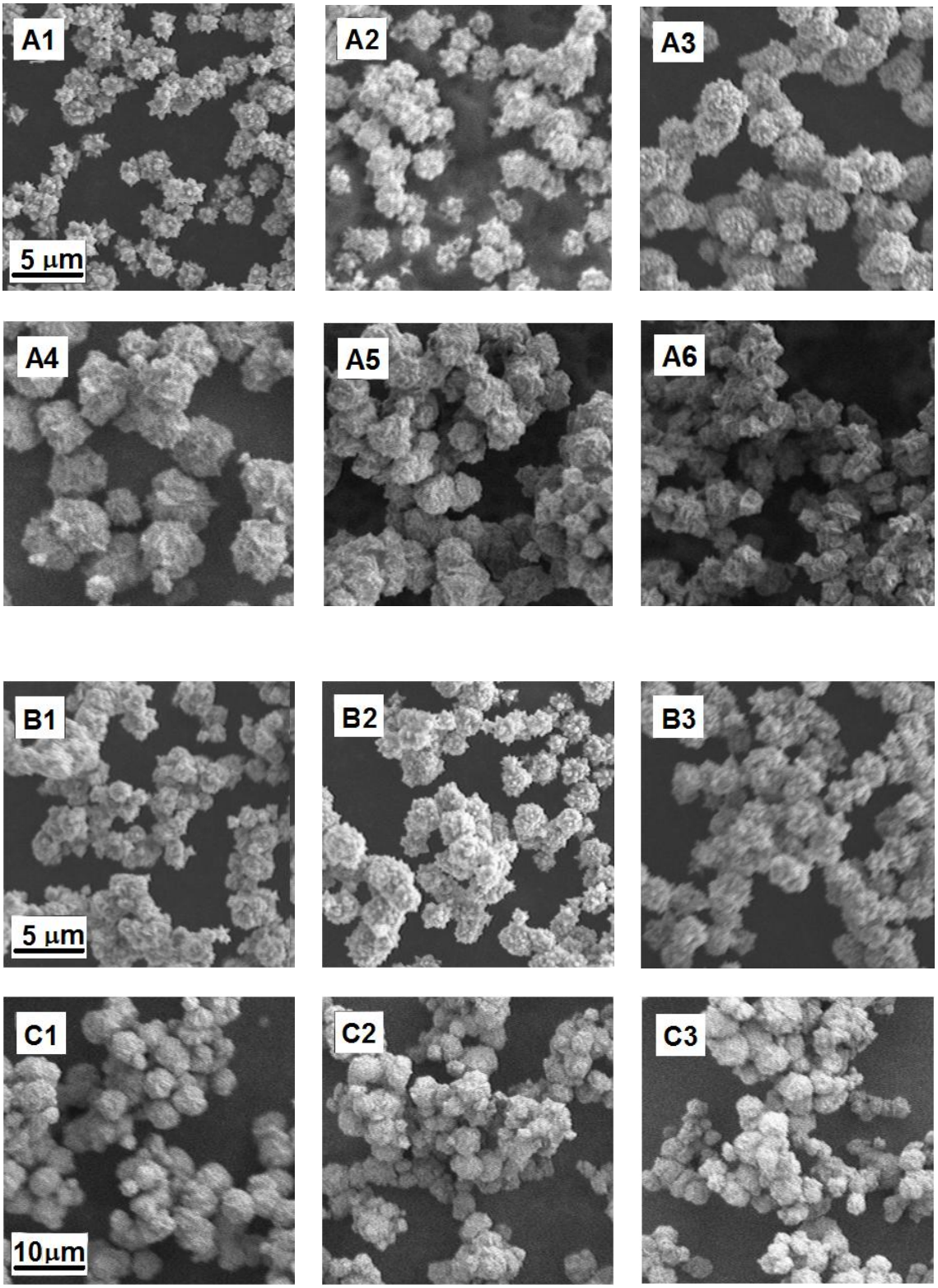

Fig. 2-12 SEM images of zinc oxide particles by the reactive crystallization (after 1 hour operation, [A1-6] initial pH: 12.90, 13.08, 13.16, 13.28, 13.33, 13.53 [-], [B1-3] feeding rate: 5, 8, 12 [mL min^{-1}], [C1-3] zinc ions concentration in the solution: 1.2, 1.6, 1.8 [g L^{-1}]).

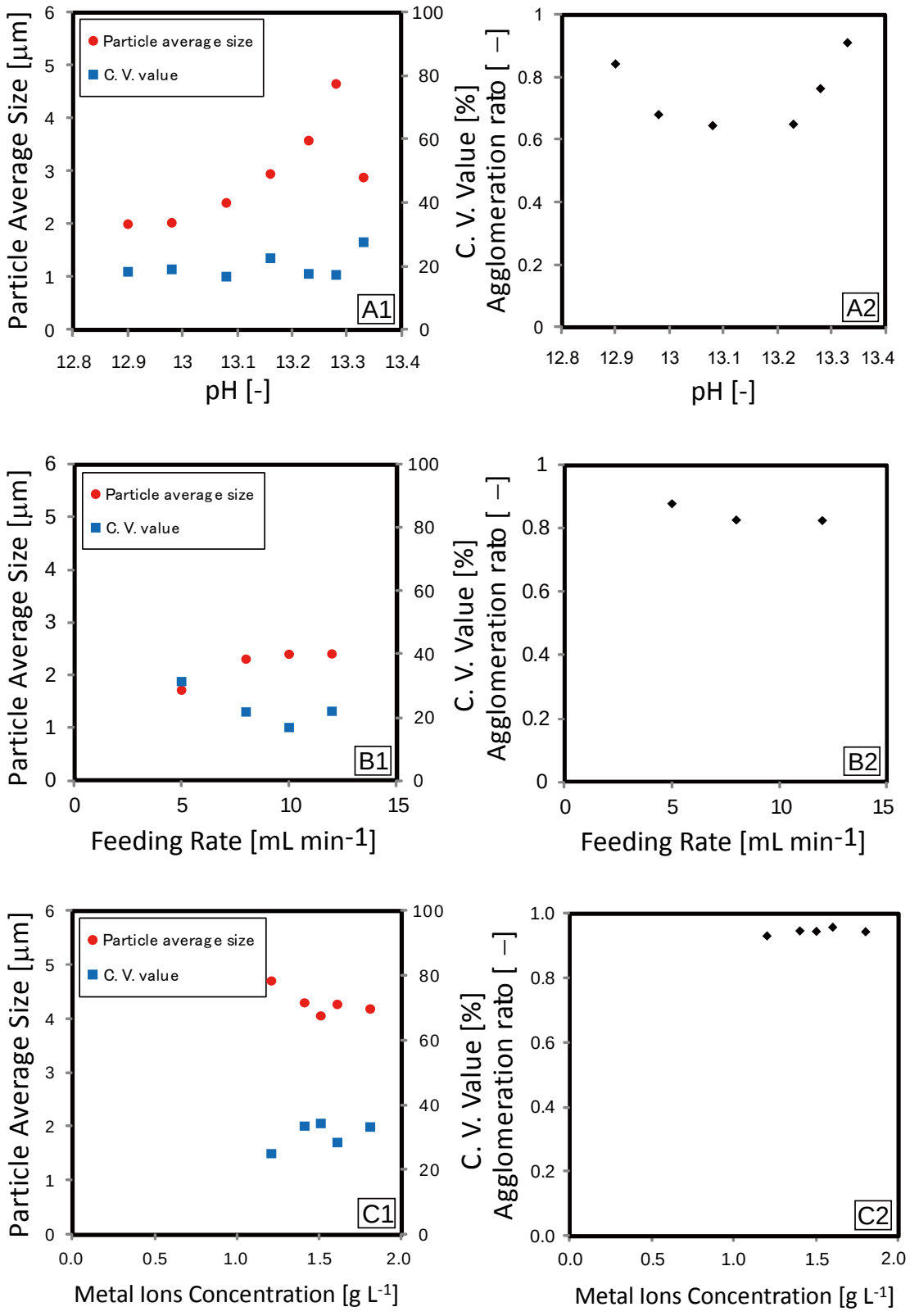

Fig. 2-13 The variation of zinc oxides average size, C. V. value and agglomeration ratio with the initial pH [A], feed rate [B] and zinc ions concentration in solution [C] (after 1 hour operation).

Nomenclature

C	metal ions concentration in the tank, kg m^{-3}
$C.V.$	coefficient of variation, %
k_r	reaction constant, -
K_{sp}	hydroxide solubility product, -
n	number of particles, #
n_a	number of aggregates, #
Q	volume of the solution, m^3
T	temperature, K
V	volume of the tank, m^3
α	agglomeration ratio, -
λ	electro-conductivity value, S m^{-1}
μ	particles mean size, μm
σ	standard deviation, μm

index

0	initial
in	the inflow
out	the outflow
Mn	manganese ions
t	time t

References

[1] C. A. J. Appelo and D. Postma, 2005, Geochemistry, groundwater and pollution 2nd edition, *A.A. Balkema Publishers.*

[2] Precipitation, 1992, *Butterworth-Heinemann Ltd.*

[3] V. C. Gopalratnam, G. F. Bennett and R. W. Peters, 1992, Effect of collector dosage on metal removal by precipitation/flotation, *J. Environ., Eng.*, **118(6)**, 923-948.

[4] R Nilsson, 1971, Removal of metals by chemical treatment of municipal waste water, *Water Res. Pergamon Press*, **5**, 51-60.

[5] C. E. Janson, R. E. Kenson and L. H. Tucker, 1982, Treatment of heavy metals in wastewater, *Environ. Prog.*, **1 (3)**, 212-216.

[6] B. M. Kim and P. A. Amodeo, 1983, Calcium sulfide process for treatment of metal-containing wastes, *Environ. Prog.*, **2 (3)**, 175-180.

[7] T. E. Higgins and V. E. Sater, 1984, Combined removal of Cr, Cd, and Ni from wastes, *Environ. Prog.*, **3 (1)**, 12-25.

[8] Shin-kogaiboshi no gijutu to hoki, 2008, *Japan Environmental Management Association for Industry.*

[9] Y. Kotaki and H. Tsuge, 1990, Reactive crystallization of calcium carbonate in a batch crystallizer, *J. Cryst. Growth*, **99**, 1092-1097.

[10] R. Sheikholeslami and M. Ng, 2001, Calcium sulfate precipitation in the presence of nondominant calcium carbonate: thermodynamics and kinetics, *Ind. Eng. Chem. Res.*, **40**, 3570-3578.

[11] T. F. Kazmlerczak, M. B. Tomson and G. H. Nancollas, 1982, Crystal growth of calcium carbonate: a controlled composition kinetic study, *J. Phys. Chem.*, **86**, 103-107.

[12] H. Zhu, E. W. Stein, Z. Lu, Y. M. Lvov and M. J. McShane, 2005, Synthesis of size-controlled monodisperse manganese carbonate microparticles as templates for uniform polyelectrolyte microcapsule formation, *Chem. Mater.*, **17**, 2323-2328.

[13] H. F. Su, Qu X.,Wen Y. X., Tong Z. F., Li X. H., 2008, Morphology control in preparation process of spherical manganese carbonate particles, *Chin. J. Process Eng.*

[14] D. Jezequel, J. Guenot, N. Jouini and F. Fievet, 1995, Submicrometer zinc oxide particles: elaboration in polyol medium and morphological characteristics, *J. Mater. Res.*, **10 (1)**, 77-83.

[15] Sossina M. Haile and David W. Johnson, Jr., Gary H. Wiseman and H. Kent Bowen, 1989,

Aqueous precipitation of spherical zinc oxide powders for varistor applications, *J. Am. Ceram. Soc*., **72 (10)**, 2004-2008.

[16] Didier J., Jean G., Noureddine J. and Fernand F., Submicrometer, 1995, zinc oxide particles: elaboration in polyol medium and morphological characteristics, *J. Mater. Res.*, **10(1)**, 77-83.

Chapter 3

Effect of seeding on metal ions recovering from the wastewater

In this chapter, against nickel and copper ions recovery, spherical metal carbonate basics are dosed in a tank preliminarily, and the reactive crystallization was performed aiming at the crystal growth on seed surfaces. The appropriate feed conditions were explored and the generalization applied to any scale systems was attempted.

3.1 Introduction

Metal ions separation and removal with the use of the precipitation method have been advanced by some researchers [1-17]. In past reports, some metal ions were shown to be taken efficiently on seeds such as quartz-sands at an optimum pH by a fluidized-bed reactor. For example, from the crystallization of silver carbonates, silver ions were removed the most effective at about pH 10.2 [3]. Nickel ions were indicated to be removed effectively about pH 9.8 [9]. Furthermore, the optimum pH for lead carbonate crystallization was ranged from 8.0 to 9.0 [7]. Also, this process has contributed to the sludge minimization; instead the removed metals became a part of dry chemical pebbles or dense precipitates incorporated directly onto pellets. However, several metals are difficult to be precipitated as crystals at any pH condition on the fluidized-bed reactor or the batch crystallizer. For producing such metal substances as crystals, rather active flow field and localized reactive point would be demanded.

From these circumstances, we proposed a new metal ions separation and recovery method using a semi-batch crystallizer. Nickel and copper ions have been crystallized by controlling pH, but the hydroxide forms are not regular. For recycling these metal ions, dispersion of their forms and sizes should be restricted. Actually, some scientists have attempted the seed growth for recovering metal ions [18-20]. And in this study, sphere metal carbonate basics are placed in a tank preliminarily and the reactive crystallization was performed aiming for the crystal growth on seed surfaces. By changing seed inputs, seed growth mechanisms have been discussed from the crystal size changes during 8 hours reactive crystallization. Furthermore, the generalization of this method has been attempted for accepting any scale of systems.

3.2 Experimental approach and measurement items

A controlled double-jet reactive crystallization was operated using a semi-batch crystallizer which was equipped with a thermostat and an agitator as shown in **Fig. 3-1** [21]. This time, spherical seeds: metal carbonate basic ($NiCO_3.2Ni(OH)_2.4H_2O$ in nickel ions recovery or $CuCO_3.Cu(OH)_2.H_2O$ in copper ions recovery, Wako Pure Chemical Industries, Ltd., Osaka, Japan) are fed in a tank preliminarily, and mixed at the adequate agitation rate, in order not to flow out their particles (**Fig. 3-1**). The geometry of a custom-made tank was like **Fig. 3-2** which was used for this crystallization. This tank is being attached four baffle plates along the sides at intervals of 90 degrees. And a four-bladed paddle for agitating is the same thing as shown in chapter 2.

As for feedstocks, $NiSO_4.6H_2O$ or $CuSO_4.5H_2O$ (Wako) solution and sodium carbonate (Wako) solution were prepared. Metal ions concentration was coordinated 1.0 g L^{-1} at first. Carbonate ions concentration in the sodium carbonate solution was regulated at sufficient amount to keep the optimum reaction molar ratio during the reaction. Each solution was provided at the feeding rate of 10 ml min^{-1} and the supernatant effluent was drained to keep the solution volume in the tank constant, 1.3 L. Each solution was calibrated and prepared by deionized water. The agitation rate was set at approximately 150 rpm so as to be constant the boundary line between crystals and supernatant from the bottom between 60 and 70 % at any experiments. And the solution temperature in the tank was maintained at 303±0.1 K. In order to investigate the mechanism of fixing metal ions onto seeds, 8 hours reactive crystallization was conducted, varying seed input from 15±0.1 to 50±0.1 g. This range of amount was appropriate for floating almost seeds evenly, and not for accumulating on the bottom of tank. Solution initial pH (IpH) was controlled each optimum value for crystallization: at 9.7±0.3 in nickel ions removal experiments and at 13.0±0.2 in copper ions removal experiments. Through the reactive crystallization, metal ion concentrations in the supernatant filtrate and produced crystal sizes were measured. Therefore, we sampled the supernatant and mixed suspension in the tank at regular interval. Metal ion concentrations were analyzed by ICP (IRIS-Intrepid, Thermo Fisher Scientific K.K., Yokohama). Formed crystals were observed with SEM (VE-8800, KEYENCE, Osaka) and crystal average sizes (L_p [μm]) were measured by the photographic method (Eq. 3-1). At this time, the number of counted particles on the photos was from 300 to 500. To determine the dispersion in obtained crystals, the coefficient of variation (*C.V.* [%]) was calculated from the equation (Eq. 2-6).

$$L_p = \frac{\sum_{i=1}^{n} n_i L_i}{\sum_{i=1}^{n} n_i} \quad (3\text{-}1)$$

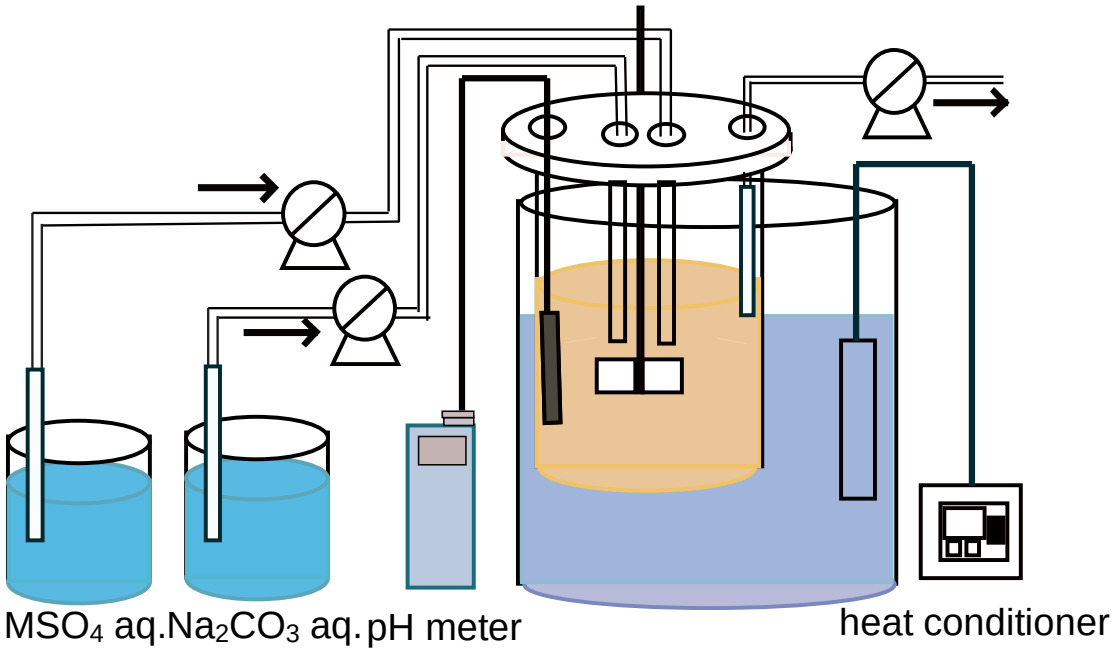

Fig. 3-1 The semi-batch crystallizer and the tank interior agitation.

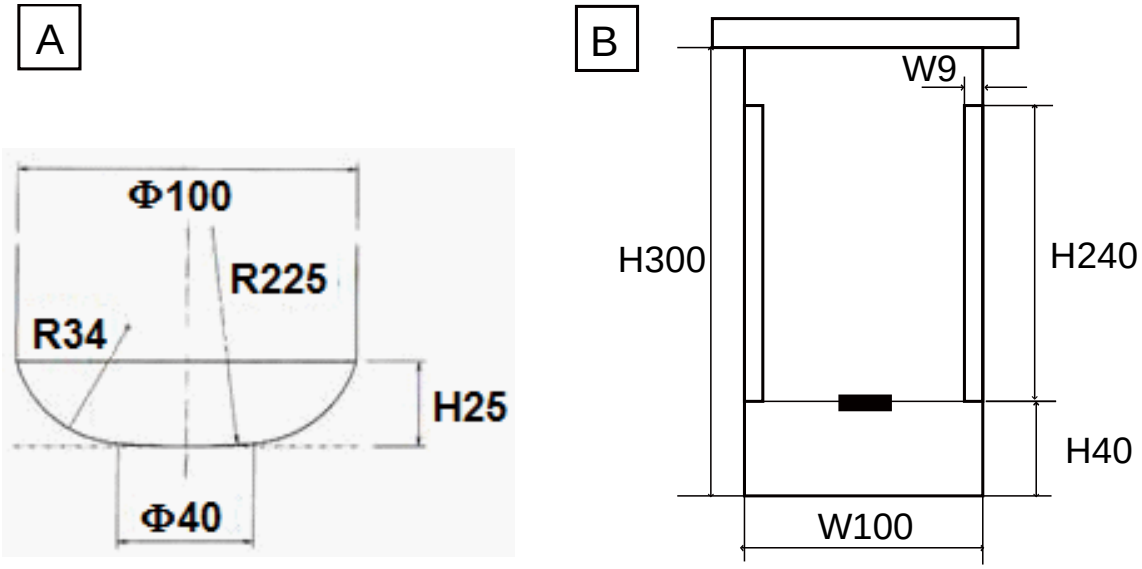

Fig. 3-2 The geometry of custom-ordered tank ([A] stirring part, [B] whole image, H: Height, W: Width, R: Radius of sphere, Φ: Inner diameter of circular cylinder, [mm]).

In Eq. 3-1, where L_p is the mean diameter of product crystals [μm], n_i is the number of counted crystals of component *i* [#], and L_i represents the measured particle size of the *i*th crystal [μm]. Furthermore, recovered crystals after the 8 hours crystallization were structurally analyzed by the multifunctional X-ray diffractometer (XRD: RINT-1100, Rigaku, Tokyo).

3.3 Obtained crystals characters

By this reactive crystallization, metal substances piled up on the surface of seeds, keeping the form sphere. Also, obtained crystals were found to be all the same materials as seeds from X-ray spectral graphs (**Fig. 3-3**). After reviewing the XRD spectrums, nickel-containing material was identified as nickel carbonate basics, $NiCO_3.2Ni(OH)_2.4H_2O$: Zaratite, and copper-containing substance was found to be copper carbonate basics, $CuCO_3.Cu(OH)_2.H_2O$: Malachite. Those materials are the same as initial seeds. According to **Fig. 3-3[B]**, XRD profiles are slight different from each other. Actually, crystals color has changed through the reaction, but peak positions of them are the same, so both can be considered to be same materials.

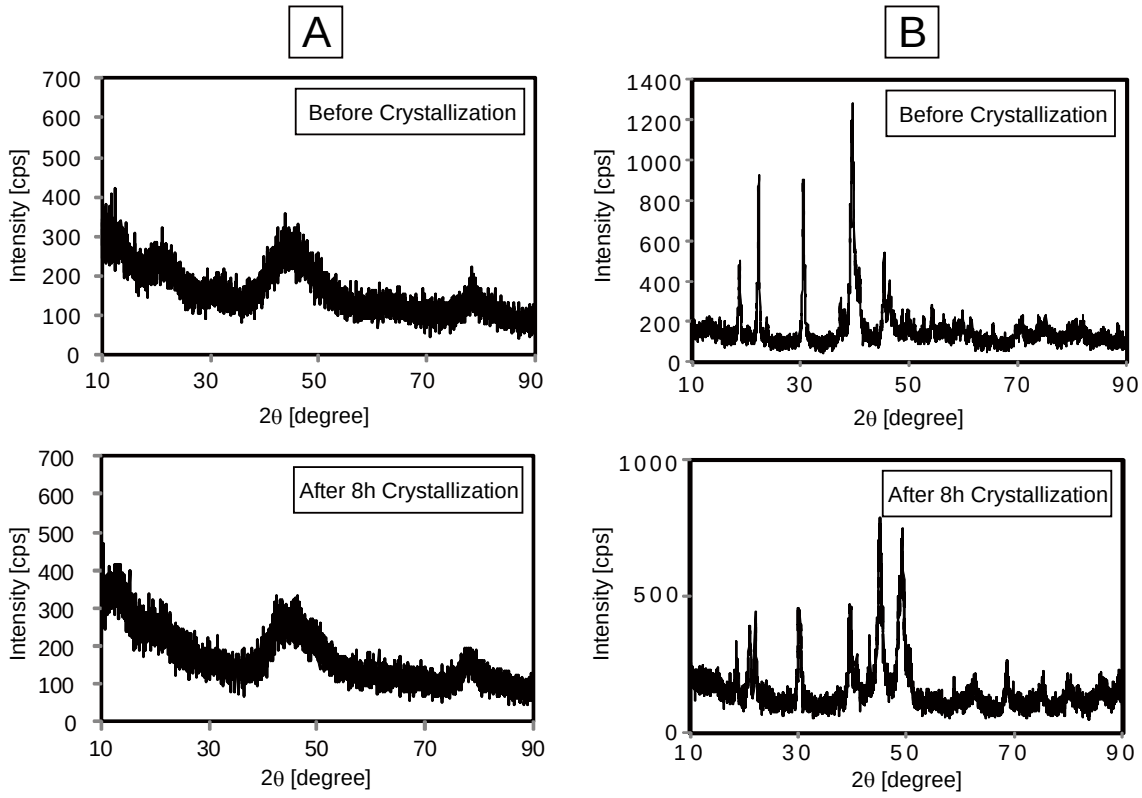

Fig. 3-3 Powder XRD patterns of seed crystals: [A] nickel carbonate basics and [B] copper carbonate basics.

3.4 Obtained crystals size data and metal ions concentration

Time dependences on recovered particles average size which was obtained from this nickel or copper ions recovering approach and each sample C.V. value are shown in **Fig. 3-4**. Dot lines in these figures mean the seed particles average sizes. These figures indicate that fine particles appearance is varied with the providing seed amount. Especially, it was suggested that the optimum seed amount for keeping crystals enlarge was 40 g in the nickel ions recovering experiment and 20 g in the copper ions recovering experiment on this tank scale. In providing seed amount below the optimum value, seeds tended to grow at first stage of reaction, however, fine particles were gradually produced and the average size turned to be decreased. Conversely, at a seed amount in excess of the optimum value, fine particles were easily produced and the average size continued to decrease from the beginning of the reaction. As for the reason of small particles production, when small amount of seeds were provided, surface of seeds were not enough for growth, and nuclei seemed to be easily produced in the bulk solution. Meanwhile, when much amount of seed was provided, seeds that created fine particles seemed to be collided frequently, accordingly, it was thought that they separated from seeds and they have grown like nuclei. In case that the optimum mass of seeds was provided, crystals were enlarged nearly along with the following growth rate equation [22] (Eq. 3-2). This equation is true under next hypotheses: [i] seeds are completely sphere, [ii] no fine particles are produced, [iii] substances are piled up on the seed surfaces uniformly.

$$L_{th} = \left\{ \frac{4\pi k_m A (c - c^*) t}{3\rho} \right\}^{\frac{1}{3}} \qquad (3\text{-}2)$$

In this equation, L_{th} is the theoretical particle size, k_m is the coefficient of mass transfer, A is the surface area of a crystal, c is the metal ions concentration in the solution, c^* is the equilibrium saturation concentration, t is the operation time and ρ is the density of solvent.

This theoretical curve was well reflected in experimental values, but strictly, in copper ions uptake experiment; actual growth was occurred a little faster at an early stage of reaction. This relates to the difference of crystal growth mechanisms, as shown in **Fig. 3-5**. In nickel ions recovery experiment, granular particles have been much produced and they accumulated on the surface of seeds. Meanwhile, in copper ions incorporation, a plenty of needle-like small particles are appeared on the surface of seeds and finally they seemed to grow from the center of seeds.

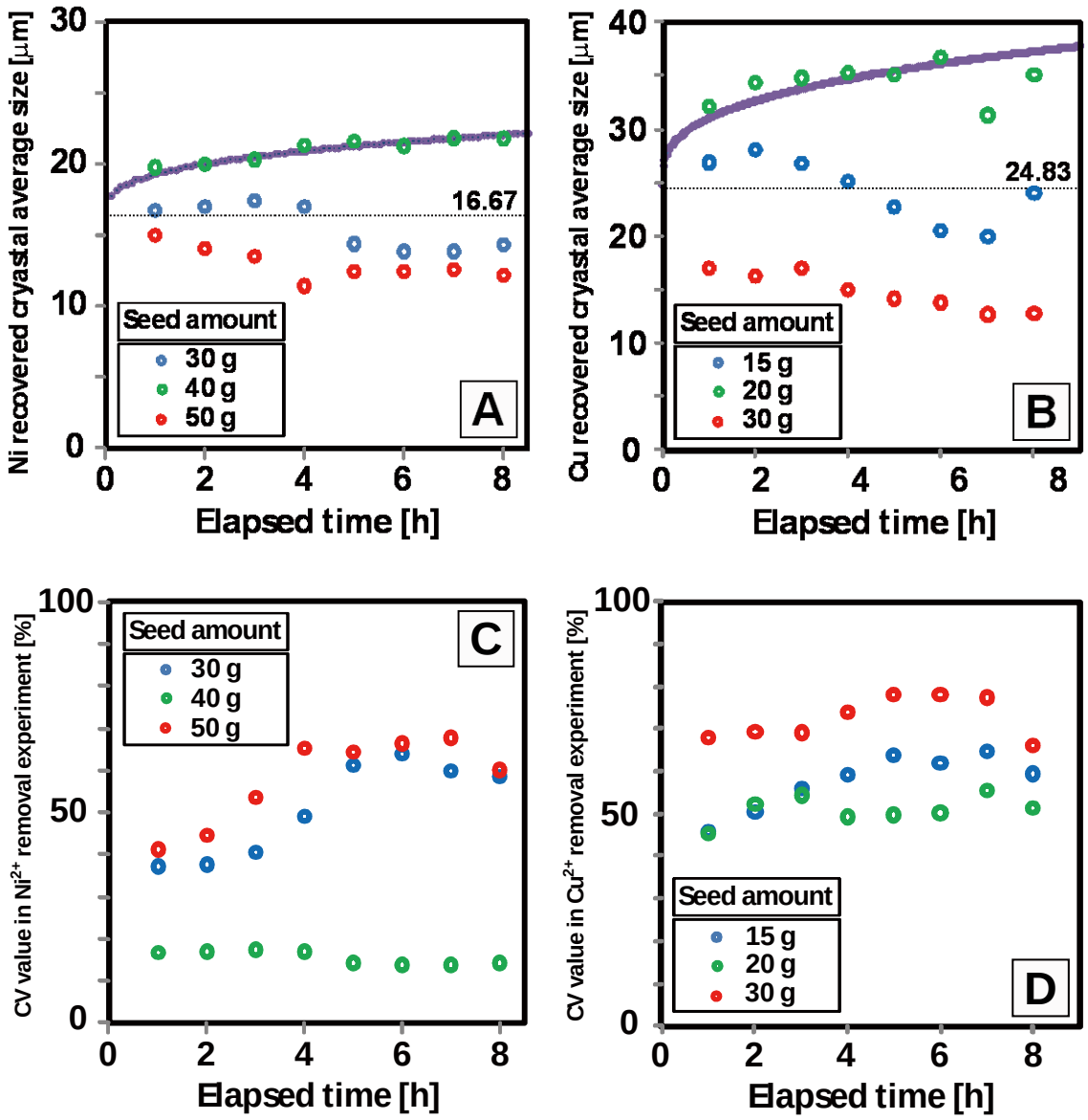

Fig. 3-4 Variation of recovered crystal average size and C.V. value with the operation time ([A, C] nickel ions recovering experiment, [B, D] copper ions recovering experiment).

Because needle-like crystals were stretched to the growth direction fast, crystals were grown large even at an early stage of reaction. Those C.V. values in the optimal condition are low in comparison with other results, thus fine particles production was demonstrated to be restricted. Furthermore, the reason that copper carbonate basics growth needs a small amount of seeds is possibly that this growth arises needle-like and growth surface area can be increased, therefore, smaller amount of seeds approached the maximum growth.

Moreover, we examined the relationship between the normalized mean size: L_p/L_s [-] and the

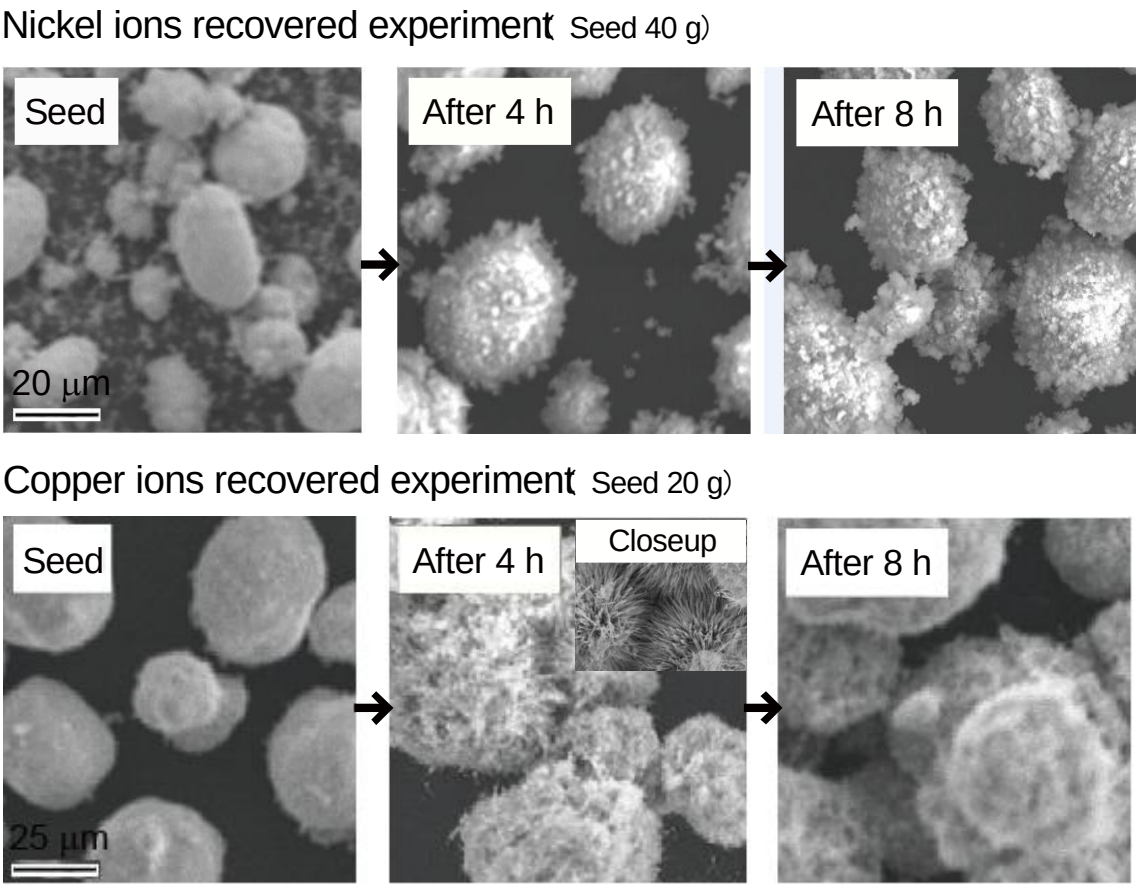

Fig. 3-5 Grown seed crystal SEM images in providing optimum amount of seeds.

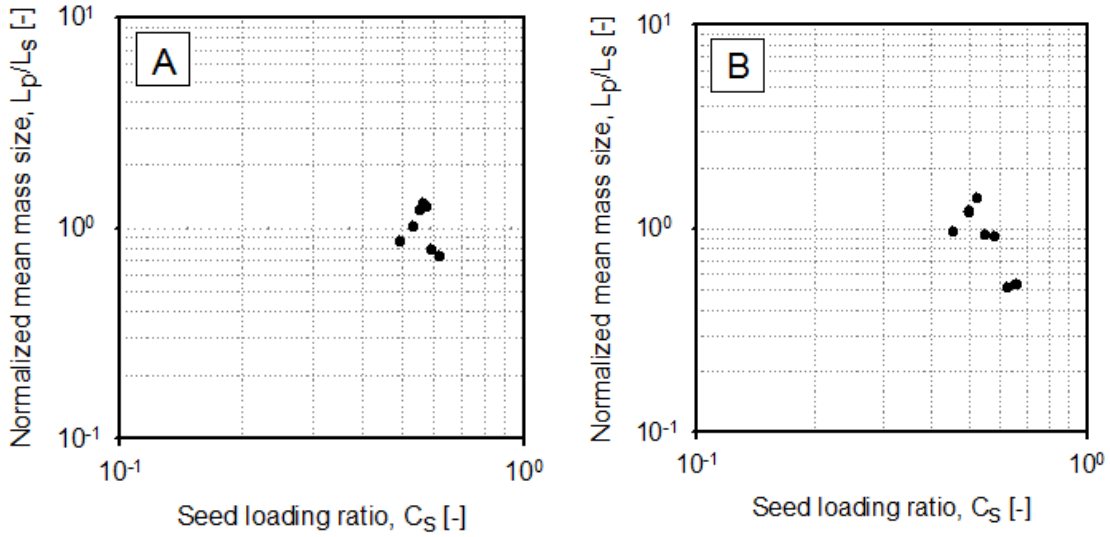

Fig. 3-6 The relationship between seed loading ratio Cs [-] and normalized mean mass size Lp/Ls [-] in the reactive crystallization ([A] nickel ions recovered experiment, [B] copper ions recovered experiment).

seeding ratio: C_s (=W_s/W_{th}) [-] after the 8 hours crystallization, as shown in **Fig. 3-6**. To determine the value of C_s, the mass of the theoretical yield W_{th} [g] is calculated by the following equations, assuming that the whole recovered metal ions are incorporated in seeds and that all crystals are the same materials.

$$W_{th} = W_s + 0.999 \cdot c_I \cdot Q \cdot \frac{w_s}{w_m} \quad (3\text{-}3)$$

The value of W_{th} needs to be remade for the reactive crystallization method. In the equation (Eq. 3-3), characters were defined as below. c_I represents the initial metal ions concentration [g L^{-1}], Q is the amount of solution supplied in this 8 hours operation [L], W_s means the seed input [g], w_s is the seed molecular weight [kg] and w_m is the metal atomic weight [kg]. The reaction rate was around 99.9 % from the result of metal ions recovery rate, as indicated later, and this ratio of metal ions in the solution was regarded to be crystallized. From those illustrations in **Fig. 3-6**, the existence of seed input maximum peak was demonstrated in each experiment, near C_s~0.53, and the values of normalized mean size L_p/L_s were much the same (~1.5) for some reason. In addition to this, the movement of C_s vs. L_p/L_s in these illustrations was found to be similar even if the target metals were different each other.

There are various theories about the seeding effect for recovering metal ions. First, about the seed growth model, the nuclei behavior can be the essential knowledge. On the basis of the summarization and the improvement of previous researches [22-27], the adsorption may largely affect to the nucleation process involving seeds. When seeds are presented in the supersaturated solution, due to the attraction of electrostatic force and van der Waals' force,

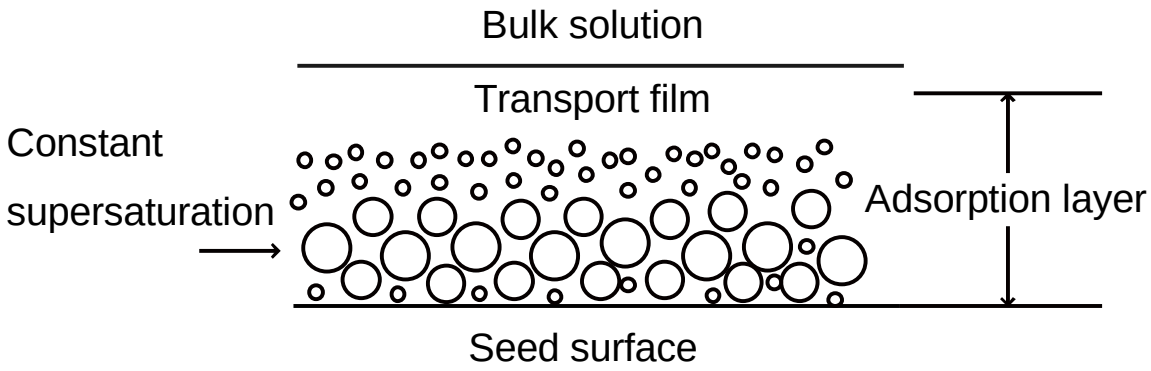

Fig. 3-7 Cluster formation in the adsorption layer.

the nucleic element in the bulk solution will be absorbed to the surface of seeds, forming an adsorption layer. Then, three phases will be formed: the seed phase, the interfacial phase (the adsorption layer) and the liquid phase [26] (**Fig. 3-7**). And the nucleation would occur much easier in the interfacial phase than in the bulk solution.

In above experiments, various nucleations would have been occurred depending on the seed loading. In providing small amount of seeds, the nucleation would occur in the bulk. At that time, nuclei could form various shapes. Meanwhile, in providing large amount of seeds, the contact nucleation (the secondary nucleation) would have been occurred near the seeds surface by the fluid-based grown seeds attrition. In that time as well, nuclei's shapes can be formed variously.

Next, the difference of seed growth mechanisms by the process of metal ions recovery will be discussed. The kinetics theory and metal carbonates morphology by changing various crystallization conditions have been explored in some articles [28-31]. From these articles, the morphology of carbonates growth can be affected by the kinetics, and also even by the crystallization conditions such as the pH and initial concentration of the solution. This forming difference has been supposed to be resulted from the nucleation rate or the growth mechanisms, deriving from the diffusion or the surface-integration. Also, guessingly, seed growth formation seems to have little to do with the kind of metals. Chen et al. [28] have indicated that rounded and floc-like crystals have been formed at higher nucleation rates ($B_0 > 1\times10^9$ [# m^{-3} s^{-1}]), depending on higher relative supersaturation. Meanwhile, needle-like crystals have been easily formed when the nucleation rate B_0 is smaller than 5×10^8 [# m^{-3} s^{-1}], and the corresponding relative supersaturation is small. And it was assumed that granular crystals growth has been dominantly occurred by the diffusion step, whereas, needle-like crystals growth has been mostly controlled by the surface integration step. In applying this theory to our experiment, metal ions supersaturation was estimated to be extremely small under the condition of existing copper carbonate basics, probably because copper seeds have incorporated copper ions so easily, and the copper ions extra concentration in the solution came to be lowered. From experiments, as we will discuss later, when metal ions in the solution are different from metal in seeds, seed growth was occurred just like when the same metals were provided. For example, granular fine particles were produced around nickel carbonate basics even if the different kind of metal ions from seeds were provided in the solution, as we see in next chapter. Therefore, the adsorption strength of metal to seeds can be the key to estimate

the products shape and the optimum seed input.

Kubota et al. have developed the seed chart theory in the cooling mode crystallization [32, 33]. This theory presents the ideal growth line, which indicates a relation between the theoretical dimensionless size L_p/L_s as a function of seed concentration C_s under the condition of no nucleation (Eq. 3-4). Also, based on these theoretical lines, the ideal crystallizer can be designed, and the optimal operation condition without occurring the nucleation can be determined. On the ideal line, the critical seed concentration C_s* has been proposed to determine the optimal operation with no nucleation.

$$\frac{L_p}{L_s} = \left\{\frac{(1+C_s)}{C_s}\right\}^{1/3} \tag{3-4}$$

However, there are some difficulties for connecting this theory to the optimal seed growth proposed in this thesis because of following reasons.

1. The critical seed concentration is not always coinciding with the optimal seed growth in the seed chart theory. In this thesis, the critical seed concentration is defined as the optimal seed amount without occurring nucleation theoretically.
2. Existing seed chart theory cannot be applied to the feed metal ions concentration change.

Then, alternative theory is needed for explaining the seeding effect via the reactive crystallization. This theory assumes that the number of metal ions in the feed solution is proportional to the metal ions concentration. And the metal ions uptake amount is assumed to be proportional to the seed surface area: the square of the seed particle average size. Then the optimum seed input W_{opt} [kg] is introduced as Eq. 3-5 if the constant value is defined as K [m^3].

$$W_{opt} = K \cdot conc. \tag{3-5}$$

The value of K comes to be $1.27 \cdot 10^{-3}$ for nickel ions recovery experiment and $0.632 \cdot 10^{-3}$ for copper ions recovery experiment. And two reminders exist in this theory: one is that seed input has its maximum limitation because if seeds are added too much, excess seeds will stay the bottom of the tank without hovering. And the other reminder is that secondary nucleation by the

collision would less happen in the condition of low metal ions concentration, so more seeds than theory will be needed for the stable seed growth.

In addition to past results, in this semi-batch operation, time dependence on metal ions concentration in the supernatant filtrate during the reaction is shown like **Fig. 3-8**. Metal ions concentration was only about 1 mg L^{-1} on an average from the supernatant during the reaction. This indicates that metal components in stock solution were removed around 99.9 %, and metal ions separation by the reactive crystallization is efficient to satisfy the water quality regulation.

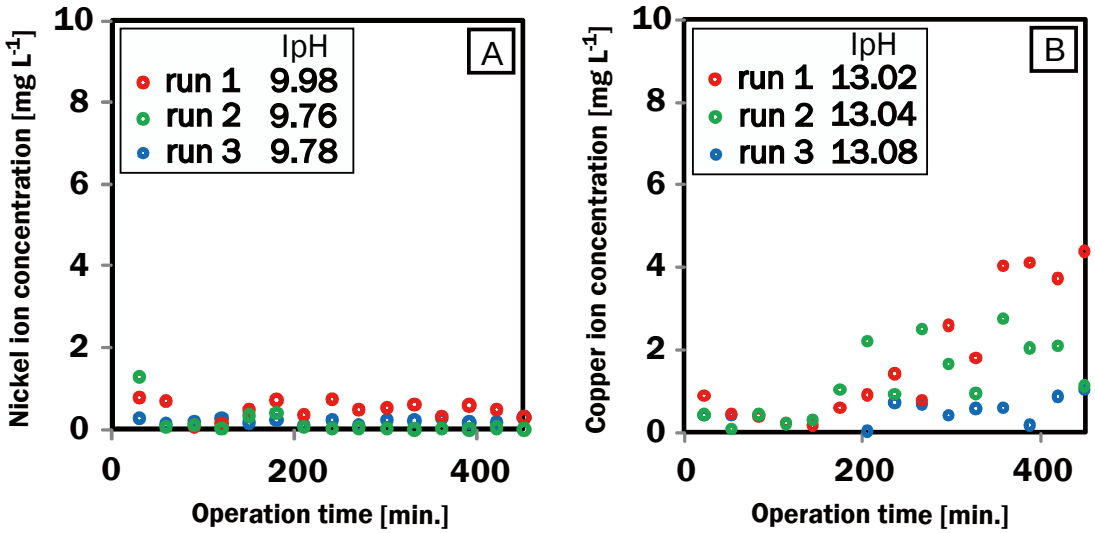

Fig. 3-8 Variation of metal ion concentration in the supernatant filtrate with operation time, optimal amount of seeds were provided in each experiment. Feed metal concentration = 1 000 mg L^{-1}, ([A] nickel ions recovered experiment, [B] copper ions recovered experiment).

3.5 The application and vision of this technology

From past results, the carbonate reactive crystallization treatment can be desirable technology for recovering metal ions from the wastewater. However, if this treatment adopts the real wastewater, many considerations present. In this section, precautions that should be regarded will be listed, and specific methods will be introduced.

At first, the composition of wastewater is considered. If the wastewater contains many types of metal ions and anions, it is recommended to be treated much of them in the preprocessing and to be improved the purity of target metals. Above details will be mentioned in Chapter 4, and here, assuming single metal ions are contained in the stock solution, the procedure for determining the optimum conditions about materials and equipment will be mainly discussed.

In above experiments, risk-free divalent metal ions were chosen and treated, but how can we deal with other metal ions such as monovalent ions or toxic ions? Silver and lithium ions produce regular and angular particles by the reaction, so different ways of the evaluation will be needed. It depends on the user's hope, but if someone desires them spherical, their ions are needed to accumulate on spherical seeds. Most of metals are likely to grow spherically when they are reacted in the presence of spherical seeds. The growth mechanism depends to a large extent on the nucleation rate as we have seen above.

From here, a case of nickel or copper recovery will mainly be focused on. Actually, in treating unitary metal ions, the volume and the shape of tank, the fluid speed, the mass of seeds, agitation speed, and so on, will be determined, in response to the desiring ability of processing [22, 23]. The apparatus will be preferable to the similarity shape of this experimental. However, depending on the space of work area, the width or the height of the crystallizer might be geared to the requirement. The essential condition is probably to make the boundary lines between crystals and supernatant, and to agitate sufficiently for accumulating metal ions on seeds. CSTR operation will be suitable because treated effluent can be flowed out simultaneously with the reaction. This optimization problem seems to be related with so many factors; however, if several initial conditions are given, the optimum seed input, the flowing speed producing desired materials, will be automatically determined [34-36]. Metal ions concentration in the tank in varying the tank volume and the flow speed will be simulated in Chapter 5. And here, the way of determining seed input in operating scale-up will be proposed on the assumption some cases.

Some considerable theories for operating the scale-up will be introduced [22, 23]. Reynolds number *Re* [-] and Froude [-] number *Fr* are often used in designing of agitators (Eq. 3-6, 3-7).

$$\mathrm{Re} = \frac{\rho \mathrm{n} \mathrm{d}^2}{\eta} \tag{3-6}$$

$$\mathrm{Fr} = \frac{\mathrm{n}^2 \mathrm{d}}{\mathrm{g}} \tag{3-7}$$

where *d* is agitator diameter, *n* is agitation speed, ρ means liquid density, η means viscosity, and *g* means gravitational acceleration. *Re* gives the ratio of the inertia and viscous forces, and *Fr* gives the ratio of centrifugal and gravitational acceleration. For exact scale-up purposes, values of both *Re* and *Fr* should be kept constant but this is generally impossible. For example, if the agitator diameter is increase to quadruple, the agitator speed must be reduced by half if *Fr* is kept to be constant ($\mathrm{n} \propto \mathrm{d}^{-\frac{1}{2}}$), but there *Re* will be octuple because other factors cannot be changed ($\mathrm{n} \propto \mathrm{d}^{-2}$). Therefore, it is impossible to satisfy both criteria, and some compromise must be made. For agitated crystallizers, scale-up is generally based on the *Re* number. Moreover, provided the same fluid is being agitated in two different units, the dependence of the agitator speed on the scale-up ratio will be presented as the following equation (Eq. 3-8).

$$\mathrm{n}_1/\mathrm{n}_2 = \mathrm{d}_2/\mathrm{d}_1 \tag{3-8}$$

Another rule for the scale-up, based on considerable practical experience suggests that at a constant magma density and residence time, the quantity R^2/T should be kept constant. Here, *R* is the agitator tip speed, and *T* is the turnover time, i.e. the next equation will be satisfied (crystallizer volume)/(volumetric liquor circulation rate).

Being constant the power per unit volume (PV) is also the most often used in the scale-up strategy because the most basic feature in the agitation process is affected by this parameter [37]. Outside of these, maintaining the geometric similarity will be requested, but this means that be conforming the shape of baffles, paddles, and the reaction tank. The dimension ratio of the crystallizer volume, the width of baffle, the span of blade will be desirable to the same.

Nomenclature

A	surface area of crystals, m^2
c	metal ion concentration in the solution, g L^{-1}
c^*	equilibrium saturation concentration, g L^{-1}
c_I	initial metal ion concentration, g L^{-1}
C_s	seed concentration (=W_s/W_{th}), -
CV	the coefficient of varience, %
d	agitator diameter, m
Fr	Froude number, -
g	gravitational acceleration, m s^{-2}
K	constant value, m^3
k_m	coefficient of mass transfer
L_i	measured diameter of the ith crystal, μm
L_p	mean diameter of produced crystals, μm
L_s	mean diameter of seed crystals, μm
L_{th}	theoretical particle size, μm
n	agitation speed, s^{-1}
n_i	number of counted crystals of component i, #
Q	supplied amount of feed in 8 hours operation, L
r	particle size, m
R	agitator tip speed, m s^{-1}
Re	Reynolds number, -
t	operation time, s
T	turnover time, s
w_m	metal atomic weight, kg
w_s	seed molecular weight, kg
W_{opt}	optimum seed input, kg
W_s	seed input, kg
W_{th}	theoretical yield of crystals, kg
η	viscosity of solution, m^2 s^{-1}
μ	mean value of the normal/Gaussian distribution, μm

ρ	density of solvent, kg m^{-3}
σ	standard deviation of particle size data, μm

References

[1] J. S. Whang, 1982, Soluble-sulfide precipitation for heavy metals removal from wastewaters, *Environ. Prog.*, **1(2)**, 110-113.

[2] B. M. Kim and P. M. Amodeo, 1983, Calcium sulfide process for treatment of metal-containing wastes, *Environ. Prog.*, **2(3)**, 175-180.

[3] D. Wilms, K. Vercaemst and J. C. Van Dijk, 1992, Recovery of silver by crystallization of silver carbonate in a fluidized-bed reactor, *Wat. Res.*, **26 (2)**, 235-239.

[4] G. Macchi, D. Marani, M. Pagano and G. Bagnuolo, 1996, A bench study on lead removal from battery manufacturing wastewater by carbonate precipitation, *Wat. Res.*, **30(12)**, 3032-3036.

[5] A. G. Chmielewski, T. S. Urbanski and W. Migdal, 1997, Separation technologies for metals recovery from industrial wastes, *Hydrometallurgy*, **45**, 333-344.

[6] P. Zhou and Ju-Chang Huang, Alfred W. F. Li and Shirly Wei, 1999, Heavy metal removal from wastewater in fluidized bed reactor, *Wat. Res.*, **33(8)**, 1918-1924.

[7] J. Paul Chen and H. Yu, 2000, Lead removal from synthetic wastewater by crystallization in a fluidized-bed reactor, *J. Environmental Science and Health, Part A*, **35(6)**, 817-835.

[8] D. Feng, C. Aldrich and H. Tan, 2000, Treatment of acid mine water by use of heavy metal precipitation and ion exchange, *Min. Eng.*, **13(6)**, 623-642.

[9] D. Guillard and A. E. Lewis, 2001, Nickel carbonate precipitation in a fluidized-bed reactor, *Ind. Eng. Chem. Res.,* **40**, 5564-5569.

[10] C. I. Lee, W. F. Yang and C. I. Hsieh, 2003, Removal of Cu(II) from aqueous solution in a fluidized-bed reactor, *Chemosphere*, **57**, 1173-1180.

[11] C. I. Lee and W. F. Yang, 2005, Heavy metal removal from aqueous solution in sequential fluidized-bed reactors, *Environ. Technol.*, **26**, 1345-1353.

[12] R. P. van Hille, K. A. Peterson and A. E. Lewis, 2005, Copper sulphide precipitation in a fluidised bed reactor, *Chem. Eng. Sci.*, **60**, 2571-2578.

[13] V. C. Taty Costodes and Alison E. Lewis, 2006, Reactive crystallization of nickel hydroxyl-carbonate in fluidized-bed reactor: Fines production and column design, *Chem. Eng. Sci.*, **61**, 1377-1385.

[14] R. Aldaco, A. Garea and A. Irabien, 2007, Particle growth kinetics of calcium fluoride in a fluidized bed reactor, *Chem. Eng. Sci.*, **62**, 2958-2966.

[15] C. Huang, J. R. Pan, M. Lee and S. Yen, 2007, Treatment of high-level arsenic-containing

wastewater by fluidized bed crystallization process, *J. Chem. Technol. Biotechnol.*, **82**, 289-294.

[16] L. Li, S. Xu, Z. Ju and F. Wu, 2009, Recovery of Ni, Co, and rare earth from spent Ni-metal hydrate batteries and preparation of spherical $Ni(OH)_2$, *Hydrometallurgy*, **100**, 41-46.

[17] S. Tait, W. P. Clarke, J. Keller and D. J. Batstone, 2009, Removal of sulfate from high-strength wastewater by crystallization, *Water Res.*, **43**, 762-772.

[18] S. McAnally and L. Benfield, 1984, Nickel removal from a synthetic nickel-plating wastewater using sulfide and carbonate for precipitation and coprecipitation, *Sep. Sci. Technol.*, **19(2&3)**, 191-217.

[19] R. W. Peters and Y. Ku, 1987, Seeding the metal hydroxide/metal sulfide reactor with activated carbon, *Environ. Prog.*, **6(2)**, 125-132.

[20] Y. Z. Sun, X. F. Song, J. Wan, Y. Luo and J. G. Yu, 2009, Seeded induction period and secondary nucleation of lithium carbonate, *Guocheng Guochang Xuebao,* **9(4)**, 652-660.

[21] Y. Shimizu and I. Hirasawa, 2012, Effect of seeding on metal ion recovery from wastewater by carbonate reactive crystallization, *Chem. Eng. Technol.*, **35(9)**, 1588-1592.

[22] J. W. Mullin, 1993, Crystallization, Third ed. *Butterworth-Heinemann, Oxford*, 202-217.

[23] A. Mersmann, 2001, Crystallization technology handbook, Second ed. *Marcel Dekker Inc., New York.*

[24] J. Garside, A. Mersmann and J. Nyvlt, 2002, Measurement of crystal growth and nucleation rates, *Institution of Chemical Engineers (IChemE).*

[25] A. Mersmann and K. Bartosch, 1998, How to predict the metastable zone, *J. Cryst. Growth*, **183 (1&2)**, 240-250.

[26] C. Y. Tai and J. F. Wu, 1992, Interfacial supersaturation, secondary nucleation, and crystal growth, *J. Cryst. Growth*, **116 (3&4)**, 294-306.

[27] R. Y. Qian and G. D. Botsaris, 1997, A new mechanism for nuclei formation in suspension crystallizers: the role of interparticle forces, *Chem. Eng. Sci.*, **52(20)**, 3429-3440.

[28] P. C. Chen, G. Y. Cheng, M. H. Kou, P. Y. Shia and P. O. Chung, 2001, Nucleation and morphology of barium carbonate crystals in a semi-batch crystallizer, *J. Cryst. Growth*, **226**, 458-472.

[29] N. Kubota, T. Sekimoto and K. Shimizu, 1990, Precipitation of $BaCO_3$ in a semi-batch reactor with double-tube gas injection nozzle, *J. Cryst. Growth*, **102**, 434-440.

[30] P. H. Nore and A. Mersmann, 1993, Batch precipitation of barium carbonate, *Chem. Eng.*

Sci., **48(17)**, 3083-3088.

[31] H. Tanaka and T. Nishi, 1989, Local phase separation at the growth front of a polymer spherulite during crystallization and nonlinear spherulitic growth in a polymer mixture with a phase diagram, *Physical Review A*, **39(2)**, 783-794.

[32] N. Kubota, N. Doki, M. Yokota and D. Jagadesh, 2002, Seeding effect on product crystal size in batch crystallization, *J. Chem. Eng. Jpn.*, **35(11)**, 1063-1071.

[33] N. Kubota, N. Doki, M. Yokota and A. Sato, 2001, Seeding policy in batch cooling crystallization, *Powder Technol.*, **121**, 31-38.

[34] D. Jagadesh, N. Kubota, M. Yokota, N. Doki and A. Sato, 1999, Seeding effect on batch crystallization of potassium sulfate under natural cooling mode and a simple design method of crystallizer, *J. Chem. Eng. Jpn.,* **32 (4)**, 514-520.

[35] J. Garside and R. J. Davey, 1980, Invited review; Secondary contact nucleation: kinetics, growth and scale-up, *Chem. Eng. Commun.*, **4**, 393-424.

[36] N. Doki, N. Kubota, A. Sato and M. Yokota, 1999, Scaleup experiments on seeded batch cooling crystallization of potassium alum, *AIChE Journal*, **45(12)**, 2527-2533.

[37] Kobelco eco-solutions co., ltd., homepage: http://www.kobelco-eco.co.jp/product/process/mixing/mixing_003.html

Chapter 4

Impurities uptake on carbonate separation for the wastewater

In this chapter, the reactive crystallization was developed with designing to separate nickel or copper ions from effluent for applying to actual industrial wastewater containing impurities. The primary reaction is the same as in chapter 3, and during the process of nickel or copper ions uptake, inhibitory effect on seed growth of impurities was investigated.

4.1 Introduction

In typical appearance, the industrial effluent raw water contains multiple kinds of metal ions. Many scientists have examined the co-precipitation, impurities uptake and separation mechanisms under each background [1-22]. Some have found the order of metal ions uptake rate to particular seeds and others have examined the pH range that metal ions can be selectively separated efficiently with the use of difference of solubility products. Impurities effect on target crystallization has been also explored from many aspects. Impurities concentration is one of factors that contribute to the seed growth inhibition. Crystals that incorporate impurities once are difficult to separate by the chemical or physical treatment, so it seems more desirable to uptake each ions separately in the process of crystallization.

In this chapter, on the basis of nickel or copper ions crystallization in the regulated solution, seeds growth inhibition mechanisms by the action of one type of heterogeneous ions were examined. In the primary reaction, a metal sulfate solution was reacted with a sodium carbonate solution. And as impurities, divalent metal ions such as cobalt, manganese, or zinc ions or anions, borate ions or phosphate ions were mixed in the stock solution and reacted. In the process of target and impurity ions uptake in seeds, crystal surface roughness, crystals size distribution and metals existence mole ratio were examined. Along with observing crystals growth over the experimental time, metal initial uptake rate was calculated. In addition, the variation of time with metal ions concentration in the effluent filtrate was analyzed. Furthermore, the centrifugation was performed to obtained materials, and the purity improvement from the difference in their specific gravities has been confirmed.

4.2 Experimental approach and measurement items

Semi-batch reactive crystallization was operated in a columned-shaped tank which was installed with a heat conditioner and an agitator in the same way as shown in chapter 3 [23] (**Fig. 3-1, 2**). Spherical seeds: metal carbonate basics (Wako Pure Chemical Industries, Ltd., Osaka, Japan) are dosed in a reaction tank preliminarily. The source of target metal ions was $NiSO_4.6H_2O$ or $CuSO_4.5H_2O$, and impurities were provided in the form of $CoSO_4.7H_2O$, $MnSO_4.6H_2O$, or $ZnSO_4.7H_2O$ as metal ions and boric acid or phosphoric acid as anions (all from Wako) solution. The solution containing 1 000 mg L^{-1} target and one type of impurity metal ions was mixed with sodium carbonate (Wako) solution on a double-jet basis. The concentration of impurity ions was coordinated at various values, and the standard value in the solution was 1 000 mg L^{-1} impurity metal ions or 0.1 M anions. Along with this, carbonate ions concentration in the sodium carbonate solution was regulated at sufficient amount to keep the optimum reaction molar ratio during the reaction. Each solution was provided at the feeding speed of 0.010 L min^{-1}, and the supernatant effluent was drained to keep the solution volume in the tank constant, 1.3 L. Each solution was calibrated and prepared by deionized water. And the solution temperature in the tank was maintained at 303±0.1 K. The agitation rate was set at about 150 rpm. To investigate the mechanism of fixing metal ions onto seeds, 8 hours reactive crystallization was conducted. The seed input was set 40±0.1 g in the nickel ion removal experiment and 20±0.1 g in the copper ion removal experiment. And, the solution initial pH was controlled at each optimum value for crystallization: at 9.7±0.2 in the nickel ions recovery experiment and at 13±0.2 in the copper ions recovery experiments.

Supernatant and mixed suspension from the tank was sampled at regular interval. Obtained crystals nature and the metal ions distribution on the produced crystals surface were observed by SEM (H8100A/200 kV, Hitachi, Ltd., Tokyo and VE-8800, KEYENCE, Osaka) equipped with energy dispersive X-ray spectrometry (EDX). And also, the content of specific metal in produced crystals was measured by X-ray Fluorescence Analysis (XRF: ZSX Primus II, RIGAKU, Tokyo). From analyzed data, metal ions uptake rate per one particle surface area R_T: for target ions and R_I: for impurity ions were determined. Suspended solution obtained after 8 hours crystallization was centrifuged at the rate of 10 000 rpm and for 30 min. by a centrifugal machine (MX-301, Tomy, Tokyo) and analyzed their purity improvement. Metal ions concentration in the supernatant filtrate was analyzed by ICP (IRIS-Intrepid, Thermo Fisher Scientific K.K., Yokohama) device.

4.3 Metal impurities uptake on seed crystals

Representative crystals obtained by this reactive crystallization are shown in **Fig. 4-1**. In the presence of manganese ions as impurities, they were reacted with carbonate ions in the early stage of the reaction, and spherical manganese carbonate grains were clearly formed. Meanwhile, in the presence of zinc or cobalt ions as impurities, they crystallized just like target ions and impurity components incorporated into seeds with uniformly. Granular fine particles were produced around nickel carbonate basics. While, needle-like crystals appeared on the surface of copper carbonate basics and finally crystals seemed to grow from the center of seeds even under the existence of impurities.

From the crystallization associated with impurities, three morphological components: seeds, compounds, and fine particles have been found out (**Fig. 4-2**). Metal ions constructed crystal groups that are misshaped and have poor dispersibility, via these crystallization operations. Then, from the analyses of the EDX image of nickel carbonate basics growth, target and impurity ions were both incorporated in fine particles and compounds at similar rate but almost all particles were found to be mainly composed of target ions. This indicates that target metal ions form crystals and are incorporated easily.

To examine metal ions uptake phenomena further, metal ions uptake rate on seed particles was calculated from XRF qualitative analyses. Time variation of the metal element existence mole ratio constructing produced crystals is described in **Fig. 4-3**. From these plot data, target and impurity ions uptake rate per unit surface area (r_T and r_I) were calculated using below mole ratio balance equation (Eq. 4-1). And in this equation, m_0 is metal mole in seeds and M_T represents target metal mole ratio in seeds. And from these data, target and impurity ions initial uptake rate per unit surface area: R_{T0} and R_{I0} were calculated using input seeds surface area A_0 (Eq. 4-2, 3). Seeds surface area was estimated from more than 300 seed particles measured sizes (Eq. 4-4). These estimated values were summarized in **Table 4-1**. The reason initial values were applied is that crystals surface area has been changing intricately during the reaction, and the uptake rate value R can also be changing.

$$M_T = (m_0 + r_T \cdot t)/(m_0 + r_T \cdot t + r_I \cdot t) \quad (4\text{-}1)$$

$$R_{T0} = r_T/A_0 \quad (4\text{-}2)$$

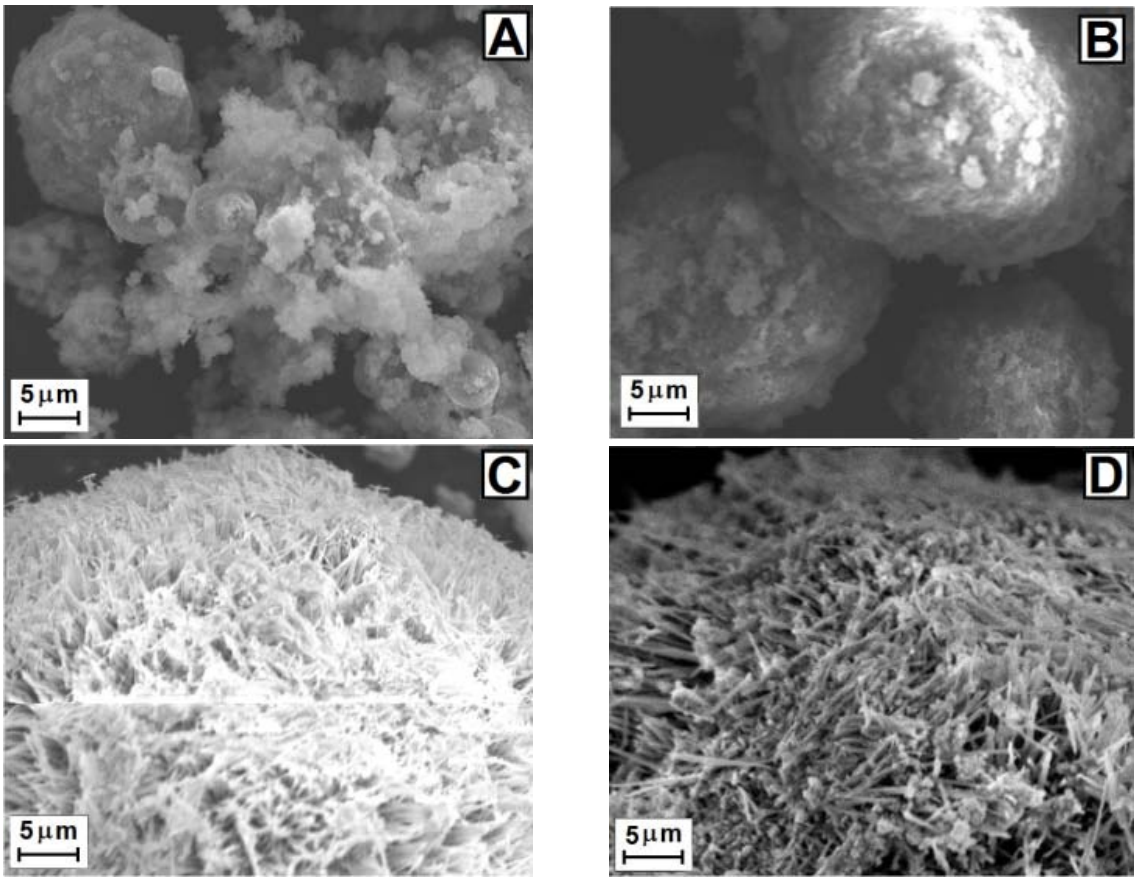

Fig. 4-1 Grown seeds SEM images observed after the reactive crystallization ([A] nickel/ manganese, [B] nickel/zinc, [C] copper/cobalt, [D] copper/zinc ions removal experiment).

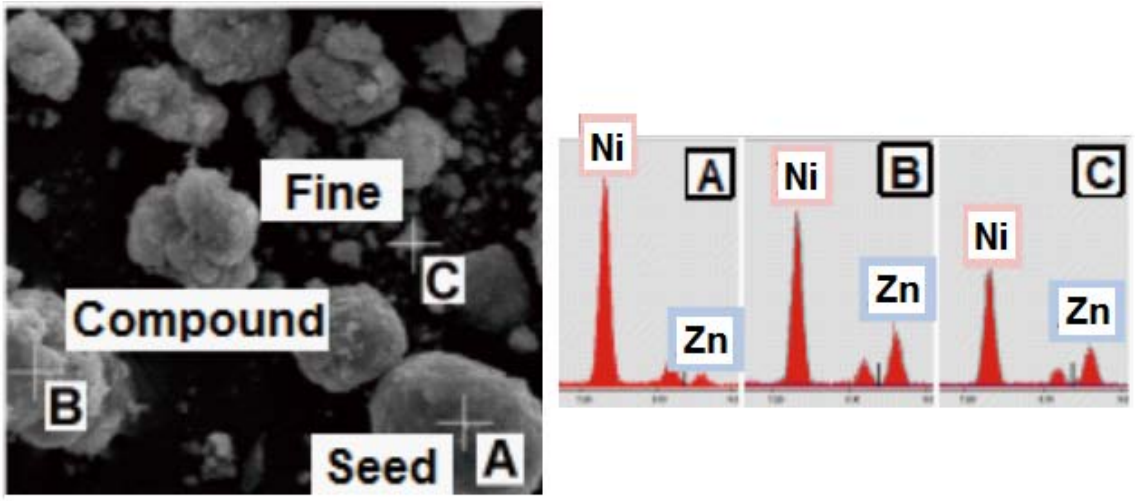

Fig. 4-2 Grown seeds SEM images observed after the crystallization and the composing metal ions number (nickel/zinc ion removal experiment. vertical scales: the number of metal ions [-] and horizontal scales: ions energy [keV], [A] seed, [B] compound, [C] fine particle).

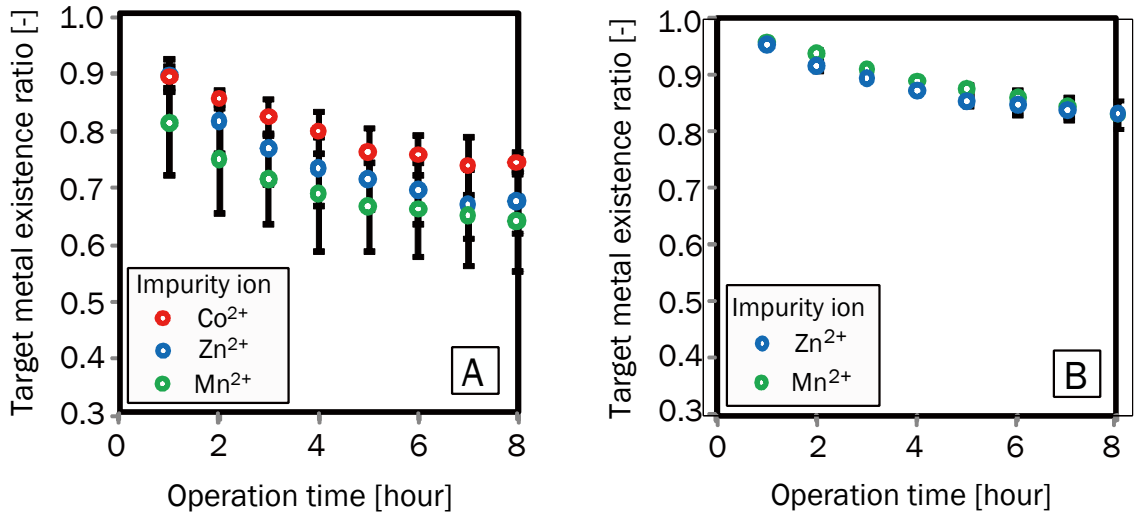

Fig. 4-3 Time variation of the existence mole ratio of target metals in sampled crystals ([A] experiments base on copper carbonate basics, [B] experiments based on nickel carbonate basics).

Table 4-1 Estimated values of metal ions uptake rate per unit surface area.

Seeds	Copper Carbonate Basic		Nickel Carbonate Basic	
Impurity	R_T [10^{-8} mol m^{-2} s^{-1}]	R_I [10^{-8} mol m^{-2} s^{-1}]	R_T [10^{-9} mol m^{-2} s^{-1}]	R_I [10^{-9} mol m^{-2} s^{-1}]
Co^{2+}	2.914	1.604	not available	not available
Zn^{2+}	2.119	1.854	1.951	0.5573
Mn^{2+}	5.756	4.074	3.030	0.8012

$$R_{I0} = r_I / A_0 \tag{4-3}$$

$$A_0 = A_{unit} \cdot N \tag{4-4}$$

The initial uptake rate against the nickel carbonate basic is not fast, and the value of R_{I0} has been about one fourth that of the value of R_{T0}. Copper and impurity ions both were incorporated readily on copper carbonate basics and the proportion of R_{I0} and R_{T0} was between half and one. The reason of this ease of uptake to copper is estimated to relate to high metal ions adsorption force. Another reason is that copper carbonate basics form needle-like products in this initial reaction and they can enlarge the uptake site.

By performing the centrifuging to obtained suspension, solid contents would be separated by the difference of specific weight. The target metal mole ratio in the condensate was also analyzed by XRF (**Fig. 4-4**). Target metal mole ratio was improved by from 10 to 20 % in the experiment based on copper carbonate basics. Meanwhile, this value did not change in the experiment based on nickel carbonate basics. Part that cannot be separated by the gravity separation was likely to be incorporated inside of crystals. Purity improvement by the physical treatment seemed to have definite ceiling in around 80 %.

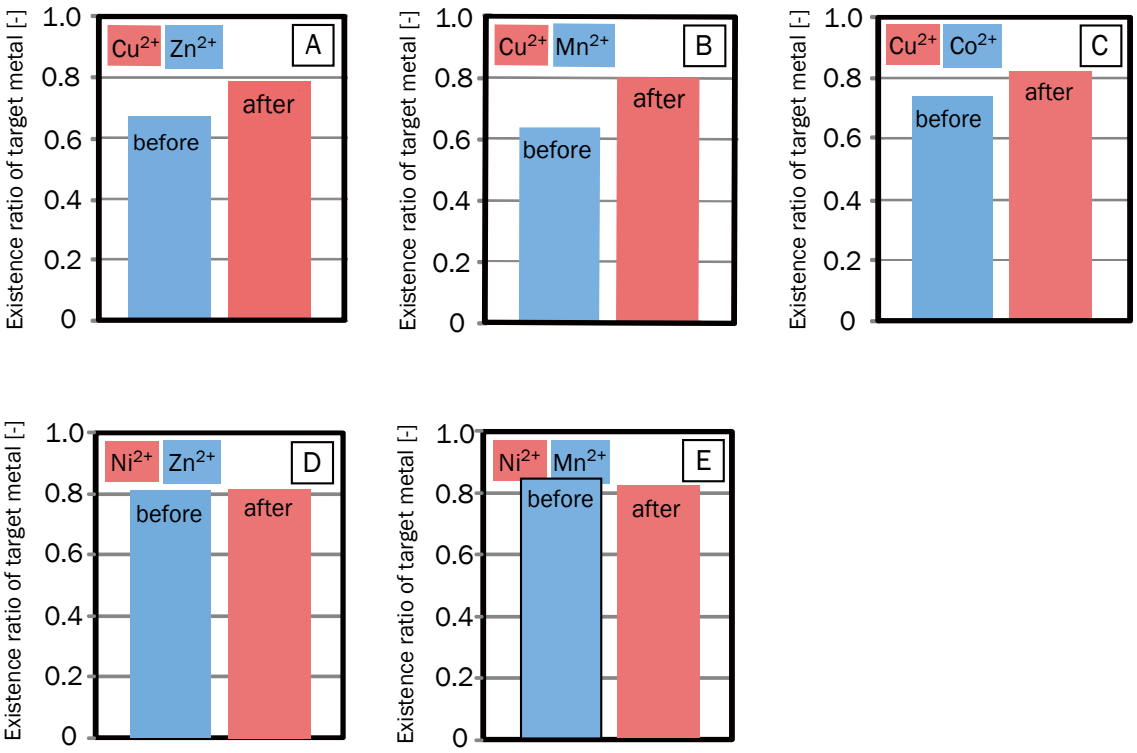

Fig. 4-4 Target metals mole ratio before and after the centrifugation ([A] copper/zinc, [B] copper/manganese, [C] copper/cobalt, [D] nickel/zinc, [E] nickel/manganese ions removal experiment).

Some scientists have examined the metal ions adsorption strength against materials during the precipitation. For example, Uzun et al.[13] proved that the ease of heavy metal ions adsorption varies from target materials. The adsorption strength was in the order of $Cu^{2+}>Ni^{2+}>Fe^{2+}>Mn^{2+}$ against activated carbon or chitosan, and in the order of $Mn^{2+}>Cu^{2+}>Ni^{2+}>Fe^{2+}$ against ager. El-korachy[17] found that metal ions uptake reaction to calcium carbonate in the form of calcite was to be in the following order: $Pb^{2+}>Cu^{2+}>Zn^{2+}>Cd^{2+}\approx Fe^{2+}$. It has been conceived that the

heavy metal ions uptake proceeds via the cation exchange and the crystallization. Handona et al. [18] examined the retardation effect of the metal ions against the crystallization of calcium sulfate (gypsum). The experiment about metal ions direct adsorption on the surface of gypsum crystals has been performed for the comparison. The precipitation speed is in the following order: $Cd^{2+}>Cu^{2+}>Fe^{2+}>Cr^{2+}$. This order has been proved to be coincident with the adsorption strength order. Moreover, Pickering [7] has examined the relationship between the metal ions adsorption strength and the pH changing. The adsorption amount of zinc ions against calcium carbonate was comparatively small at pH<6.5, increasing to near the double of this value in the pH range from 6.5 to 7.6.

As we have seen, it was assumed that crystals growth inhibitor ions can retard or block the growth process, and these effects can be explained by their preferential adsorption at active growth sites on crystal surfaces. For establishing the inhibitory effect in the crystallization, it is effective to examine the adsorption strength against objective materials. The degree of inhibition may be interpreted in terms of Langmuir adsorption isotherm theory (Eq. 4-5) [24-26].

$$\theta = \frac{R_0}{R_0 - R_i} \tag{4-5}$$

where θ is the surface coverage [-], R_0 is the growth rate without impurity [m s^{-1}] and R_i means the growth rate with impurity [m s^{-1}].

Kubota et al. [27-30] have presented a mathematical model describing crystal growth rates in the aqueous solution by the use of above Langmuir adsorption isotherm. This model assumes that the step velocity decreases linearly to zero with increasing surface coverage (θ_{eq}) by impurities adsorbed on the growing crystals, and a proportionality constant α is introduced to consider the effectiveness of impurities (Eq. 4-6). When $\alpha>1$, the step velocity is stopped at $\theta_{eq}<1$, (incomplete coverage of active sites for adsorption). In the case of $\alpha=1$, the velocity reaches zero just at $\theta_{eq}=1$ (complete coverage), and for $\alpha<1$, it never becomes zero even at $\theta_{eq}=1$ but approaches a limiting value.

$$V/V_0 = 1 - \alpha\theta_{eq} \tag{4-6}$$

In equation 4-6, V means the step velocity and V_0 is the step velocity in a pure system [m s^{-1}]. They also have examined the relationship between the crystal growth rate and the solution supersaturation in the presence of impurities. Impurities generally retard the crystal growth [31, 32]. When impurities present in the reaction solution, the crystal growth will be inhibited at the same supersaturation. And with the increase of the critical relative concentration as a function of impurity concentration, crystals growth rate depressed at that rate. As for the mechanism of adsorption, it was proposed that the growth rate controlled by the surface integration process at low solution supersaturation, and mainly by the diffusion process at high supersaturation.

Some researchers also have examined the metal ions adsorption behavior and indicated some ideas against metals separation. Verbann [15] has examined the impurity uptake behavior via the reactive crystallization from the view of ions adsorption. By varying operation parameters, conditions so as not to incorporate impurity ions to seeds have been explored. In general, the impurities uptake was found to be depressed at low pH and elevated temperatures. Also, adsorption experiments were performed with and without seeds, and in general the impurities uptake was found to be depressed in the presence of seeds.

Some researches proved impurity ions concentration also affect the seed growth. Berner et al. [4] have examined the role of magnesium ions in the calcite crystal growth and found that at level less than about 5 mole % magnesium ions concentration, magnesium ions have little or no effect on calcite growth. By contrast, in containing from 7 to 10 mole % magnesium carbonate solution caused the rate inhibition due to its incorporation within the calcite crystal structure. Michael et al. [5, 6] have also studied the inhibition of calcium carbonate crystallization by magnesium ions and obtained the similar results. They found that small concentration of magnesium ions (10^{-5} M) had almost no inhibitory effect on crystallization. While, magnesium concentration at 10^{-3} M nearly stopped calcite growth. Compared to phosphate ions, known as calcite growth inhibitor, it has been found that magnesium ions were not the effective inhibitor.

Metal ions uptake mechanism somewhat relates to the co-precipitation process. Some scientists have defined five major types of co-precipitation such as the following [1, 15].

a. Surface adsorption: Impurities are not incorporated into the internal crystal structure, but stay absorbed to the outer surface of the precipitate. This involves a primary adsorbed ion

layer, which is held tightly, and a counter-ion layer, which is held more or less loosely. Surface properties of the forming solid phase (including electrostatic charge) serve to attract or repel secondary constituents in the surrounding aqueous matrix.

b. Occlusion: In this case, impurities are not incorporating in the crystal lattice, but are adsorbed during the growth of the crystals and give rise to the formation of imperfections in the crystal. Adsorptions during the crystals growth are primarily responsible for the amount of occlusion.
c. Isomorphic inclusion (mixed crystal formation): Impurities fit nicely incorporate into the crystal lattice and they do not change the lattice regular structure. Mixed crystal formation amount depends on the adsorption degree during the reaction.
d. Mechanical entrapment: This involves the physical enclosure of a small portion of the mother liquor with tiny hollows or flaws that form during the rapid growth and coalescence of crystals. These pockets remain filled with the mother liquor and eventually become completely enclosed by the precipitate.
e. Post-precipitation: The precipitate is allowed to stand in contact with the mother liquor, and a second substance will slowly from a precipitate with the precipitating reagent. This type of precipitate contamination is closely associated with surface adsorption.

Regardless of the type of co-precipitation, the initial incorporation of the impurity into the solid phase is the result of adsorption. This adsorption may be due to chemisorptions, occurring from the coordination between the impurity and one or more constituent ions of the crystal lattice constructed by electrostatic interactions, Van der Waal's forces, or dipole-dipole interactions. From the elements of physical adsorption, metal atoms that adsorbed to seeds are easily desorbed by the physical operation, because Van der Waal's forces are comparatively slight mutual effects. This can account for the result of the uptake and the centrifugal separation. And another thing, the same metal ions as seeds were not well separated by the physical operation so this proved that target metal ions incorporated to seeds by highly stronger connection.

It can be concluded that metal components that can be separated by the physical treatment such as centrifuging were incorporated mainly by the adsorption described above type a. And probably, metal components that cannot be separated by these treatments were likely to be constructed mainly by the co-precipitation described above type of b, c, d or e.

Next, time variation of metal ions concentration in the effluent filtrate during 8 hours operation was summarized in **Fig. 4-6**. From these figures, target and impurity ions concentration in the effluent supernatant filtrate were both almost below 10 mg L^{-1} on an average during the reaction. This indicates that target metal components and impurities in stock solution were removed around 99 %. And this means that metal ion separation operation by reactive crystallization is efficient to remove metal ions. Also in the next stage, separation and purification of obtained crystals will come to be notable questions.

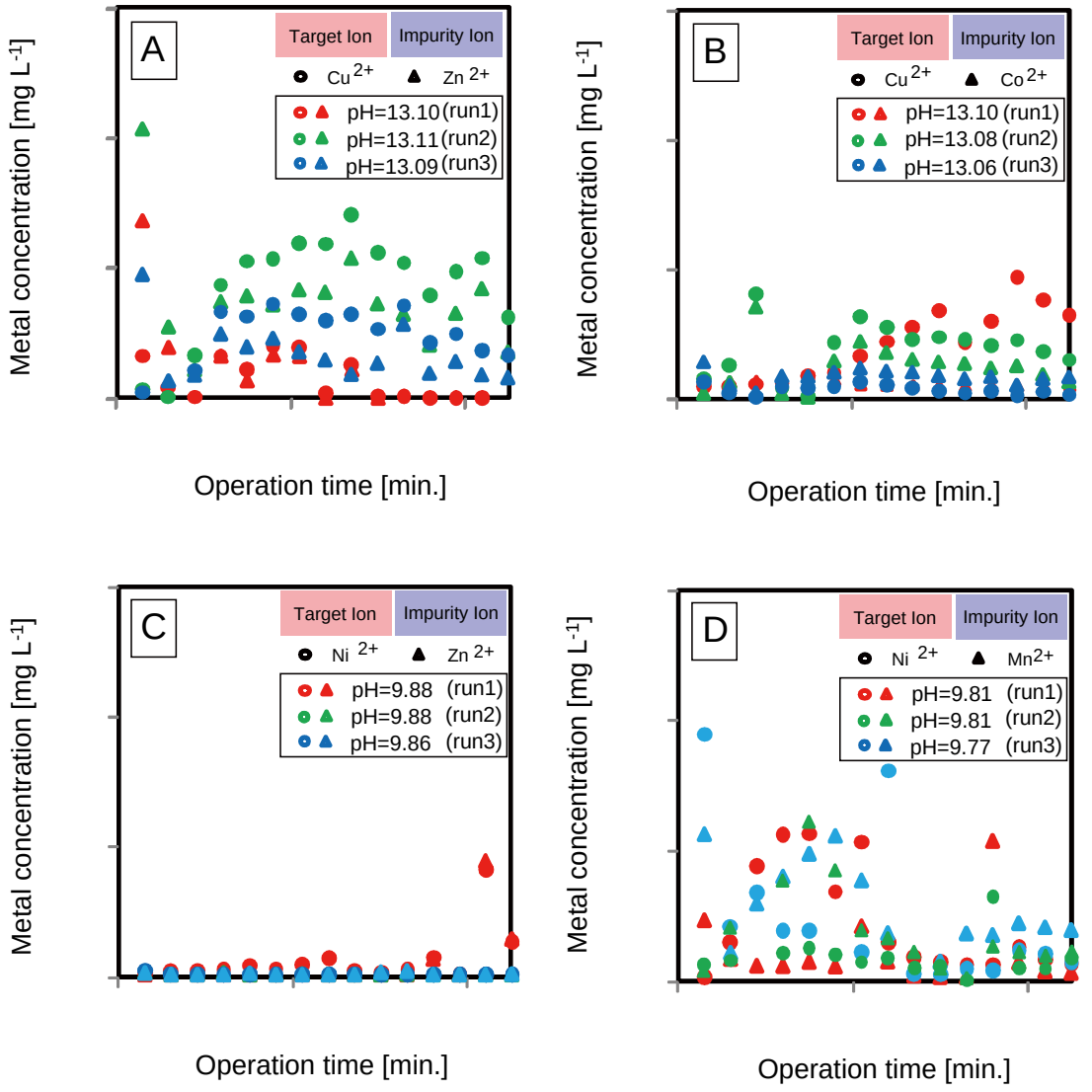

Fig. 4-6 Time transition of metal ions concentration in the supernatant filtrate ([A] copper/zinc, [B] copper/cobalt, [C] nickel/zinc, [D] nickel/manganese ions removal experiment).

4.4 Anion impurities uptake on seed crystals

In providing boric acid and phosphoric acid as anion impurities during the 8 hours reaction, time variation of produced crystals appearance, average size and C. V. value are described as following figures (**Figs. 4-7, 8**). It has been found that the seeds growth mechanism was different by the kind of anions. When borate ions were provided as impurities, seeds surface has gotten rough but the particles average size has been enlarged gradually because the particulates production was restricted. Meanwhile, in providing phosphate ions as impurities, with the increase of the anions concentration, more fine particles have been produced and the particles average size has been smaller. Especially in this case, it has been found that even the existence of low concentration anions enormously affected the seed growth. And these results indicate that the kind of anions give the various effect to this reaction. As for the C. V. value, the regular change by the anions addition has not been found out.

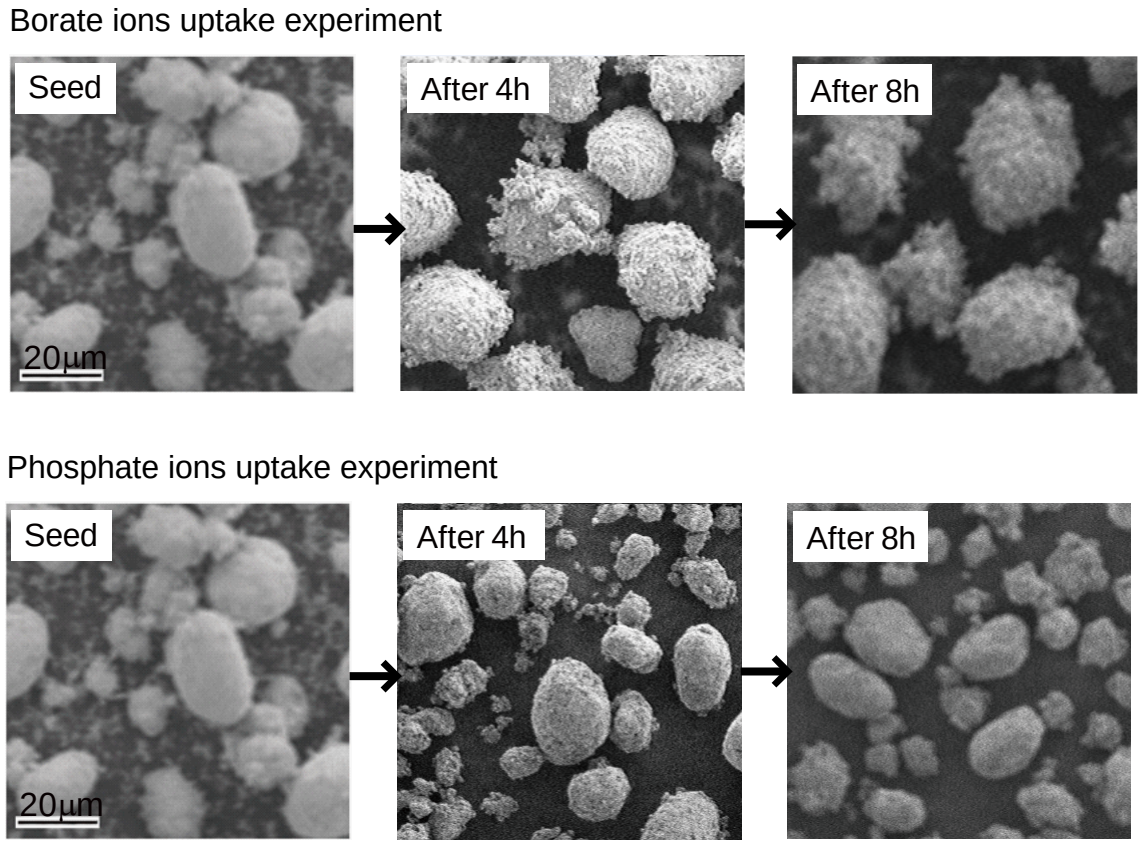

Fig. 4-7 Grown seed crystal SEM images in providing 0.1 M anion impurities.

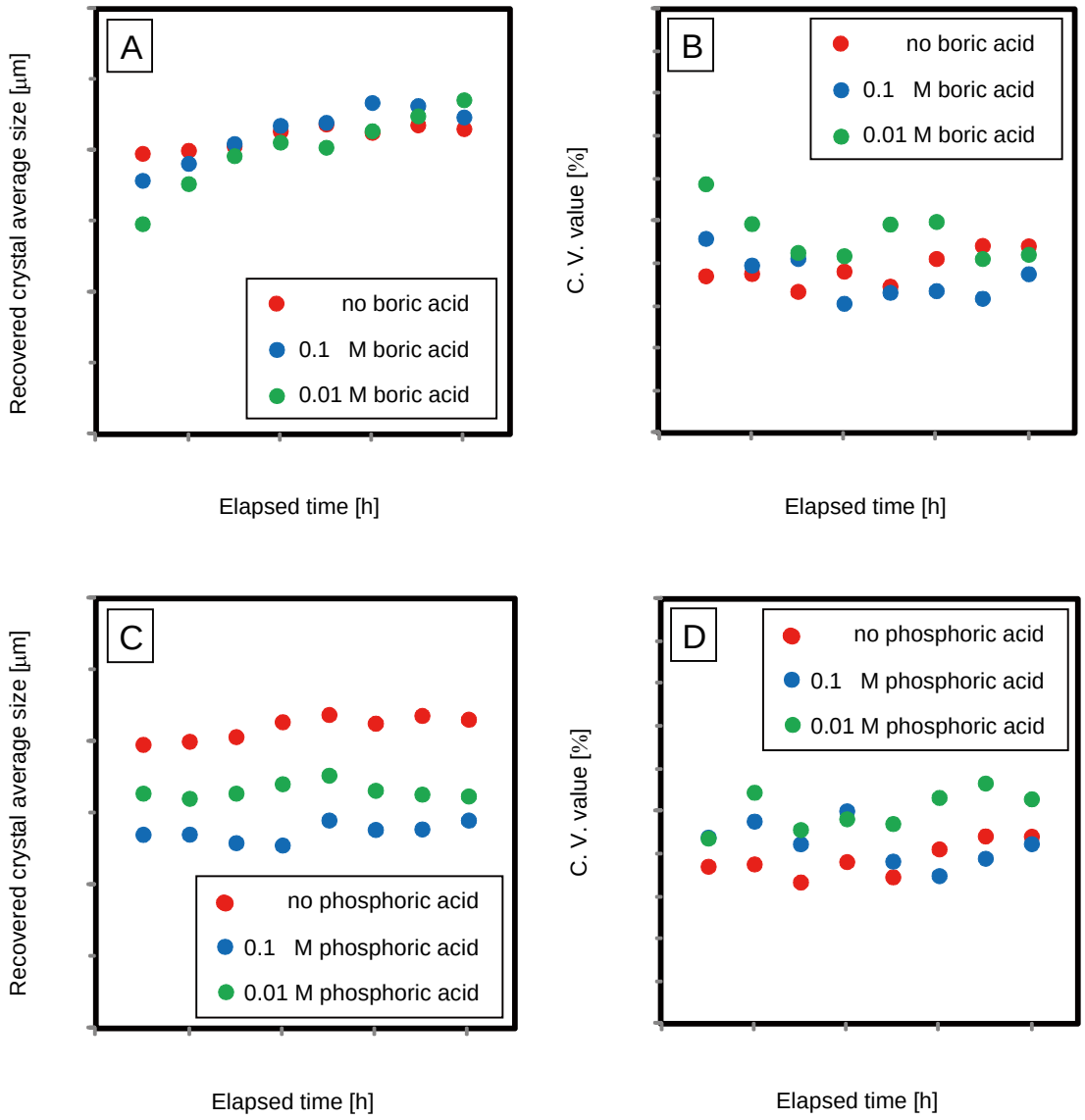

Fig. 4-8 Time variation of produced crystal average size and C. V. value in adding anions as impurities ([A, B] in providing borate ions as impurities, [C, D] in providing phosphate ions as impurities.

4.5 Strategies for Impurities-Free Crystallization

Some researchers attempted to separate metal ions from the wastewater by pH controlling with the use of solubility difference. If this theory applies to the real wastewater management, dual or triple stages of treatment equipment will be prepared.

Soya et al. [20] have examined the selective sulfidation of nickel-zinc-copper mixed solution with calcium sulfide (CaS) at different pH. At pH range from 1.9 to 2.0, copper ions were selectively precipitated and in a range from 4.0 to 6.0, zinc ions were selectively sulfurized. Fukuda et al. [22] also have attempted to separate copper, zinc and nickel component contained in plating wastewater by the sulfuration treatment. Coordinated plating solutions containing these metals were treated with sodium sulfides (Na_2S). In the pH range from 1.4 to 1.5, copper ions were first separated from the solution as copper sulfides. Next, zinc sulfides were formed in the pH range from 2.4 to 2.5. Subsequently, nickel sulfides were formed in the residual solution at pH 5.5-5.6. At that time, copper, zinc and nickel ions in plating wastewater can be recovered separately as metal sulfides. This method can recycle each metal through the operation, but cannot be well paid attention to the point of utilizing as uniform materials.

In our metal carbonate experiments, almost all metal ions react with carbonate ions and produce precipitates in the basic solution, so it is difficult to separate metal ions by such above method. Therefore, the mechanism of metal ions or anions incorporating should be clarified. Kolthoff et al. [1] have proposed some strategies for separating co-precipitation. In a study of the precipitates purity, it is important to distinct the boundary line between the adsorption and co-precipitation. If a precipitate produced as a flocculated colloid, it has a layer of flocculating ions rigidly adsorbed at its surface. These adsorbed ions can be partly removed by washing out or by centrifuging. If a co-precipitation takes place, the impurities are present in the interior of crystals and cannot be removed by physical procedures.

In this time experimental system, washing out and sweating are difficult choices for separating a number of metal ions. Against metal ions with similar properties in crystals, solvent that dissolves either of them would not be present. Also, products melting point is high: about several hundred degrees Celsius, and their values are near, therefore, separating by the difference of temperature will also be difficult. For releasing the connection arisen from

co-precipitation, another method, for example, in the process of crystallization, improvement of technology that accumulates metal ions with regularity will be expected.

Nomenclature

A	Seed surface area, m^2
m	Metal mole in seed, mol
M	Metal mole ratio in seed, -
N	Number of seed crystals, #
r	Metal ions uptake rate, mol s^{-1}
R	Metal ions uptake rate per surface area, mol m^{-2} s^{-1}
t	Operation time, s
V	Step velocity, m s^{-1}
θ	Surface coverage, -

Index

0	Initial/ in a pure system
eq	Equilibrium
I	Impurity metal ions
T	Target metal ions
unit	Mono

References

[1] I. M. Kolthoff and E. Pearson, 1932, "Theory of coprecipitation" the formation and properties of crystalline precipitates, *J. Phys. Chem*., **36**(**3**), 860-881.

[2] I. V. Kavich, I. V. Savitskii and G. I. Il'kiv, 1964, The introduction of impurities in the crystal lattice of mercuric sulfide, UDC 548. 73.

[3] R. Nilson, 1971, Removal of metals by chemical treatment of municipal waste water, *Water Res.,* **5**, 51-60.

[4] R. A. Berner, 1975, The role of magnesium in the crystal growth of calcite and aragonite from sea water, *Geochim. Cosmochim. Acta*, **39**, 489-504.

[5] Michael M. R., 1977, Crystllization of calcium carbonate in the presence of trace concentrations of phosphorus-containing anions, *J. Cryst. Growth*, **41**, 287-295.

[6] Michael M. R. and K. K. Wang, 1980, Crystallization of calcium carbonate in the presence of metal ions, *J. Cryst. Growth*, **50**, 470-480.

[7] W. F. Pickering, 1983, Extraction of copper, lead, zinc or cadmium ions sorbed on calcium carbonate, *Water, Air, Soil Pollut.*, **20**, 299-309.

[8] S. D. Faust and C. M. Schultz, 1983, The efficiency of removal of heavy metals from water by calcite, *J. Environ. Sci. Health*, **A18(1)**, 95-102.

[9] T. E. Higgins and V. E. Sater, 1984, Combined removal of Cr, Cd, and Ni from wastes, *Environ. Prog.*, **3 (1)**, 12-25.

[10] S. McAnally and L. Benfield, 1984, Nickel removal from a synthetic nickel-plating wastewater using sulfide and carbonate for precipitation and coprecipitation, *Sep. Sci. Technol.*, **19(2&3)**, 191-217.

[11] M. H. Salimi, J. C. Heughebaert and G. H. Nancollas, 1985, Crystal growth of calcium phosphates in the presence of magnecium ions, *Langmuir*, **1**, 119-122.

[12] G. M. P. Morrison, 1987, Bioavailable metal uptake rate determination in polluted waters by dialysis with receiving resins, *Environ. Technol. Lett.*, **8**, 393-402.

[13] I. Uzun and F. Guzel, 2000, Adsorption of some heavy metal ions from aqueous solution by activated carbon and comparison of percent adsorption results of activated carbon with those of some other adsorbents, **24**, 291-297.

[14] D. Feng, C. Aldrich and H. Tan, 2000, Treatment of acid mine water by use of heavy metal precipitation and ion exchange, *Miner. Eng.*, **13(6)**, 623-642.

[15] C. M. Verbann, 2000, Impurity uptake during gypsum crystallization in wastewater

treatment, *Mcgill Univ., Montreal*.

[16] W. X. Wang, 2001, Comparison of metal uptake rate and absorption efficiency in marine bivalves, *Environ. Toxicol. Chem.*, **20(6)**, 1367-1373.

[17] S. A. El-Korashy, 2003, Studies on divalent ion uptake of transition metal cations by calcite through crystallization and cation exchange process. **38**, 1709-1719.

[18] S. K. Handona and U. A. Al Hadad, 2007, Crystallization of calcium sulfate dehydrate in the presence of some metal ions, *J. Cryst. Growth*, **299**, 146-151.

[19] L. Li, S. Xu, Z. Ju and F. Wu, 2009, Recovery of Ni, Co, and rare earth from spent Ni-metal hydrate batteries and preparation of spherical $Ni(OH)_2$, *Hydrometallurgy*, **100**, 41-46.

[20] K. Soya, N. Mihara, D. Kuchar, M. Kubota, H. Matsuda and T. Fukuta, 2010, Selective sulfidation of copper, zinc and nickel in plating wastewater using calcium sulfide, *Int. J. Civ. Environ. Eng.*, **2(2)**, 93-97.

[21] V. C. Gopalratnam, G. F. Bennett and R. W. Peters, Effect of collector dosage on metal removal by precipitation/flotation, 923-938.

[22] T. Fukuda, T. Ito, K. Sawada, Y. Kojima, H. Matsuda and K. Yagishita, 2003, Improvement of nickel-precipitation from aqueous nickel solution by sulfuration with sodium sulfides, *J. Chem. Eng. Jpn.*, **36**, 493-498.

[23] Y. Shimizu and I. Hirasawa, 2013, Impurities effect on carbonate reactive crystallization for wastewater containing metal ions, *ISRN Chem. Eng.* Article ID 984163.

[24] B. Salbu, E. Steinnes and H. Bjornstad, Use of difference physical separation techniques for trace element speciation studies in natural waters, *Separation techniques for trace element speciation*, 203-213.

[25] P. G. Koutsoukos, Z. Amjad and G. H. Nancollas, 1981, The influence of phytate and phosphonate on the crystal growth of fluorapatite and hydroxyapatite, *J. Colloid Interface Sci.*, **83(2)**, 599-605.

[26] I. Langmuir, 1916, The constitution and fundamental properties of solids and liquids, *J. Amer. Chem. Soc.*, **38**, 2221-2295.

[27] N. Kubota and J. W. Mullin, 1995, A kinetic model for crystal growth aqueous solution in the presence of impurity, *J. Cryst. Growth*, **152**, 203-208.

[28] N. Kubota, M. Yokota and J. W. Mullin, 1997, Superssturation dependence of crystal growth in solutions in the presence of impurity, *J. Cryst. Growth*, **182**, 86-94.

[29] N. Kubota, M. Yokota and J. W. Mullin, 2000, The combined of supersaturation and impurity

concentration on crystal growth, *J. Cryst. Growth*, **212**, 480-488.

[30] N. Kubota, M. Yokota, N. Doki, L. A. Guzman, S. Sasaki and J. W. Mullin, 2003, A mathematical model for crystal growth rate hysteresis induced by impurity, *Cryst. Growth Des.*, **3(3)**, 397-402.

[31] J. W. Mullin, 1993, Crystallization, 3rd ed., Butterworth-Heinemann, Oxford.

[32] A. Mersmann, 2001, Crystallization technology handbook, 2nd Ed., Tech. Univ. of Munich, Germany.

Chapter 5

Particle growth rate analyses for the reactive crystallization

In this chapter, based on experiments in past chapters (from 2 to 4), phenomena in the reaction tank has been modeled by the numerical simulation. For example, metal ions concentration in the tank and the crystals growth rate were analyzed. And the generality of this reactive crystallization technology was attempted and problems were clarified.

5.1 Introduction

In past chapters, metal ions separation and recovery efficiency from the wastewater were examined by operating the experimental method. However, experiments have limitations of time, condition involving extremeness, complexity, and dangerousness. The simulation method is the optimum tool for detecting results in any circumstances. And if the internal appearance of the reaction tank is replicated by something of the numerical simulation method, much information which could not been obtained in the experiment can be found out. Also, simulation sometimes contributes to prove the discussion. Facts that are not cleared by the experiment will be found out in this chapter. The aim of this attempt is that the clarification of spherical particles' growth mechanism. In the reactive crystallization, it was determined that the particle growth rate varies with the difference of operation apparatus/conditions or existence/non-existence of seeds.

At first in numerical analyses, time variation of metal ions concentration in the tank during the reactive crystallization was clarified. And then, with the use of these analytical supersaturation data, the behavior of crystals nucleation rate B [# m^{-3} s^{-1}] and the growth rate G [μm s^{-1}] were estimated. And at the same time, the coefficient value of nucleation rate and growth rate: k_b [# m^{-3} s^{-1}], k_g [m s^{-1}], and the order value of them: b [-], g [-] were each optimized by the mathematical simulation from the real experimental CSD data. Mathematical and physical meanings of them were discussed and the growth mechanisms of the reactive crystallization were embodied. Numerical simulations in this chapter have been performed by MATLAB: matrix laboratory and the numerical programs have been all shown in Appendix A, end of this thesis.

5.2 Simulation of metal ions concentration in the tank

At the first of simulation, metal ions concentration in the reaction tank during the reactive crystallization was replicated. Especially, when the continuous stirred-tank reactor: CSTR (chapter 2) and the semi-batch crystallizer (chapter 3 and 4) were used, fundamental equations that describe time change of metal ions concentration during the reaction are each indicated below, Eq. 5-1 and 2.

$$\frac{dC}{dt} = \frac{Q_{in} \cdot C_{in} - Q_{out} \cdot C(t)}{V} - k_r \cdot C(t) \quad (5\text{-}1)$$

$$\frac{dC}{dt} = \frac{Q_{in} \cdot C_{in}}{V} - k_r \cdot C(t) \quad (5\text{-}2)$$

Here, C means metal ions concentration in the tank [kg m^{-3}], k_r is the reaction constant [s^{-1}], Q is the flow rate of the raw solution [m^3 s^{-1}] and V is the tank volume [m^3]. And the index *in* represents the inflow and *out* means the outflow.

The difference of these equations is the term of the outflow feed. In the CSTR method, the suspension liquid in the tank was directly fed out and the term $-\frac{Q_{out} \cdot C(t)}{V}$ was inserted. Meanwhile, in the semi-batch crystallizer, the suspension was hovering at the bottom of tank so almost no metal ions existed in the upper side and the outflow. There, the second term was considered to be ignorable. In the simulation, numerical parameter was set the same value as the experiment indicated in chapter 2 and 3. The value of reaction constant k_r is required to set carefully because this value affects time before reaching the steady states in this simulation. This time, k_r was set the value in consideration of the approximate steady states in experimental conditions. Time variation of the metal ions concentration in the reaction solution, varying the feeding speed and the initial metal ions concentration, can be described like **Fig. 5-1, 2**.

From these results, metal ions concentration in the tank was increased in certain period of time after the reaction occurred, and becomes constant in a low level. Metal ions concentration in the tank increases with the feeding rate and the initial metal ions concentration in the feed increasing (**Fig. 5-1**). This offers supporting evidence that the particles growth rate and their size correlate with the supersaturation ratio in the reaction solution as mentioned in chapter 2 (**Fig. 2-9 and 12**). About the operation apparatus, the metal ions concentration in the tank is estimated to be higher in the semi-batch crystallizer. The reason is considered that metal ions in the tank are not flowed out and much metal ions were remained in the semi-batch crystallizer.

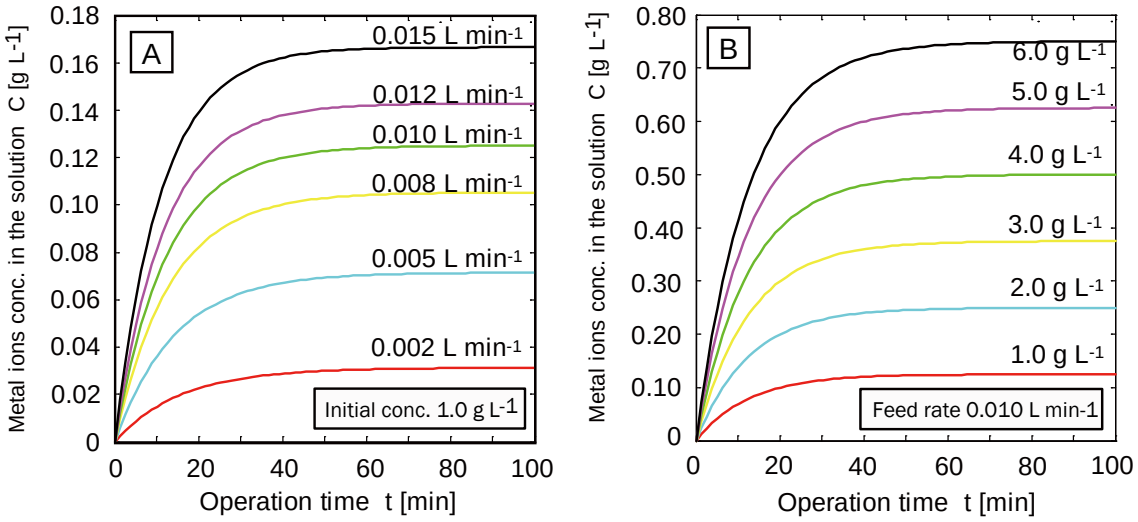

Fig. 5-1 Time variation of metal ions concentration in the reacting solution under the condition of various feeding rates [A] and initial metal ions concentrations [B] (when the CSTR method was applied referring chapter 2, volume of tank: $1.0 \cdot 10^{-3}$ m³).

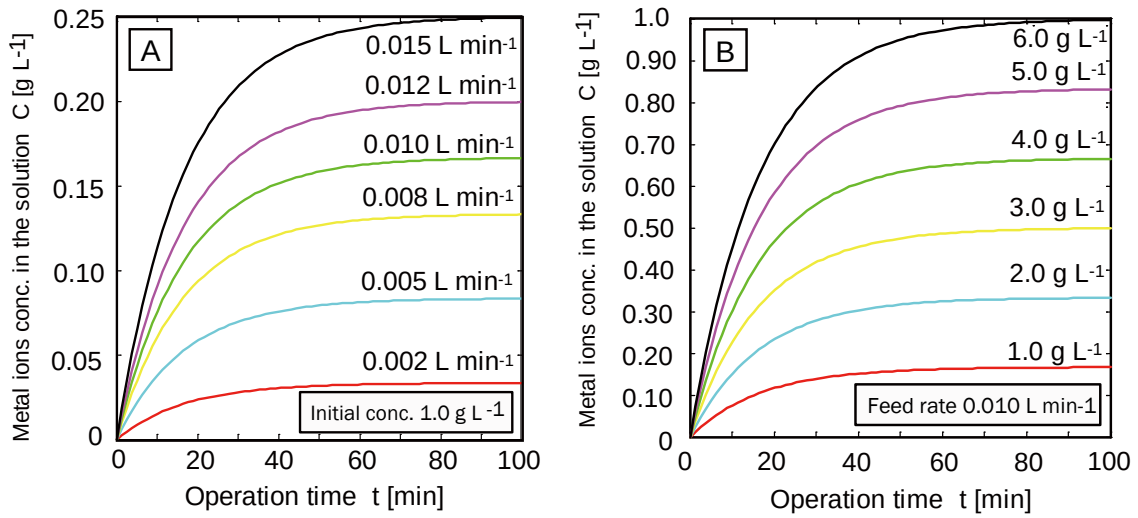

Fig. 5-2 Time variation of metal ions concentration in the reacting solution under the condition of various feeding rates [A] and initial metal ions concentrations [B] (when the semi-batch method was applied referring chapter 3 or 4, volume of tank: $1.0 \cdot 10^{-3}$ m³).

In addition, time variation of metal ions concentration in the reacting solution with changing the volume of solution was similarly simulated, as shown in **Fig. 5-3**. When the volume of solution was large, the metal ions concentration in the tank came to be small, but the transition of raising the metal ions concentration was similar in each condition. Next, in case of applying this

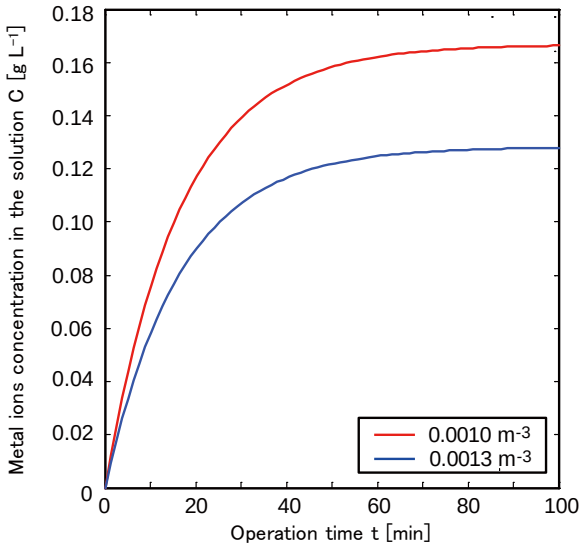

Fig. 5-3 Time variation of metal ions concentration in the reacting solution with the solution volume changes (when the semi-batch crystallizer method was applied, feeding rate: 0.010 L min^{-1}, initial metal ions concentration: 1 000 mg L^{-1}).

model to the real tank-scale, time variation of metal ions concentration in the reaction solution was similarly simulated. As a result of tries and errors, to make the same behavior of metal ions concentration in the tank, next equation have to be satisfied. In fact, as for the feed rate, the reproducibility of recovery rate will be kept by setting to be proportional to the tank volume.

$$\frac{\text{Tank volume}}{\text{Feed rate}} = \text{constant value} \tag{5-3}$$

5.3 Mathematical interpretation about crystal growth mechanisms

Numerical analyses regarding the particle growth mechanisms by the reactive crystallization have been performed [1-12]. The equation of particle growth rate R_G [kg m^{-2} s^{-1}] applies this situation (Eq. 5-3). In the study of particles growth, numerical analyses were operated from two aspects. One is that evaluating the value of k_G: coefficient of growth speed [kg m^{-2} s^{-1}] and g: the order of growth speed [-] by fitting the experimental data to the Eq. 5-3. The other is that estimating PSD profiles from the population balance theory as mentioned below.

$$\mathrm{R_G} = \mathrm{k_G}\Delta\mathrm{C^g} \tag{5-4}$$

Ku et al. [1] have discussed PSD theory for the removal of copper and nickel by the numerical method. The concept of the population balance for a mixed-suspension/mixed-product removal (MSMPR) system states that the number of discrete particles must be conserved in a dispersed system [2]. This concept applies the particle size distribution density function: crystals number near the size L represents $\mathrm{dN} = \mathrm{n(L)dL}$. In considering the mass balance in the minute space, below equation can be held. The assumptions that should be considered for the MSMPR operation are as follows. I a certain amount of tank volume, II steady inflow and outflow, III not containing particles in the influent, IV well-mixing, and V not occurring birth and death of particles due to attrition.

$$\mathrm{n} = \mathrm{n^0 exp}\left(-\frac{\mathrm{L}}{\mathrm{G\tau}}\right) = \frac{\mathrm{B}}{\mathrm{G}}\exp\left(-\frac{\mathrm{L}}{\mathrm{G\tau}}\right) \tag{5-5}$$

where n represents the population density [# L^{-1} m^{-1}], L is the characteristic particle size [m], G is the particle growth rate [m min^{-1}] and τ is the reactor residence time [min]. When the cumulative particle size distribution is plotted in the field, ndL integration yields as below:

$$\mathrm{N(L,\infty)} = \int_0^\infty \mathrm{n^0 exp}\,(-\mathrm{L/G\tau})\mathrm{dL} = \mathrm{n^0 G\tau exp}\,(-\mathrm{L/G\tau}) \tag{5-6}$$

where N is the total number of particles per unit volume in the size range from L to ∞. Plots of ln N vs. L yield a straight line of slope $-1/G\tau$ and intercept $ln(n^0 G\tau)$ theoretically, but the N value drops off this line in L near zero. The birth rate B^0 is computed from the product of n^0 and G in Eq. 5-6.

$$B^0 = n^0 G \tag{5-7}$$

Next, based on the experiment introduced in Chapter 3, an approach of analysis about spherical obtained particles growth rate has been attempted. The method is that particles growth rate *G* has calculated from CSD data, mainly using Eq. 5-4 and 5-5 (**Fig. 5-4**). After that, the coefficient of growth rate k_G [kg m^{-2} s^{-1}] and the order of growth rate *g* [-] have been estimated. Numerical programs were introduced in Appendix at the end of this thesis.

Growth rate based on recovered particles average size were calculated from Eq. 5-4. Growth rate of nickel carbonate basics was roughly 1.3×10^{-9} [m s^{-1}] and that of copper carbonate basics was about 2.5×10^{-9} [m s^{-1}]. The difference of values was due to the shape of grown particles, as explained in Chapter 4. Then, the coefficient of growth rate k_G [kg m^{-2} s^{-1}] and the order of growth rate *g* [-] have been estimated from Eq. 5-3. This equation indicates that the particles growth rate is proportional to the reaction time. Time variation of particles growth rate can be represented as below Fig. 5-4. The slope in these graphs indicate the term $k_G \Delta C^g$. In fact, the value of nickel carbonate basics is 3.43×10^{-2} and the value of copper carbonate basics is 4.89×10^{-4}. Even if the value of ΔC has been found out, these two parameters will not be cleared at the same time. Then, rough value range of them needs to be understood. Now, the mathematical and physical meanings of k_g and *g* will be discussed.

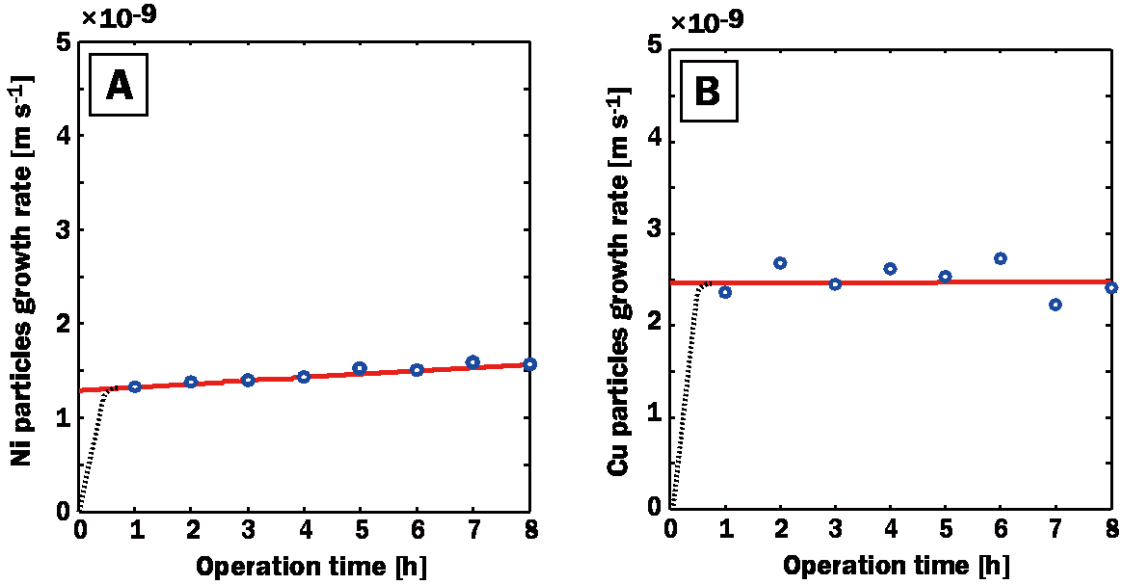

Fig. 5-4 Growth rate fitting against nickel carbonate basic [A] and copper carbonate basic [B].

As it has been seen, the value of k_g and g both can largely alter particles growth. The term g always refers to the power which gives a factor proportional to the rate of an elementary reaction [3]. So if the surface reaction is first order, g comes to be near 1. And many types of inorganic crystallization from aqueous solution gives g will be in the range from 1 to 2. Therefore, setting the g value between 1 and 2 and evaluating the k_G value will be the adequate measurement.

By another simulation, nucleation rate and growth rate are estimated to increase with the operation in accordance with the metal ions concentration in the stock solution. There, they are thought to keep increase until the steady states are reached. Dot lines in Fig. 5-4 are indicated the conceivable curve to reach the steady value.

5.4 Possible application of this system for the model wastewater

Experiments in this thesis target at only five kinds of metal ions, however, how the other metal ions react? If metal sulfates have high water solubility and metal carbonates have low water solubility, metal ions can easily be solidified via the reaction. This holds true about univalent and trivalent ions, instead, it will not come to that if the water solubility of sulfate or carbonate is different. Metal substances indicated in **Table 2-1** are obtained as crystals but the shape cannot be determined by the estimation. If the sphere seeds are provided prior to the reaction, metal ions will be assumed to incorporate in seeds and grow spherically.

From chapter 2 to chapter 4, the application of the reactive crystallization method for simple model wastewater has been attempted. However, actual wastewater containing metal ions is wide variety and this system needs to make more improvements. Some strategies for separating impurity ions from the real wastewater will be discussed in this section.

1. Chemical and physical separation treatment

Generically thinkable methods for improving purity of target metal ions from crystals incorporating impurity ions include washing and centrifuging. Washing is one of separation treatments that utilize the difference of the degree of solubility or ionization tendency against particular solvent. Solvents include rather strong acid like nitric acid and hot concentrated sulfuric acid. In this instance, the solvent which melts metal ions selectively should be chosen. Centrifuging and ultrasonic shaking are physical treatments to separate plural kinds of metal ions. These treatments can remove metal components that are incorporated by the adsorption.

2. Selective precipitation by changing pH

In the basic solution, many kinds of metal ions were precipitated in the wide range of pH. Because it is difficult to separate precipitates and crystals, metal ions will not be obtained particularly by the difference of pH like in the acid solution. If sphere seeds are presented during the reaction, any metal ions may be piled up on seeds and this behavior should be largely utilized. But in this regard, any metal ions are incorporated to seeds so eventually. Other separation treatments will be needed for obtaining only particular metal components.

3. Selective precipitation by the difference of metal ions uptake speed

If the reaction was occurred under the existence of seeds, target metal purity will be large just after the reaction. In this study, target metal ions were found to be incorporated more easily than impurity ions, so it seems to be effective to utilize the difference of uptake speed to seeds for separating metal ions in this reaction. The more the difference is large, the more easily metal ions can be separated. Procedures of separation will include that recovering products soon after the reaction and exchanging the initial state solution any number of times.

4. Selective precipitation by adding protecting group

This is a method for not occurring some reactions, as is often found in chemical and biological reactions. Introducing inactive functional group to metal ions can be a strategy for separating plural ions. However, it is difficult to find agents for binding particular metal ions selectively.

Nomenclature

B	particles nucleation rate, $m^{-3}\ s^{-1}$
C	metal ions concentration in the tank, $kg\ m^{-3}$
ΔC	$C - C*$ (C*=metal ions saturated concentration)
g	the orger of growth rate, -
G	particle growth rate, $m\ min^{-1}$
k_G	coefficient of growth rate, $kg\ m^{-2}\ s^{-1}$
k_r	reaction constant, s^{-1}
L	characteristic particle size, m
n	population density, $\#\ L^{-1}\ m^{-1}$
N	total number of particles per unit volume in the size range from L to ∞
Q	flow rate of the raw solution, $m^3\ s^{-1}$
R_G	particle growth rate, $kg\ m^{-2}\ s^{-1}$
V	volume of tank, m^3
τ	residence time, min

index

0	initial
in	inflow
out	outflow
t	time

References

[1] Y. Ku, R. W. Peters, 1988, The effect of complexing agents on the precipitation and removal of copper and nickel solution, *Part. Sci. Technol*., **6**, 441-466.

[2] A. D. Randolph and M. A. Larson, 1971, Theory of particulate processes, *Academic Press, New York*.

[3] J. W. Mullin, 1993, Crystallization, Third ed. *Butterworth-Heinemann, Oxford*.

[4] A. Mersmann, 2001, Crystallization technology handbook, Second ed. *Marcel Dekker Inc., New York.*

[5] H. Tsuge, I. Kuge and K. Fujii, 2004, The effective utilization of beneficial resources dissolved in seawater –crystallization characteristic of lithium carbonate-, *Bull. Soc. Sea. Water Sci. Jpn.*, **58**, 579-584.

[6] H. Tanaka and T. Nishi, 1989, Local phase separation at the growth front of polymer spherulite during crystallization and nonlinear spherulitic growth in a polymer mixture with a phase diagram, *Phys. Rev. A*, **39(2)**, 783-794.

[7] H. D. Keith and F. J. Padden Jr., 1963, A phenomenological theory of spherulitic crystallization, *J. Appl. Phys.*, **34(8)**, 2409-2421.

[8] P. C. Chen, G. Y. Cheng, M. H. Kou, P. Y. Shia and P. O. Chung, 2001, Nucleation and morphology of barium carbonate crystals in a semi-batch crystallizer, *J. Cryst. Growth*, **226**, 458-472.

[9] T. F. Kazmierczak, M. B. Tomson and G. H. Nancollas, 1982, Crystal growth of calcium carbonate. A controlled composition kinetic study, *J. Phys. Chem.*, **86**, 103-107.

[10] R. Sheikholeslami and M. Ng, 2001, Calcium sulfate precipitation in the presence of nondominant calcium carbonate: thermodynamics and kinetics, *Ind. Eng. Chem. Res.*, **40**, 3570-3578.

[11] Y. Kotaki and H. Tsuge, 1990, Reactive crystallization of calcium carbonate in a batch crystallizer, *J. Cryst. Growth*, **99**, 1092-1097.

[12] N. Kubota, T. Sekimoto and K. Shimizu, 1990, Precipitation of $BaCO_3$ in a semi-batch reactor with double-tube gas injection nozzle, *J. Cryst. Growth*, **102**, 434-440.

Conclusions

CONCLUSIONS

In this thesis, the method of separating and recovering metal ions in the wastewater by the carbonate reactive crystallization was developed. Materials such as manganese carbonates and zinc oxides are obtained spherically, and particles size, surface roughness, metal ions recovery rates, mono-dispersion, and C. V. value are controlled to some extent by coordinating the inflow conditions (i.e. metal ions concentration in the stock solution, the inflow feeding rate, and solution's initial pH, and so on). The particles growth rate has been estimated to roughly correlate with the supersaturation ratio in the reactive solution from the particles sizes data.

In applying isolated metal ions to this technology, recovered crystal sizes, forms, and dispersibilities can be highly controlled by adjusting the seed inputs or the stock solution inflow conditions. Meanwhile, against solutions containing impurities, foreign metal ions produced compounds and fine particles. Impurities were strictly incorporated into crystals or adsorbed on the surface of seeds. Considering metal ions uptake rate per surface area, copper components can take in metal ions rapidly but nickel component cannot so fast. In addition, target metal mole ratio was improved by from 10 to 20 % by the centrifugation in copper carbonate basic based experiment. Anions impurities like borate or phosphate ions caused the effect of damaging the surface of seeds or producing many fine particles during the reactive crystallization. Through these experiments, metal ions in the drainage can be recovered almost over 99 % in any semi-batch crystallization. Especially, in semi-batch crystallization without impurities, the recovery rate was indicated about 99.9 %. This method can be used secondarily against the highly extraction liquid after the solvent extraction or the electrolytic refining. Reactive crystallization method can be concluded to contribute to both the wastewater treatment and the materials construction from fresh direction.

FUTURE WORKS

Actual wastewater contains many types of metal ions and anions, and most of ions can be recovered as solids by the carbonate crystallization method. Moreover, target metal ions purity

will be improved to some extent by the physical separation. This technology is considered to move toward practical use after conducting additional improvements indicated as the following.

1. For recycling metal carbonates as materials, the metal purity is required to be further improved. Development of washing technology or any other physical treatment that separate metal ions may be the key to improve the purity of target metal.
2. Technology that does not incorporate foreign metal ions in the crystallization process will also effective. For example, modifying the target ions or other ions by the functional group will be the method of recovering metal ions selectively. Or exploring the method of metals selective incorporation by the use of the difference of uptake speed also has possibilities.
3. For applying to the real scale treatment, the construction of theory about geometric items and treatment conditions will be needed. In this thesis, theoretical formula about the best seed input that applies to the reactive crystallization has been developed. It will be required to confirm the adequacy and lead the most appropriate value in any operation condition.

Appendixes

Numerical computing programs (MATLAB programs) using in this thesis

1 Metal ions concentration in the reactive solution (in Chapter 5-1)

```
Simpara.C0=[0]; %initial concentration [ppm]
Simpara.qin=[0.002;0.005;0.008;0.010;0.012;0.015]; %inflow feed [L/min]
Simpara.Cin=[1000]; %inflow manganese concentration [ppm]
Simpara.qout= [0.004;0.010;0.016;0.020;0.024;0.030]; %outflow feed [L/min]
Simpara.V=1.0; %reaction tank volume [L]
Simpara.t0=0; %reaction initial time [min]
Simpara.tf=100; %reaction end time [min]
Simpara.k=0.06; %reaction coefficient [min-1]
Simpara.N=80; %separation number [#]
Simpara.tspan=linspace(Simpara.t0,Simpara.tf,Simpara.N);
Simpara.index=1;

result=[];
figure(1);
for i=1:6
    Simpara.index=i;
    options=odeset('RelTol',1e-4,'AbsTol',[1e-4]);
    [t,C]=ode45(@f_concentration,Simpara.tspan,Simpara.C0,options,Simpara);
    result=[result t C];
end
%plot(t,C(:,1));
plot(result(:,1),result(:,2),'r',result(:,3),result(:,4),'c',result(:,5),result(:,6),
'y',result(:,7),result(:,8),'g',result(:,9),result(:,10),'m',result(:,11),result(:,12
),'k');
legend('0.002 L min-1','0.005 L min-1','0.008 L min-1','0.010 L min-1','0.012 L
min-1','0.015 L min-1');
ylabel('metal ions concentration in the solution C [ppm]');
xlabel('time t [min]');
```

```
function dCdt=f_concentration(t,C,Simpara)

p=Simpara;
dCdt=zeros(1,1);
dCdt(1)= (p.qin(p.index)*p.Cin-p.qout(p.index)*C(1)-p.k*C(1)*p.V)/p.V;

end
```

Above is the example of metal ions concentration in the reaction solution based on eq. 5-1.

2 Fitting of metal ions uptake rate per seed surface area for copper reactive crystallization (in Chapter 4-5)

```
%Excel file loading__impurity uptake
Outdata1x=xlsread('Impurity_MetalRatio.xlsx','Cubase_XRF','W5:W13');
Outdata2x=xlsread('Impurity_MetalRatio.xlsx','Cubase_XRF','W20:W28');
Outdata3x=xlsread('Impurity_MetalRatio.xlsx','Cubase_XRF','W36:W44');

Outdata1y=xlsread('Impurity_MetalRatio.xlsx','Cubase_XRF','AB5:AB13');
Outdata2y=xlsread('Impurity_MetalRatio.xlsx','Cubase_XRF','AB20:AB28');
Outdata3y=xlsread('Impurity_MetalRatio.xlsx','Cubase_XRF','AB36:AB44');

%data curve fitting／the calculation of optimum R value
time=0:0.01:8; %reaction time[h]
options=optimset('Display','iter','TolFun',1e-3,'DiffMinChange',1e-2);
Tr=@(R,time)(0.1673+R(1).*time)./(0.1673+R(1).*time+R(2).*time); %time variation of
target metal mole ratio

param0=[0.01 0.01];
LB=[0 0];
UB=[10 10];

coefEsts1=lsqcurvefit(Tr,param0,Outdata1x,Outdata1y,LB,UB,options);
coefEsts2=lsqcurvefit(Tr,param0,Outdata2x,Outdata2y,LB,UB,options);
```

```
coefEsts3=lsqcurvefit(Tr,param0,Outdata3x,Outdata3y,LB,UB,options);
figure(1);

%optimparam=[0.0804 0.0569]
subplot(311)
plot(Outdata1x,Outdata1y,'o')
title('Cu mol Ratio in Seeds using Mn as Imp.'); xlabel('time [h]'); ylabel('Main Metal
Ratio [-]');
hold on
line(time,Tr(coefEsts1,time),'Color','r')

%optimparam=[0.0407 0.0224]
subplot(312);
plot(Outdata2x,Outdata2y,'o')
title('Cu mol Ratio in Seeds using Co as Imp.'); xlabel('time [h]'); ylabel('Main Metal
Ratio [-]');
hold on
line(time,Tr(coefEsts2,time),'Color','r')

%optimparam=[0.0296 0.0259]
subplot(313);
plot(Outdata3x,Outdata3y,'o')
title('Cu mol Ratio in Seeds using Zn as Imp.'); xlabel('time [h]'); ylabel('Main Metal
Ratio [-]');
hold on
line(time,Tr(coefEsts3,time),'Color','r')
end
```

---

3 Fitting seed growth rate by the experimental grown size (Chapter 5-2)

```
%Particles growth fitting

%Excel file loading__particles grown average size

Outdata1x=xlsread('粒径分布_Ni.xlsx','NiSeed_40','D7:K7');
Outdata2x=xlsread('粒径分布_Cu.xlsx','CuSeed_20','D7:K7');
```

```
Outdata1y=xlsread('粒径分布_Ni.xlsx','NiSeed_40','D373:K373');
Outdata2y=xlsread('粒径分布_Cu.xlsx','CuSeed_20','D326:K326');

%Fitting particels growth rate value

time=0:0.01:8; %reaction time[h]
options=optimset('Display','iter','TolFun',1e-3,'DiffMinChange',1e-2);

R=@(c,time)(time.*c(1)+c(2));                    %Equation of particles growth

param0=[1 1.5];
LB=[0 0];
UB=[10 3];

coefEsts1=lsqcurvefit(R,param0,Outdata1x,Outdata1y,LB,UB,options);
coefEsts2=lsqcurvefit(R,param0,Outdata2x,Outdata2y,LB,UB,options);

%optimparam=[0.0343 1.2844]
figure(1);
plot(Outdata1x,Outdata1y,'o')
title('Ni particles growth rate'); xlabel('time [h]'); ylabel('Ni particles growth rate
[-]');
hold on
line(time,R(coefEsts1,time),'Color','r')

%optimparam=[4.8877e-04 2.4657]
figure(2);
plot(Outdata2x,Outdata2y,'o');
title('Cu particles growth rate'); xlabel('time [h]'); ylabel('Cu particles growth rate
[-]');
hold on
line(time,R(coefEsts2,time),'Color','r')
```

Acknowledgement

I thank Professor Izumi Hirasawa for many helpful discussions and advices about this thesis. I appreciate his supporting my participation of international conference and Global COE program. I also thank for Professor Joakim Ulrich, Professor Suguru Noda and junior associate professor Fukashi Kohori for critical comments on the original version of my thesis.

I'm very grateful for Global COE program "Center for Practice Chemical Wisdom" by MEXT during my doctoral course, from 2009 to 2012. With the assistance of this program, I preceded my research smoothly and developed the philosophy about research. I improved the skill of international communication in various global aspects. This study was sophisticated as a result of financially supported and trained in many aspects from this program. Also we appreciate the designing and creating custom-ordered flask of the Fujimoto Kagaku Co, Ltd.

After the doctoral course, I really appreciate Dr. Hiroshi Takahashi, Dr. Masahiro Abe, and Mr. Kiyotaka Suzuki in doctoral career center in Waseda University for the employment assistance. In the doctoral practice training, I greatly appreciate Dr. Yoshida and Dr. Isaka in Hitachi Plant Technology Co, Ltd. for their helping my research environment assistance and advising about my life even if they are in a busy schedule.

I thank all senior associates and junior associates through the study duration.
Finally, I would like to express the best gratitude to my parents against all their help and encouragement.